Physiochemical controls on the formation and stability of atacamite in the soil surrounding the Spektakel mine, Northern Cape Province, South Africa

by

Stephan Gerhard le Roux

Thesis presented in fulfilment of the requirements for the degree
Master of Science in Geology/Environmental Geochemistry
Stellenbosch University

Supervisor: Dr. Catherine Clarke
Co-supervisor: Prof. Alakendra Roychoudhury
Faculty of Science

March 2013

Declaration

By submitting this thesis/dissertation electronically, I declare that the entirety of the work contained therein is my own, original work, that I am the sole author thereof (save to the extent explicitly otherwise stated), that reproduction and publication thereof by Stellenbosch University will not infringe any third party rights and that I have not previously in its entirety or in part submitted it for obtaining any qualification.

February 2013

_____

Abstract

The Northern Cape Province of South Africa has played host to numerous mining activities for over a century. To date, most of the mining activity has ceased, leaving the area laden with derelict mine sites and unlined tailings dumps. One such site is the Spektakel mine situated to the west of the town of Springbok. The unlined copper and sulphide rich tailings at the site have the potential to leach elevated concentrations of copper and acidic water into the Buffels River downslope of the site. This poses a threat to the surrounding communities that rely mainly on the river to supply water for drinking, livestock and irrigation.

The soil surrounding the tailings dumps was characterised in terms of its mineralogical and chemical properties. The results indicate that the soil contains elevated concentrations of Cu^{2+}, which is bound in the soil in the form of the secondary copper hydroxy mineral atacamite ($Cu_2(OH)_3Cl$). No other secondary copper minerals were identified at the site. Analysis of the solution present on the surface of the tailings dumps indicate that the tailings are the main source of the high Cu^{2+}, Mg^{2+} and SO_4^{2-} concentrations observed in the surrounding soils. As this solution migrates through the tailings dumps, into the soil, it accumulates Cl^- through halite dissolution. The resulting acidic Cu^{2+}, Mg^{2+}, SO_4^{2-} and Cl^- solution reacts with the calcite in the soil, replacing it with atacamite.

To determine why only a copper chloride mineral formed in the sulphate rich environment a synthetic solution with the composition of a solution in equilibrium with the soil was evaporated, both in the presence and absence of calcite. The results indicate that when the solution comes into contact with calcite, atacamite immediately precipitated, removing the Cu^{2+} from the solution. In the absence of calcite Cu^{2+} remains conservative, accumulating in the solution without precipitating a copper sulphate mineral. This establishes that the elevated Mg^{2+} concentration of the solution induces the formation $MgSO_4$ aqueous complexes that reduce the activity of free sulphate, thus restricting copper sulphate mineral formation.

The results from the soil characterization indicate that the atacamite stabilization mechanisms (circumneutral pH, high Cl^- concentration and calcite) in the soil are diminishing. During sporadic rain events the acidic tailings solutions dissolve the calcite and temporarily reduce the Cl^- concentration of the soil. To determine how these decreases will influence Cu^{2+} mobility in the soil, the stability of atacamite was tested by reducing the pH both in the presence and the absence of chloride. The results indicate that an elevated Cl^- concentration and a pH > 6 stabilizes atacamite. A decrease in either of these parameters destabilizes atacamite and favours its dissolution.

The study concludes that the current chemical conditions in the soil at Spektakel favour the stability of atacamite. However, continued sporadic rain events will reduce the Cl^- concentration in the soil by increasing the SO_4^{2-} concentration. This acidic solution will dissolve the calcite in the soil, thus reducing the buffering capacity of the soil, leading to the instability of atacamite, resulting in the leaching of large quantities of Cu^{2+} into the surrounding water bodies.

Opsomming

Die mynbou bedryf was die ekonomiese dryfkrag van die Noord-Kaap Provinsie van Suid-Afrika vir meer as ‘n eeu. Die area was die gasheer vir ‘n verskeidenheid mynbou aktiwiteite tot die mynmaatskappye besluit het om mynproduksie te staak en die gebied te verlaat. Die mynmaatskappye het geen rehabilitasie aan die myne en mynhope verrig nie. Die verlate myne lê verspreid in die area met oop mynhope wat koper en ander swaar metale in die grond, sowel as in die water, na omliggende areas kan versprei. Een van dié verlate myne is die Spektakel myn 40 km wes van Springbok. Die mynhope by Spektakel kan moontlik koper en ander swaar metale in die Buffelsrivier, wat langs die myn verby loop, loog. Dit dien as ‘n bedreiging vir die omliggende gemeenskappe wat staatmaak op die water vir drinkwater en besproeiing.

Die grond rondom die mynhope was ge-analiseer om te bepaal hoe erg ‘n bedreiging die mynhope vir die omgewing is. Die resultate dui daarop dat die grond hoë konsentrasies Cu^{2+} bevat wat vasgebind is in die sekondêre koper mineral atakamiet ($Cu_2(OH)_3Cl$). Geen ander sekondêre koper minerale is in die grond geïdentifiseer. Die analise van die oplossing wat bo-op die mynhoop aangetref is dui aan dat dié oplossing suur en gekonsentreerd is t.o.v. Cu^{2+}, Mg^{2+} en SO_4^{2-}. Terwyl die oplossing deur die mynhoop migreer los dit haliet in die grond op wat Cl^- tot die oplossing byvoeg. Wanneer hierdie suur en Cu^{2+}, Mg^{2+}, SO_4^{2-} en Cl^- ryke oplossing met die kalsiet in die grond reageer word die kalsiet vervang met atakamiet (Garrels en Stine, 1948).

Om vas te stel waarom slegs 'n koperchloried mineraal vorm in die sulfaat ryke grond was ‘n oplossing, met ‘n samestelling soortgelyk aan 'n oplossing in ewewig met die grond, verdamp in beide die teenwoordigheid en afwesigheid van kalsiet. Die resultate van die eksperiment dui daarop dat wanneer die oplossing in kontak kom met kalsiet atakamiet onmiddellik neerslaan en Cu^{2+} uit die oplossing verwyder. In die afwesigheid van kalsiet bly Cu^{2+} konserwatief in die oplossing; die Cu^{2+} hoop op in die oplossing en slaan nooit neer nie. Daar is vasgestel dat die verhoogde Mg^{2+} in die grondoplossing $MgSO_4$ water komplekse vorm wat die aktiwiteit van SO_4^{2-} verlaag en verhoed dat kopersulfaat minerale kan vorm.

Verdere navorsing dui aan dat die chemiese meganismes wat atakamiet in die grond stabiliseer besig is om te kwyn. Gedurende sporadiese reën buie word die kalsiet in die grond opgelos deur die suur mynhoop oplossings wat die pH van die grond verlaag. Die mynhoop oplossing verryk ook die grond t.o.v SO_4^{2-} wat die Cl^- konsentrasie verlaag. Om te bepaal hoe hierdie afname in Cl^- konsentrasie en pH die migrasie van Cu^{2+} beïnvloed was atakamiet oplossbaarheid bepaal. Atakamiet was onderskeidelik geplaas in ‘n suiwer water en chloried oplossing tewyl die pH verlaag was om te bepaal hoe atakamiet oplos in elk van

die oplossings. Die resultate dui aan dat 'n verhoogde Cl^- konsentrasie en pH > 6 atakamiet stabiliseer. Die afname van beide hierdie veranderlikes het veroorsaak dat atakamiet makliker ontbind en Cu^{2+} vrystel.

Die gevolgtrekking van die studie is dat die huidige chemiese toestande in die grond by Spektakel gunstig is vir die stabiliteit van atakamiet. Met sporadiese reën buie neem die Cl^- konsentrasie in die grond af en los kalsiet op. Hierdie afname in pH en Cl^- konsentrasie maak atakamiet meer onstabiel wat gevolglik Cu^{2+} in die grond en water rondom Spektakel vrystel.

Acknowledgements

This project would not have been possible without all the people that supported me for the past six years. First and foremost I would like to thank Dr. Cathy Clarke for all the time and effort she invested in me and the project. Without your knowledge and patience, I would not have been able to produce and finish the project on time, thank you for everything. I would like to thank the Nation Research Foundation (NRF) (Grant Number 80400) for funding the running costs of this project. I would like to thank Inkaba yeAfrica for providing me with a bursary which enabled me to do this MSc. Thank you to all the staff at Stellenbosch University that aided me with all my lab work and analysis namely Nigel Robertson, Matt Gordon, Esmé Spicer and Riana Rossouw. I would like to thank Remy Bucher at iThemba Labs who helped with X-Ray Diffraction analysis. I would also like to thank Robert Hansen for his help in the field and acquiring information of the site. This said, I want to thank my parents, Gerhard and Nilia, and brother Jacques for their constant motivation and support, never doubting me and helping me when it felt that the project was never going to end. My dear friends Joanie Smit, Andrea Baker, Duncan Hall, Raimund Rentel and Claudia Struwig thank you for all the good times we had together, I will never forget all the fun time we had, I hope that this will continue in the future. Duncan, Joanie and Andrea thanks for the last minute read through, you helped me more than you can imagine. Thank you to Prof. AN Roychoudhury for aiding in the understanding of the chemistry and always being available when help was required. Lastly thank you to Jeremy Donnelly for sponsoring me a new laptop when my old one decided to die.

Table of Content

List of Figures

List of Tables

1 Introduction

1.1 Overview

The Northern Cape province of South Africa has played host to large scale mining activity for more than two centuries. Due to the lack of regulations governing the disposal of mine waste and the initially primitive mining techniques, some depleted mine sites have been abandoned without any rehabilitation. The most prominent problem at these sites is the presence of unlined and exposed sulphide-rich mine tailings dumps. One such a site is the derelict Spektakel mine situated in the Buffels River valley.

To date only limited research has been conducted in order to determine the potential threat the Spektakel site poses to the surrounding environment. Preliminary studies by Hohne and Hansen (2008) and Newmark (2010) indicate that the largest threat posed by the site is the dispersion of copper-bearing acid mine drainage solutions into the soil and water systems surrounding the site. This corresponds with research performed on similar sites that noted that unlined sulphide-rich mine tailings are the main source of acid mine drainage at abandoned mine sites (Vigneault *et al.*, 2001). As these solutions move through the tailings dumps they have the potential to leach metals from the tailings (Geller *et al.*, 1998) into the surrounding soil profile and nearby water bodies. This is problematic in the case of the Spektakel site, which is situated upslope of the Buffels River and unconfined Buffels River aquifer. The Buffels River is the main water source of the largest aquifers in the region, namely the Spektakel, Buffels River and Kleinsee aquifers (Benito *et al.*, 2010). These aquifers contribute a large proportion of the drinking and irrigation water to the surrounding communities. Possible leaching of these acidic copper rich solutions from the tailings into these water systems could have disastrous consequences for the people in the area.

Preliminary studies found that the secondary copper mineral atacamite is present in the soil surrounding the mine tailings (Hohne and Hansen, 2008; Newmark, 2010). It is still uncertain whether or not atacamite is the only secondary copper mineral phase in the soil surrounding the site. Nevertheless the presence of atacamite does illustrate the secondary copper mineral forming potential of the soil. To date, little is known about the conditions governing the formation and dissolution of atacamite in soils, although some research has indicated that that atacamite is the prevailing secondary Cu mineral present in supergene oxide zones of Cu deposits in the Atacama Desert (Hannington, 1993). Additionally it has been reported that atacamite forms at high Cl^- concentrations and pH conditions similar to normal sea water (Woods and Garrels, 1986) which is contrary to the acidic characteristic of the site.

This leads to the question as to how the continuous supply of acidic solutions from the tailings influences the stability of atacamite, as no research to determine its dissolution potential has been conducted.

Aside from the preceding observations little is understood about the chemistry of the soil surrounding the site. Due to the arid evaporative climate (Hahn *et al.*, 2005) and sporadic rainfall (MacKellar *et al.*, 2007), the soil at Spektakel is exposed to a range of different chemical conditions. It is also still uncertain as to how the climate contributes to the chemistry of the soil and the formation of atacamite. Although atacamite has been detected in the soil, a question arises as to why the sulphate equivalent (brochantite [$Cu_4(OH)_6SO_4$]) is not present. The stability of secondary Cu phases under current and future (more acidic) soil conditions is still unknown. The geographical position of the mine as well as the sensitivity of the local ecosystem make an understanding of secondary Cu mineral formation and stability essential to understand the potential risks the contaminated soils pose to the environment.

1.2 Aims and objectives

The overall aim of this study is to characterise the chemical environment within the Spektakel soils in order to understand and predict the conditions needed for the formation and stability of secondary Cu minerals in the soil.

This will be achieved through the following objectives:

- Characterization of the soil surrounding the tailings in terms of mineralogy and physical and chemical properties, with the aim of determining what other secondary copper minerals are present in the soil, as well as the concentration of soluble ions in the soil.

- Determining the composition of the solutions at the surface of the tailings dumps in order to define how it contributes to the chemistry of the soil.

- Investigating the influence that the absolute Cl^- and SO_4^{2-} concentrations have on the formation of atacamite and brochantite in the presence of calcite.

- Determine how a solution that is in equilibrium with the soil surrounding the tailings dumps evolves chemically during evaporation, both in the presence and the absence of calcite, to establish how evaporation aids the formation of atacamite or other secondary copper minerals.

- Investigating the stability of atacamite under the chemical conditions present in the soil, as well as under conditions of decreased salinity and increased acidity.

1.3 Spektakel site location and description

The derelict Spektakel mine is situated in the Northern Cape province of South Africa (29°39'30.41"S, 17°35'1.65"E), 40km west of the town of Springbok on the R355 (Figure 1.1). It is the easternmost Cu mine of the Okiep Copper District (OCD) and is situated at the foot of the Nababeep plateau in the Buffels Rivier Valley. The valley is bound by the edge of the Sandveld coastal plain, 50km from the Atlantic coast at an approximate elevation of 200m above sea level. On the southern side of the site, adjacent to the road, there are signs of old exposed dump sites as well as the remnants of a leaching pond. One of the troubling aspects about the site is the proximity of the Buffels River which borders on the south of the site (Figure 1.2).

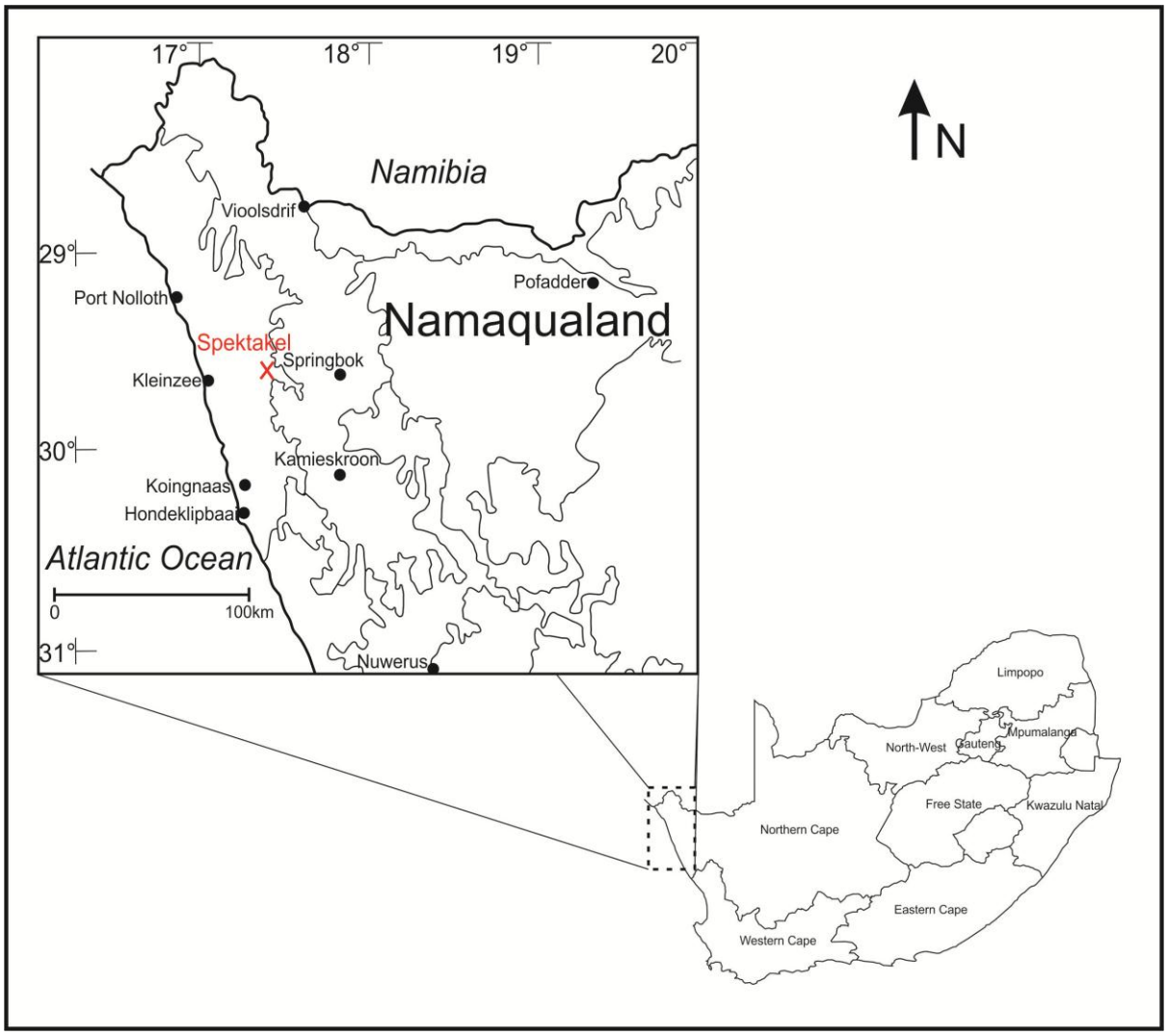

Figure 1.1: Position of the Namaqualand region relative to the Northern Cape province in South Africa. The location of the Spektakel mine is indicated by a red X.

During the life span of the mine both underground and opencast mining were practiced. The mine shaft was sunk to the north of the site adjacent to the Open Pit (Figure 1.2). Four tailings dumps are located to the west and east of the shaft (Figure 1.2). Tailings Dump 1 is the remnant of the original tailings dump and contains large quantities of unprocessed ore material which is a result of initially crude mining techniques. At some stage in the mines history heap leaching was performed on this dump in order to try and extract the remaining unprocessed material. The remnants of the heap leaching process are visible in Tailings Dump 3 and adjacent Leach Pond. Tailings Dump 2 was created at a later stage of active mining. The improved mining techniques produced less unprocessed material producing a potentially “less hazardous” tailings dump relative to Tailings Dumps 1, 3 and the Leach Pond. The Open Pit is approximately 450m^2 in diameter and contains water at the base.

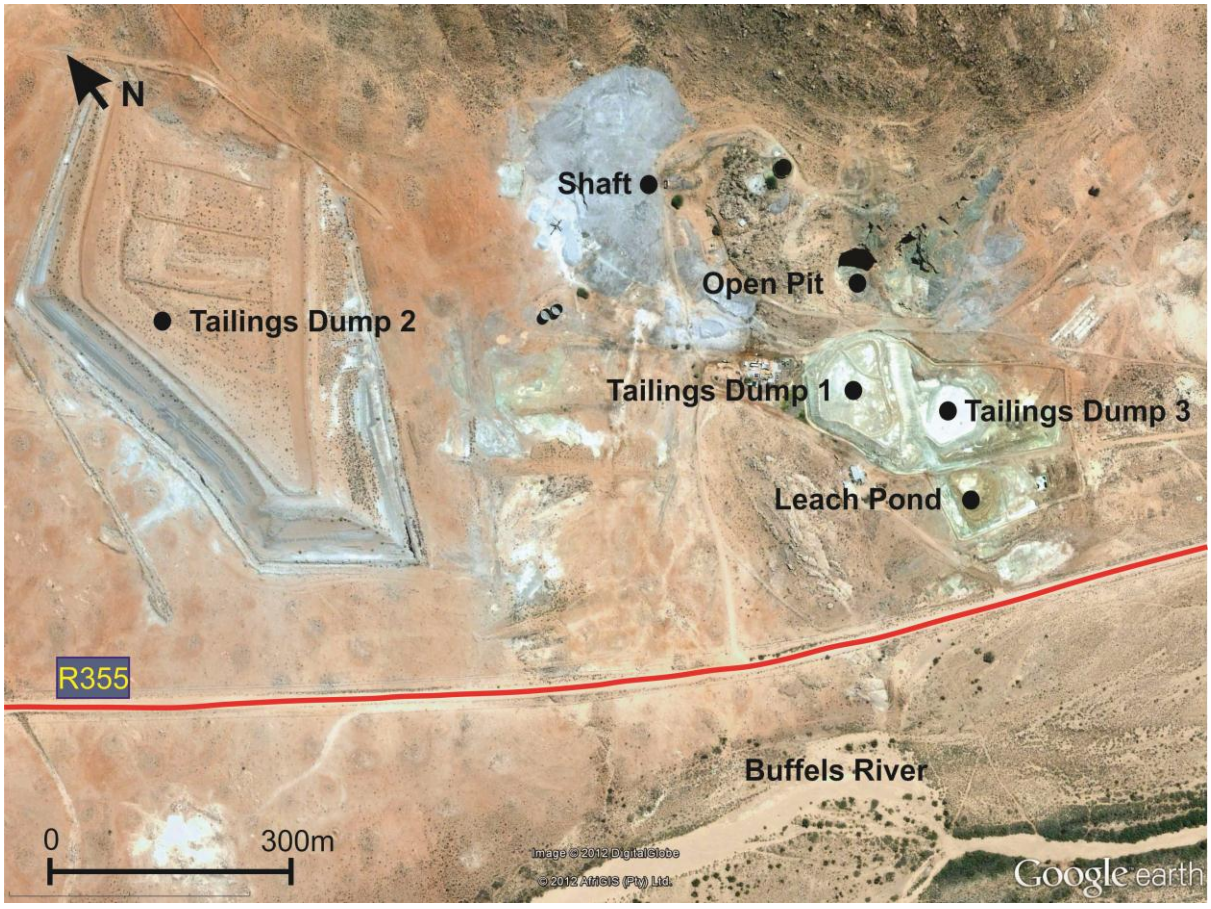

Figure 1.2: Google Earth image of the Spektakel mine site labelling each of the key physical features at the site. The red line indicates the road (R355) that accesses the Spektakel mine and each dot marks a key physical feature at the site.

During its existence, the mine was repeatedly opened and closed as the copper price fluctuated. This is reflected by the fact that the mine has played host to an array of different mining activities, as is evident from the current observations of the site. The Okiep Copper Company (OCC) operated three mills in the area prior to 1975, one at Carolusberg, one at Okiep and another at Nababeep, with a maximum yearly milling rate of 3 million tons during

1971 and 1972 (Gadd-Claxton, 1981). However, the mill at Okiep was closed in April 1975 and relocated to the Spektakel mine site to resuming production in early 1981. Remnants of this milling activity, in the form of poorly covered dump sites and leach ponds are still visible at the site (Gadd-Claxton, 1981).

It is not certain what remediation work was conducted prior to closure. There is evidence to suggest that soil from around the site has been used to cover the tailings material of Tailings Dump 2 (Figure 1.2), in an attempt to rehabilitate the tailings and reintroduce some of the local vegetation. This can be seen on the western side of the tailings where the surface soils have been scraped and underlying calcrete and dorbank subsoil horizons are exposed. This attempt to cover the tailings is inadequate as the tailings are still exposed, allowing material to be blown onto the surrounding land cover, farmland and into the Buffels River.

1.4 Background information of the region and area surrounding Spektakel

1.4.1 Historical overview of the Okiep region

The Okiep Copper District (OCD) is located in the western part of the Namaqua Metamorphic Complex. Exploration of copper by the Namaqua tribes in the OCD predates the arrival of the Dutch Settlers in 1652 (Miller, 1995). By 1661 the trade of copper between these tribes and settlers gave rise to the idea that mineral wealth could be found in this area. The first copper discovered by the Dutch settlers in 1685 was located in the Koperberg area east of current town Springbok. Due to the remoteness and harsh conditions of the area, exploration only began in earnest in the 1840s (Gibson and Kisters, 1996). In 1852 the Okiep District became the first proclaimed mining district in the Namaqualand region. Although the froth flotation process was first patented in 1860, it was only after the 1950s that it reached real efficiency as an extraction method. Thus during this early period hand cobbing was the only means of extracting copper from the easily mineable ores.

During the period of active mining, the district was controlled by the Cape Copper Company (1862-1919) and the Namaqua Copper Company (1888-1931) (Smalberger, 1975) who managed the Nababeep, Okiep and Spektakel mines (Clifford *et al.*, 1975). Mining ended after the closure of the Namaqua Copper Company, but was re-opened by the Okiep Copper Company (OCC) in 1940 (Clifford *et al.*, 1975) until, in the mid-1980's Gold Fields of South Africa took control of OCC (Kisters *et al.*, 1996).

The revival of mining by the OCC in 1940 was accomplished by large scale exploration in an effort to try and find additional minable deposits. To date more than 30 deposits have been mined, ranging in size from 0.2 – 37.5 Mt with grades ranging between 1.71 – 14% Cu (Cairncross, 2004). Total copper production in the district from 1940 till 1998 amounted to

105,6Mt of ore at 1,75% copper. This implies that an enormous quantity of waste material (slimes and tailings) must have been left behind as a legacy of the copper mining. Mining in the OCD finally ceased altogether with the closure of the Carolusberg mine in 1998 (Cairncross, 2004).

1.4.2 Namaqualand

1.4.2.1 Physical landscape

The Namaqualand region is located in the north-west corner of South Africa (Figure 1.1). The Orange River marks the region's northern boundary as well as the international border between South Africa and Namibia. The southern boundary of the region is defined by the Olifants River and Bokkeveld escarpment (Desmet, 2007). Namaqualand forms part of the western escarpment of South Africa and includes the coastal plain, the mountain ranges and the escarpment itself and covers approximately 45 000 km^2 (Desmet, 2007). In general the landscape of the region consists of steep slopes, rock sheets and gravel plains. The inland region is comprised of quartzite mountain complexes and some complex geology consisting mainly of metamorphic and igneous terrains (Desmet, 2007).

1.4.2.2 Geology

The Namaqualand region is characterised by large granite-gneiss domes that contrast with the dominantly flat topography of the surrounding areas, Steinkopf and Bushmanland, to the north and east respectively (Kisters *et al.*, 1996). The area comprises Namaqua-age (1000-1250 Ma) voluminous, stratified, sub-horizontal granite gneisses and granites which intrude and dismember the older granitoid gneisses and metavolcanosedimentary rocks (Benedict *et al.*, 1964; Clifford *et al.*, 1975; Holland and Marais, 1983; Lombaard and The Exploration Department Staff of the O'okiep Copper Company Ltd, 1986). Intrusive into these granite-gneiss successions are dyke- and sill-like structures of the Koperberg Suite (Kisters *et al.*, 1996; Lombaard *et al*, 1986). These bodies are mainly anorthitic and dioritic in composition, although noritic and pyroxenitic varieties of the Koperberg Suite are developed in places (Lombaard *et al*, 1986; Schoch and Conradie, 1990). To the west of the Okiep Copper District the granitic basement is overlain by the late Proteozoic to early Phanerozoic clastic sediments of the Nama Group (Kisters *et al.*, 1996).

To date no literature indicates which primary copper minerals are present at the Spektakel mine. Research conducted on the mines surrounding Spektakel indicates that major sulphide minerals are the dominant primary copper minerals of the Okiep Copper District and consist mainly of bornite, chalcopyrite and chalcocite. Some accessory minerals associated with these ores include vallerite, millerite, niccolite, molybdenite, linnaeite,

melonite, sylvanite, hessite, coloradoite and tetradymite. The main secondary copper minerals observed in the oxidized zones are chrysocolla and subordinate malachite and brochantite (Gadd-Claxton, 1981).

1.4.2.3 Soil

According to the land type survey (Land Type Survey Staff, 1987) the soils on the lower terrain units of the Buffels river valley are comprised of red, shallow, base rich soils. The soils on the foot slope terrain unit (where the actual mine is situated) are comprised mainly of shallow eutrophic Hutton soils while the soils on the valley floor (downslope of the mine) are largely alluvial Dundee soils. Unfortunately no modal profile data is available for the map unit in which Spektakel falls (Land Type Survey Staff, 1987)

The soil surrounding the Spektakel mine consists mainly of red sands. Even though they are described as deep sands there is abundant evidence for differentiation into horizons for example, bleaching, clay elluviation and secondary cementing by silica and carbonate. There is little information available on the Namaqualand soils, making soil studies in this area especially challenging as there is no reference material available (Francis *et al.*, 2007).

The formation of hardpans is a prominent feature in the soils of the Namaqualand soil. Three dominant types of hardpans are found in SA namely dorbank, silcrete and calcrete. These three formations can occur in the same landscape and can form in different erosional surface soil horizons (Ellis and Lambrechts, 1994). These hardpans are a prominent feature in the soil profiles around the Spektakel mine site as is the presence of ancient termite mounds, locally known as “heuweltjies”. These termite mounds occur in the soil as hard circular subsoil features consisting of more alkaline, calcareous and sodic rich soil enriched with silica (Ellis, 2002)

1.4.2.4 Climate and vegetation

Namaqualand is classified as a semi-arid winter rainfall region, (MacKellar *et al.*, 2007) with high diurnal and seasonal temperature ranges. The maximum temperature rarely exceeds 37 °C in the summer whereas sub-zero temperatures can be experienced in the winter months (Hahn *et al.*, 2005). The rainfall in the region is low, 50 - 70 mm per annum on average, with the lowest rainfall figures occurring in the west, near the coast close to Spektakel (Kelso and Vogel, 2007). Contrary to this, the area occasionally experiences extremely wet years, during which the annual precipitation may increase to up to 400 mm (MacKellar *et al.*, 2007).

The climate and topography of the region provide ideal conditions to sustain its unique succulent biome. Recent studies indicate that the flora of the Succulent Karoo is part of the

Greater Cape Floral Kingdom (Desmet, 2007) and is also one of only two desert regions worldwide that is recognised as a global bio-diversity hotspot. The Succulent Karoo contains an estimated 3500 species in 1354 families and 724 genera's of flora covering approximately 25% of Namaqualand (Desmet, 2007).

1.5 Thesis layout

This thesis presents research conducted in an effort to determine the chemical conditions in the soil at the Spektakel mine site that contribute to the formation and dissolution of secondary copper minerals

- This chapter provides an overview of the project describing; the area surrounding Spektakel and the site itself, the position of Spektakel within South Africa, the physical landscape of the region surrounding Spektakel, the history of mining in the area and at the site, and a general overview of the climate and vegetation in the area.

- Chapter 2 provides a detailed description of the analytical techniques performed on the samples collected during the experiments.

- Chapter 3 describes the bulk chemistry and mineralogical characteristics of the soil at the Spektakel site. The chemical composition of solutions in equilibrium with the soil was determined to acquire an understanding of the solubility of the secondary minerals in the event that the soil becomes waterlogged after a rain event.

- Chapter 4 firstly details how the absolute SO_4^{2-} and Cl^- concentration in the soil influence secondary copper mineral formation in the presence of calcite. Secondly it details the chemical evolution, during evaporation, of a solution in equilibrium with the soil at Spektakel both in the presence and absence of calcite to determine how evaporation influences copper mineral formation.

- Chapter 5 describes how increasing acidity and decreasing salinity influence atacamite dissolution.

- Chapter 6 provides an overall discussion which relates the experimental work to the processes occurring within the soil in order to make a deduction regarding the risk that the secondary mineral phases in the soil pose to the environment.

- Chapter 7 concludes the research and suggests further work

2 Analytical techniques

The experiments that follow in the study all make use of the following analytical techniques and equipment. In each of the following chapters reference will be made as to the specific techniques employed for the various analyses. All the techniques are described in full detail in the following section. All the analyses were conducted at Stellenbosch University excluding the X-Ray Diffraction which was conducted at iThemba Labs.

Cation analysis – ICP-AES and ICP-MS

The major cation analysis was conducted using a Varian ICP-AES (Inductively Coupled Plasma - Atomic Emission Spectroscopy) and the trace cation analysis using an Agilent 7700 ICP-MS (Inductively Coupled Plasma - Mass Spectrometer). A quality control standard was analysed prior to the sample runs to verify the accuracy of the calibration standards, while control standards were used throughout the analyses to monitor accuracy and instrument drift. On the ICP-MS, internal standards were continuously introduced with the samples and standards to correct for drift due to high matrix load.

Ion chromatography (IC)

The anion concentrations were analysed using a Metrohm 761 Compact Ion Chromatograph (IC) with a Metrohm Metrosep A Supp 5 - 250/4.0mm Anion Column. To quantify the results each time new eluent was prepared the IC was calibrated with the Fluka range of IC calibration standards. It was calibrated for the following anions, Cl^-, SO_4^{2-}, NO_3^-, PO_4^{3-} and F^- with the following concentration ranges, 0.3 - 30ppm for F^-, PO_4^{3-} and NO_3^- and 1 - 400ppm for Cl^- and SO_4^{2-}.

X-Ray fluorescence (XRF)

X-ray Fluorescence (XRF) analysis was conducted using an Axios from PANalytical with a 2.4kW Rh X-ray Tube. The international (NIST®) and national (SARM®) standards were used in the calibration procedures and quality control (precision and accuracy) for both major and trace element analyses of the XRF. Detection limits for the elements quoted, depending on the matrix (combination of elements present), are approximately 0.5 ppm for trace elements on a pressed pellet and approximately 0.001 wt% for major elements on a fused bead.

X-Ray diffraction (XRD)

XRD analysis was performed at iThemba Labs using a BRUKER AXS (Germany) with a D8 Advance diffractometer and measurement of ϑ-ϑ scan in locked coupled mode. The tube used Cu-Kα radiation at ($\lambda K\alpha_1$=1.5406Å) with a 1600 Channel PSD Vantec-1, Gas detector.

Measurements were conducted at a tube voltage of 40kV, tube current of 40mA with variable slits at V20 and a measurement time of 1 sec/step which is statistically satisfactory. The analysis does not indicate the presence of specific mineral orientations but measures the bulk abundance of all the minerals present, regardless of orientation. It should be kept in mind that XRD analysis is not strictly a quantitative technique and that the results are only semi-quantitative at best.

pH and Electrical conductivity (EC)

The pH measurements were conducted using a Metrohm 905_1 pH Electrode and the EC was measured with a Eutech Instruments CyberScan Series 60 Waterproof EC Meter.

3 Morphological, chemical and mineralogical characteristics of the soil at Spektakel

3.1 Introduction

The Northern Cape province of South Africa has played host to large scale mining activity since the mid 1800's (Cairncross, 2004). Due to the lack of regulations for the disposal of mine waste and the initial primitive mining techniques, some mine sites were abandoned without any rehabilitation. The most prominent problem at these sites is the unlined and exposed sulphide rich mine tailings dumps. One such a site is the derelict Spektakel mine situates at the base of the Spektakel Pass in the Buffels River valley.

The limited research that has been conducted at the site indicates that the tailings and soil surrounding the site contain elevated concentrations of trace metals, especially copper (Hohne and Hansen, 2008). The results of the a fore mentioned study found bulk copper concentrations of up to 6.2 wt% in soil samples collected at Spektakel. The work conducted by Newmark (2010) and Hohne and Hansen (2008) found the secondary copper hydroxyl chloride mineral, atacamite ($Cu_2(OH)_3Cl$), to be present in the soil surrounding the site.

The limited studies performed at the site indicate that extended research is required in order to acquire a more informed understanding of the chemical mechanisms active in the tailings and soil at Spektakel. Research performed at sites similar to Spektakel has found that unlined sulphide rich mine tailings are the main source of acid mine drainage at abandoned mine sites (Vigneault *et al.*, 2001). The presence of these acidic solutions can potentially leach major and trace metals from the tailings into the soil and water bodies around the tailings, constituting a threat to the surrounding environment (Geller *et al.*, 1998).

To date atacamite is the only documented secondary Cu mineral phase in the soil at Spektakel and little is known about the formation of other secondary copper minerals. The aim of this chapter is to characterise the mineralogical and chemical conditions in which these minerals form to determine whether or not atacamite is the only secondary copper mineral present in the soil.

3.2 Materials and methods

3.2.1 Sample description and collection

Sample collection was performed during the dry season (January 2011) at varying distances downslope of Tailings Dump 1 (Figure 3.1).

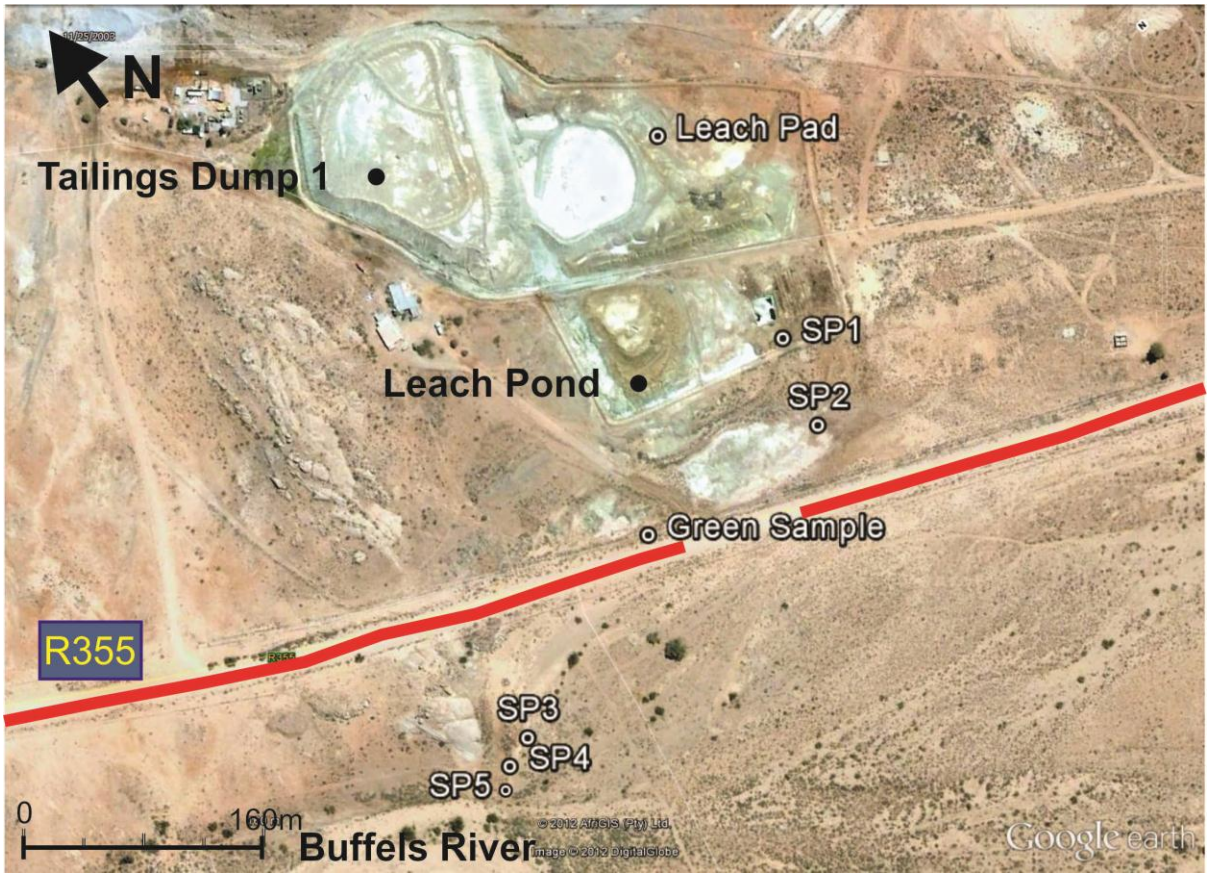

Figure 3.1: Google Earth image indicating the samples collection sites near the Spektakel Mine. The red line indicates the road (R355) that accesses the Spektakel mine. The dots indicate a key physical feature and the sample collection sites.

Sampling sites were chosen based on visible evidence of contamination (salt crusts and/or denuded vegetation). River sediments within the Buffels River (SP3 to SP5) were also sampled (Figure 3.1). Soils were sampled by means of a soil auger and were collected from every identifiable horizon within the soil profiles, to a maximum depth of 1 m. Sample SP1 was collected by Newmark (2010) as part of her unpublished Honours research. Sample SP2 was collected in one of the old leach ponds and samples SP3 to SP5 were collected south of the R355 close to the Buffels River. A green soil horizon was identified and collected adjacent to the R355 (Green Sample). Profile descriptions of the sampled soils were made (Table 3.1) and, where possible, soils were classified according to the South African Soil Classification System (Table 3.1: Soil Classification Group, 1991).

At the time of sampling the leach pond on the tailings dump (Figure 3.2a) was dry, and thus a crust sample of the evaporate salts was collected (Figure 3.2b) in order to determine the composition of water leaching from the dumps. Unfortunately pond solution could not be collected, as no means of storage was available at the time to collect the fluid.

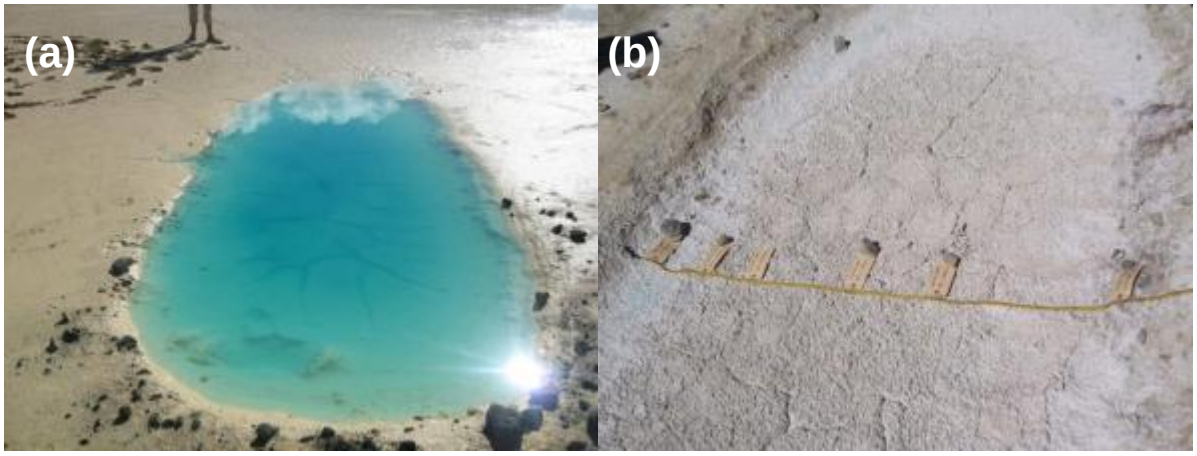

Figure 3.2: a) Acid water ponded on the surface of the tailings dump (photo taken November 2010) and (b) salt crust of the same pond (photo taken January 2011)

The soil and crust samples were placed in plastic bags and sealed to prevent loss of water. Each section was labelled according to the depth at which they were collected. Samples were transported to the laboratory and stored in the refrigerator at 4 °C. The soil samples were sieved through a 2mm sieve, in their field moist condition, to remove any coarse fragments. These sieved samples were placed in air tight containers and refrigerated at 4 °C to try and eliminate moisture loss. All further analyses were conducted on these field moist fine earth fractions (<2mm) correcting for moisture content as discussed below.

3.2.2 Chemical analysis

The salt crust, sampled from the leach pad, was dissolved in MilliQ water using a 1:5 solid liquid ratio. The solution was filtered through 0.2µm GVS Cellulose Acetate Membrane Syringe Filters before analysis.

The moisture content of the soil was determined by weighing off 10g of the field moist sample and drying it at 104 °C for 24 hours. The samples were re-weighing and the moisture loss was calculated. The EC and pH of the soil samples was determined using a 1:2.5 soil to water ratio by adding 10g of soil with known water content and 25ml of DI water in a 50ml centrifuge tube. The samples were shaken for 30 min and left to settle for 10 min before the pH and EC were measured in the supernatant.

A saturated paste was made with the collected soil samples; 200 g of each soil sample was placed in glass acid washed containers and dried overnight at 102 °C. The dried soil

samples were milled in a tungsten carbide mill to help achieve rapid equilibration of the solution with the solid phase. The saturated paste was prepared by adding deionised water to the milled sample until the soil formed a glistening paste. The container and paste were weighed to determine the amount of water added to the soil sample. The container was covered with Parafilm to limit water loss, and left to equilibrate for 24 hours before the fluid was extracted (Sparks *et al.*, 1996). Prior to extraction the EC and pH of the paste were measured (*Refer to Chapter 2*). The solution of each sample was extracted under vacuum, into 50 ml centrifuge tubes through Whatman filter paper using a Buchner funnel. The extracts were filtered a second time through 0.45 µm GVS Cellulose Acetate Membrane Syringe Filters to remove any particles still suspended in the fluid. The alkalinity of the solution extracts were determined by manual titration using 0.001M HCl. The concentration of dissolved silica in the samples was determined colorimetrically following the method of Mortlock and Froelich (1989). The solution samples were analysed for major and trace ions through ICP-MS, ICP-AES and IC analysis (*Refer to Chapter 2*).

3.2.3 Mineralogical analysis

Mineral analysis was performed on dry clay powder extracts and powdered soil samples. The clay extract was prepared on 50g of milled dry soil material. The milled soil samples were suspended in 500ml of deionized water. During continuous stirring the pH was adjusted to just above 9.5 by the drop wise addition of a 2M Na_2CO_3 solution. To aid in the deflocculation of the clay, two drops of calgon (1g hexametephosphate in 100ml deionized water) were added to the solution. The samples were left to settle for 30 min in order to determine whether or not the clay remained deflocculated. If the clay flocculated, the samples were stirred up and more calgon was added until the clay particles remained in a deflocculated state. Once the clay remained in a deflocculated state, the suspension was allowed to settle for 4 hours. The top 5cm (approximately 80ml) of suspension was removed and placed into two 50 ml centrifuge tubes (40 ml in each). The clay suspension was flocculated by adding 10ml of KCl and $MgCl_2$ respectively. The pH of the $MgCl_2$ solution was lowered to 5 using 0.1M HCl to prevent the precipitation of brucite. The samples were centrifuged for 4 minutes at 1500rpm to flocculate the clay particles. The supernatant that remained after centrifuging was decanted and 25ml of the same KCl and $MgCl_2$ solutions was added to the flocculated clay. After the clays had equilibrated with the newly added salt solution the samples were centrifuged for 4 minutes at 1500 rpm. The clay particles were washed repeatedly with 25ml of both deionised water and methanol, the supernatant was decanted and tested for Cl^- using $AgNO_3$ until no more precipitated formed. The samples were washed for a final time with 95% acetone, the clay extracts were dried overnight before it was sent for XRD analysis. (*Refer to Chapter 2*)

The powdered soil samples were prepared by milling dried soil samples by hand in an agate mortar and pestle. Some white and green flecks visible in the soil samples were also collected and milled. All the milled samples were sent for XRD analysis (*Refer to Chapter 2*).

3.3 Results

3.3.1 Soil classification and description

The soil samples collected at the Spektakel Mine (SP) are numbered according to their proximity to the mine, SP1 being the closest and SP5 the furthest (Table 3.1). The sample depth ranges are between 35cm and 120cm with noticeable visual changes occurring along the length of the profiles. No vegetation was present at the sample sites.

During sample preparation green and white mottles were observed in the SP3 B and SP3 C soil horizons. The white mottles were friable, approximately 3mm in diameter and did not react with 10% HCl. The green mottles were more solid, approximately 3mm in diameter and dissolved when reacted with 10% HCl.

The green soil sample that was collected consists of a green soil horizon with a 5cm top soil cover. The total depth of the horizon was not determined; the horizon remained green to a depth of 20 cm (Figure 3.3). The green soil was slightly moist, sandy loam, containing coarse fragments and some green mottles were present.

Figure 3.3: Image of the green soil collected for the Green Sample next to the R355. Geological hammer is 30 cm in length.

Table 3.1: Profile description of sample SP1 to SP5 (descriptions were performed in the field): Each description starts at the soil surface and moves down the soil profile. Descriptions were performed according to the South African Soil Classification Guideline (Soil Classification Group, 1991).

Horizon		Depth (cm)	Description	Diagnostic Horizon	Form
SP1	**A**	0-7	Slightly Moist, Yellow Brown, Fine Sandy Loam, Apedal, Slightly Friable, No Reaction With HCl, Abrupt Transition.	Orthic A	Witbank
	B1	7-17	Slightly Moist, Green, Fine Sandy Loam, Friable, Pure Aggregates (Green slightly striated aggregates with some yellow zones) No Reaction with HCl. Gradual Transition.		
	B2	17-27	Moist, Brown, Loam/Clay, Apedal, Slightly Friable, Slight Reaction With HCl, No Green Mottles in soil material	Manmade soil deposit	
	B3	27-37	Moist, Brown, Fine Sandy Loam, Apedal, Loose, Abrupt transition, Strong Reaction With HCl.		
SP2	**A**	0-5	Dry, Yellow Brown, Silty Clay, Massive, Brittle Consistency, Few Green Mottles, Abrupt Transition, No Reaction with HCl.	Orthic A	Hutton/Witbank
	B	5-40	Slightly Moist, Red Brown, Sandy Loam, Apedal, Loose, Black Lenses, Small Green mottles, Large Course Fragments, Root Fragments, No Reaction with HCl.	Red Apedal B/ Man made deposit	
SP3	**A**	0-15	Slightly Moist, Moist Brown, Silty Clay, Very Fine - Sub-Angular Blocky, Slightly Friable, Thin Clay Layers, Depositional, Many White Salt Flakes, No Reaction with HCl.	Orthic A	Dundee
	B	15-30	Slightly Moist, Light Green, Sandy Loam, Apedal, Loose, Few White Salt Lenses, Green Mottles, No Reaction with HCl.	Stratified Alluvium	
	C	30-35	Slightly Moist, Light Green, Sandy Loam, Apedal, Loose, Few White Salt Lenses, Green Mottles, Reacted with HCl.		
SP4	**A**	0-24	Slightly Moist - Moist, Silty Clay/Loam, Apedal, Loose	Orthic A	Dundee
	B	24-67	Moist, Brown, Clay, Friable, Fine Angular Blocky, Yellow Mottles, Few Glade Mottles, Few Orange Mottles, No Reaction with HCl.		
	C	67-94	Moist, Yellow/Orange/Brown, Sandy Loam, Apedal, Friable/Loose, Many Gravel Fragments, No Reaction with HCl.	Stratified Alluvium	
SP5	**A**	0-20	Dry, Light Brown, Coarse/Medium , No Reaction with HCl.Sand, Apedal, Loose, Fine and Course Fragments, Few Roots	Orthic A	Dundee
	B	20-35	Slightly Moist, Yellow Brown, Fine Angular Blocky, Sandy Clay, Apedal, Loose, Few Fine Roots, Clay Lenses, No Reaction with HCl.		
	C	35-57	Slightly Moist, Yellow Brown, Sandy Loam, Apedal, Loose, Few Roots, Large Clay lenses, Possible Green Lenses, No Reaction with HCl.	Stratified Alluvium	
	D	57-92	Slightly Moist, Orange Brown, Sandy, Apedal, Loose, Some Very Coarse Fragments, No Reaction with HCl.		
	E	92-120	Wet, Yellow Orange, Sandy, Apedal, Loose, Free Water		

3.3.2 Soil chemistry

3.3.2.1 Bulk chemical composition of the soil surrounding the Spektakel mine tailings

As a comparison, the bulk trace element concentrations are displayed alongside the Dutch Soil Standard Guideline (DSSG) (Table 3.3). To date the Dutch Soil Standard Guidelines (DSSG) is the most comprehensive set of soil screening guidelines available (Dutch Soil Screening Guidelines, 2009). The results indicate that the most abundant major ions in the soil are SiO_2>Al_2O_3>K_2O>Fe_2O_3>CaO>=MgO>=Na_2O (Table 3.2) and the most abundant trace elements are Cu>S>Ba>Sr>Rb>Cr (Table 3.3). The CaO, MgO and Na_2O concentrations vary in each of the soil profiles. In some cases the MgO concentration exceeds the Na_2O and CaO concentration and in other cases vice versa (Table 3.2). The Na_2O concentration is most elevated in the top horizons of the soil profiles and decreases moving down the profile.

The highest Cu concentrations are in samples SP1 B1, SP1 B2 and SP2 A, however Cu is elevated relative to the DSSG in all the horizons of each soil profile (Table 3.3). The Cu concentration in SP1 increases abruptly moving from the A to B horizon and decreases further down the profile. A decrease in Cu is observed in sample SP2 A moving down the profile and the same decrease is again observed in SP3. The Cu concentration in sample SP4 increases moving down through horizon SP4 A and SP4 B and decreases at SP4 C.

The change in S concentration defines two different trends in the soil profiles. In sample SP2 and SP4 the S concentration decreases moving down the profile and in SP3 the S concentration increases moving down the profile (Table 3.3). The Cr concentration only exceeds the DSSG in SP1 B1 and SP4 B (Table 3.3).

Table 3.2: Bulk major elemental composition of each soil horizon collected down soil profiles SP1 to SP4. Data from sample SP1 was collected by (Newmark, 2010)

Sample	Horizon	Depth (cm)	Al_2O_3	CaO	Cr_2O_3	Fe_2O_3	K_2O	MgO	MnO	Na_2O	P_2O_5	SiO_2	TiO_2	LOI	H_2O	SUM
			Concentration (wt%)													
SP1	**A**	0-7	11.97	1.71	0.01	2.79	4.60	1.55	0.06	2.00	0.15	68.51	0.51	4.73	0.80	99.40
	B1	7-17	13.05	5.16	0.04	5.82	3.45	2.80	0.08	2.07	0.66	55.70	0.54	8.06	0.70	98.13
	B2	17-27	12.03	1.97	0.01	3.00	4.48	1.73	0.06	1.89	0.16	63.96	0.44	6.92	1.99	98.63
	B3	27-37	12.78	2.63	0.01	3.73	4.23	2.77	0.07	1.81	0.19	63.03	0.54	6.45	1.08	99.30
SP2	**A**	0-5	13.68	1.66	-	4.52	3.90	1.66	0.14	1.84	0.18	59.92	0.68	9.94	2.15	100.28
	B	5-40	12.24	1.57	0.01	2.83	4.75	0.87	0.10	1.94	0.17	69.75	0.42	3.94	0.96	99.55
SP3	**A**	0-15	13.62	4.58	0.02	6.70	3.02	2.40	0.12	2.46	0.24	51.32	0.80	14.15	2.51	101.94
	B	15-30	11.32	3.76	-	3.04	4.04	1.04	0.08	1.68	0.12	62.48	0.52	9.53	2.26	99.87
	C	30-35	10.44	6.92	-	2.78	3.56	1.28	0.06	1.76	0.12	56.58	0.44	15.02	3.00	101.96
SP4	**A**	0-24	15.12	2.15	0.02	6.02	3.31	1.98	0.15	2.34	0.19	55.96	0.81	11.70	2.19	101.94
	B	24-67	16.14	1.36	0.04	9.70	3.28	2.62	0.10	1.36	0.28	55.32	0.88	9.59	1.09	101.76
	C	67-86	15.13	1.05	0.02	9.55	3.50	2.11	0.07	1.55	0.26	55.95	0.91	9.26	2.04	101.40

Table 3.3: Bulk trace elemental composition of each soil horizon collected down soil profiles SP1 to SP4 displayed along the Dutch Soil Standard Guidelines (Dutch Soil Screening Guidelines, 2009) Data from sample SP1 was collected by (Newmark, 2010)

		Depth (cm)	V	Cr	Co	Ni	Cu	Zn	Ga	Rb	Sr	Zr	Nb	Ba	Ce	Pb	Th	U	S
Sample	**Horizon**	**Concentration (mg/kg)**																	
SP1	**A**	0-7	54	44	67	29	4175	48	14	218	198	236	13	647	135	38	46	8	-
	B1	7-17	85	249	88	206	20335	131	18	157	500	163	8	819	181	39	26	11	-
	B2	17-27	53	56	42	37	14442	64	13	208	210	184	9	511	115	42	34	10	-
	B3	27-37	65	43	60	28	3123	62	16	205	200	198	13	617	137	40	46	8	-
SP2	**A**	0-5	107	89	79	80	11389	271	17	217	163	284	17	595	138	52	41	14	7841
	B	5-40	55	54	51	53	6770	104	15	220	209	337	12	698	88	81	44	15	3836
SP3	**A**	0-15	84	146	31	71	2972	113	18	178	439	194	17	357	106	38	39	12	13050
	B	15-30	61	52	32	16	1579	50	14	198	249	310	13	556	92	40	43	11	16546
	C	30-35	52	50	30	18	1293	44	13	174	257	260	12	446	75	29	32	12	32104
SP4	**A**	0-24	115	126	40	66	2222	163	20	211	169	234	20	484	160	43	41	13	6523
	B	24-67	163	282	57	85	3841	133	23	206	217	180	20	602	162	42	43	17	4945
	C	67-86	172	153	59	60	3419	113	22	239	173	216	23	600	164	37	47	19	3333
DSSG		-	250	180	190	100	190	720	-	-	-	-	-	-	-	130	-	-	-

3.3.2.2 The chemical composition of solutions in equilibrium with the soil (saturated paste extract) and the fluids of the tailings ponds

The EC of the soil solutions decreases down each of the soil profiles (Table 3.4) with similar decreases being observed in the samples moving away from the mine site. The pH of the soil falls largely in the circumneutral range with the exception of SP2 A (4.87). The abundance of the soluble major elements follows a similar trend in most of the profiles with $Cl^{-}>SO_4^{2-}>Na^{+}>Mg^{2+}>Ca^{2+}>K^{+}>NO_3^{-}$ (Table 3.4). The Cu^{2+} concentration in SP2A (2.95 mmol/l) is elevated compared to the other soil horizons, which have Cu^{2+} concentrations between 0 and 0.04 mmol/L. The Cl^{-}, Na^{+}, SO_4^{2-} and Mg^{2+} concentrations are highest in the A horizon of SP1-SP4 decreasing in concentration down the profile, while the concentrations of these same elements vary with depth in the SP5 profile. The alkalinity of the samples is low. The concentration of dissolved salts decreases with distance away from the site in the direction of the Buffels River.

The chemical composition of the solution comprised of the redissolved leach pad crust indicates that the solution in the ponds on the surface of the tailings contained a range of soluble major and trace elements, $SO_4^{2-}>Mg^{2+}>Cu^{2+}>Mn^{2+}>Na^{+}>Cl^{-}$ (Table 3.5). The Na^{+} and Cl^{-} concentration of this solution is depleted relative to the equilibrium soil solutions. The Cu^{2+} concentration in the solution exceed the Cu^{2+} concentration of the equilibrium soil solution to a large extent.

Table 3.4: Chemical composition of the solution in equilibrium with soil (saturated paste extract) of samples SP1 to SP5. The elemental concentrations of the solutions are expressed in mmol/l

Profile	Horizon	Depth (cm)	EC (mS/cm)	pH	Soluble ion concentrations (mmol/l)											
			1:2.5 Solid Soil Solution		Silica	HCO_3^-	Ca^{2+}	Mg^{2+}	Na^+	K^+	Cl^-	SO_4^{2-}	NO_3^-	F^-	Cu^{2+}	Mn^{2+}
SP1	A	0-7	38.91	6.83	0.25	0.31	13.46	67.04	86.97	13.89	96.96	71.73	0.66	0.25	0.01	0.03
	B1	7-17	26.8	6.51	0.27	0.27	14.68	36.22	45.20	9.66	50.02	41.28	0.10	0.11	0.01	0.02
	B3	27-37	25.65	7.59	0.39	0.43	24.33	35.27	46.48	9.04	35.13	53.85	0.06	0.23	0.00	0.00
SP2	A	0-5	20.93	4.87	1.10	0.17	23.05	223.37	247.21	15.28	495.51	142.54	0.26	1.66	2.95	14.96
	B	5-40	3.73	6.23	0.36	0.35	16.49	34.85	24.84	5.84	27.45	52.06	0.22	0.07	0.03	2.94
SP3	A	0-15	29.03	7.23	0.17	0.40	40.30	134.36	651.32	7.67	810.04	62.39	0.37	0.39	0.01	0.22
	B	15-30	11.11	7.68	0.40	0.65	25.21	39.48	203.31	3.61	218.00	43.79	0.13	0.72	0.00	0.06
	C	30-35	12.07	7.84	0.41	0.85	29.86	47.90	231.87	3.86	296.51	49.54	0.15	0.47	0.00	0.02
SP4	A	0-24	21.05	6.75	0.33	1.30	41.21	132.13	349.35	7.54	568.23	54.21	0.00	0.17	0.04	2.13
	B	24-67	3.56	5.39	0.94	0.25	20.14	13.38	38.01	2.68	36.37	28.72	0.48	0.02	0.04	0.35
	C	67-86	3.25	5.18	1.01	0.37	7.44	10.35	41.48	2.70	45.26	11.54	0.23	0.00	0.02	0.05
SP5	A	0-20	1.587	7.24	0.18	1.30	6.64	8.08	58.10	0.48	64.09	6.69	0.15	0.16	0.00	0.01
	B	20-35	2.3869	6.62	0.16	0.37	9.43	12.39	74.98	0.49	94.33	7.47	0.19	0.09	0.00	0.01
	C	35-57	6.625	5.04	0.37	0.21	9.23	12.37	80.72	0.74	102.88	6.98	0.22	0.03	0.03	0.04
	D	57-92	0.79	6.07	0.11	0.30	2.33	2.98	29.40	0.32	28.09	2.56	0.10	0.15	0.00	0.00
	E	92-120	3.283	6.37	0.07	0.57	11.16	18.61	120.94	0.79	156.16	9.10	0.08	0.08	0.00	0.05

Table 3.5: Solution composition of the redissolved tailings crust (LP). The elemental concentration of the solutions are expressed in mmol/l

	pH	Silica	Ca^{2+}	Mg^{2+}	Na^+	Cl^-	SO_4^{2-}	NO_3^-	F^-	Cu^{2+}	Mn^{2+}
	Concentration (mmol/l)										
LP	4.46	0.25	12.52	276.33	11.58	21.48	381.16	0.08	5.68	90.20	12.56

3.3.3 Mineralogical composition of the soil surrounding the Spektakel mine

A mineralogical study was performed on milled whole soil samples (Figure 3.4a and Figure 3.4b), dried clay extractions (Figure 3.5) and the green soil and mottles collected in the soil profiles (Figure 3.6 and Figure 3.7). Some of the peaks in the whole soil samples and clay extract could not be identified.

The whole soil samples (Figure 3.4) contain elevated quartz concentrations which tend to mask the other smaller mineral peaks. The dominant primary mineralogy, however, remained identifiable, being made up of quartz, micas (biotite, muscovite) and feldspars (albite, microcline). The secondary minerals present are halite, gypsum, anhydrite, bassanite, kaolinite and atacamite. The gypsum concentration is elevated in the SP3 soil profile and the A horizon of SP2 relative to the other profiles. Halite is elevated in the surface horizons of the soil profiles. The copper hydroxy chloride mineral atacamite ($Cu_2(OH)_3Cl$) is observed in SP1 B1 and SP2 A.

The clay extraction aids in the interpretation of the XRD analysis by minimizing the masking effect the quartz peak has on the other mineral peaks. The XRD analysis of the clay fraction (Figure 3.5) indicates that the clay fraction has a mineral composition similar to that of the whole soil fraction, although an increase in calcite abundance is observed moving down the profiles. The abundance of calcite in SP2 and SP4 is reduced compared to SP3. The results obtained from the clay fraction indicate that kaolinite is the major secondary clay mineral.

In the case of the mottles only the peaks relevant to the mottles were identified (Figure 3.6 and Figure 3.7). The green mottles (Figure 3.6) were identified as atacamite. The soil of the green horizon was found to consist mainly of atacamite type minerals and the white fleck collected from the SP3 B soil profile (Figure 3.7) consists of the gypsum ($CaSO_4 \cdot 2H_2O$) and bassanite ($2CaSO_4 \cdot H_2O$).

The black dashed lines on the XRD patterns (Figure 3.4a, Figure 3.4b and Figure 3.5) indicate the position on the graphs where the brochantite peak would be expected. As can be seen, neither brochantite, nor any other copper sulphate minerals were identified in any of the soil samples.

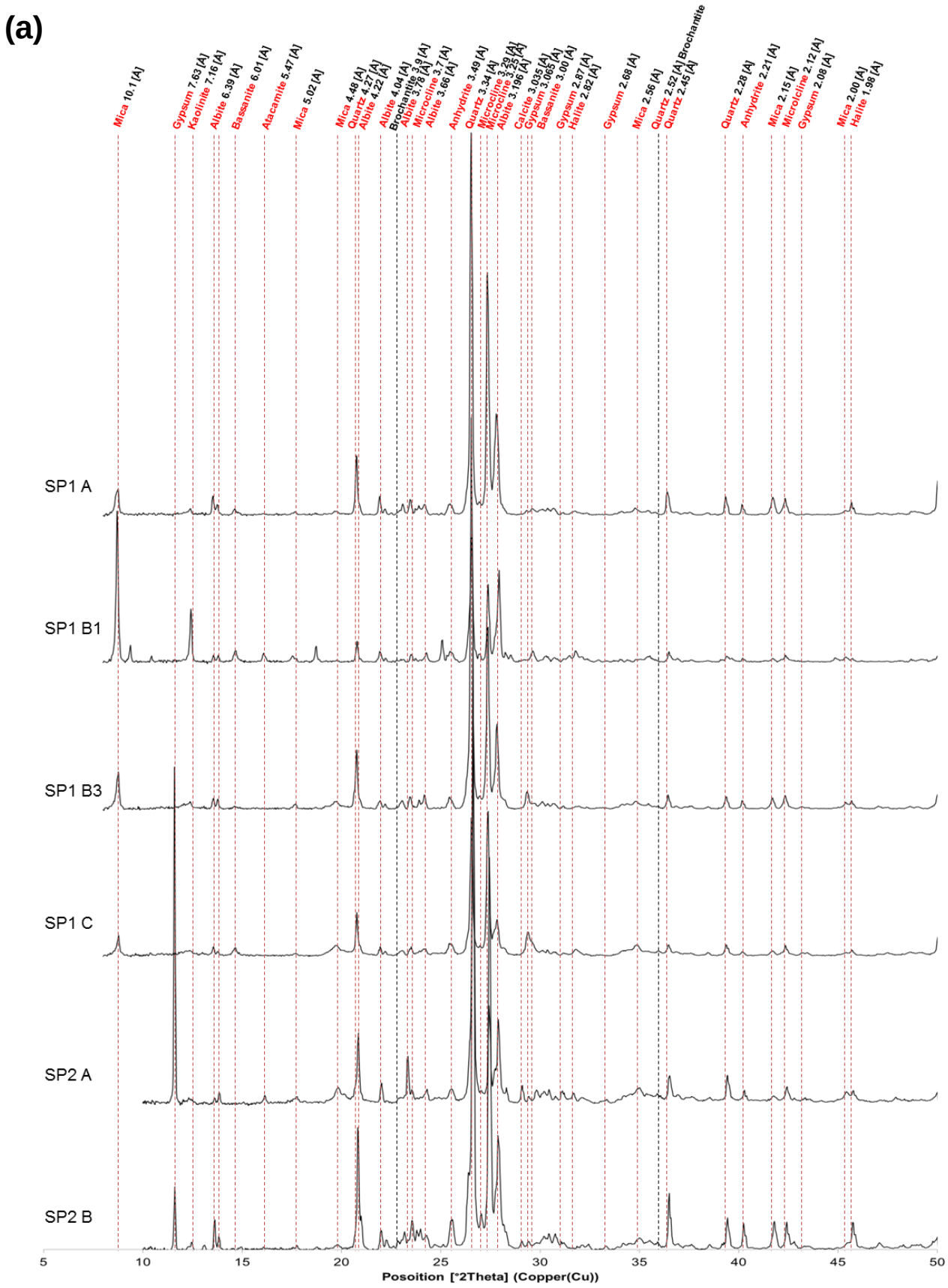

Figure 3.4: Powder XRD patterns of each horizon in sample SP1 to SP2. The red dashed lines indicate the dominant peaks of each mineral identified, along with their d-distance value and mineral name. The absent brochantite peak positions are indicated with black dashed lines.

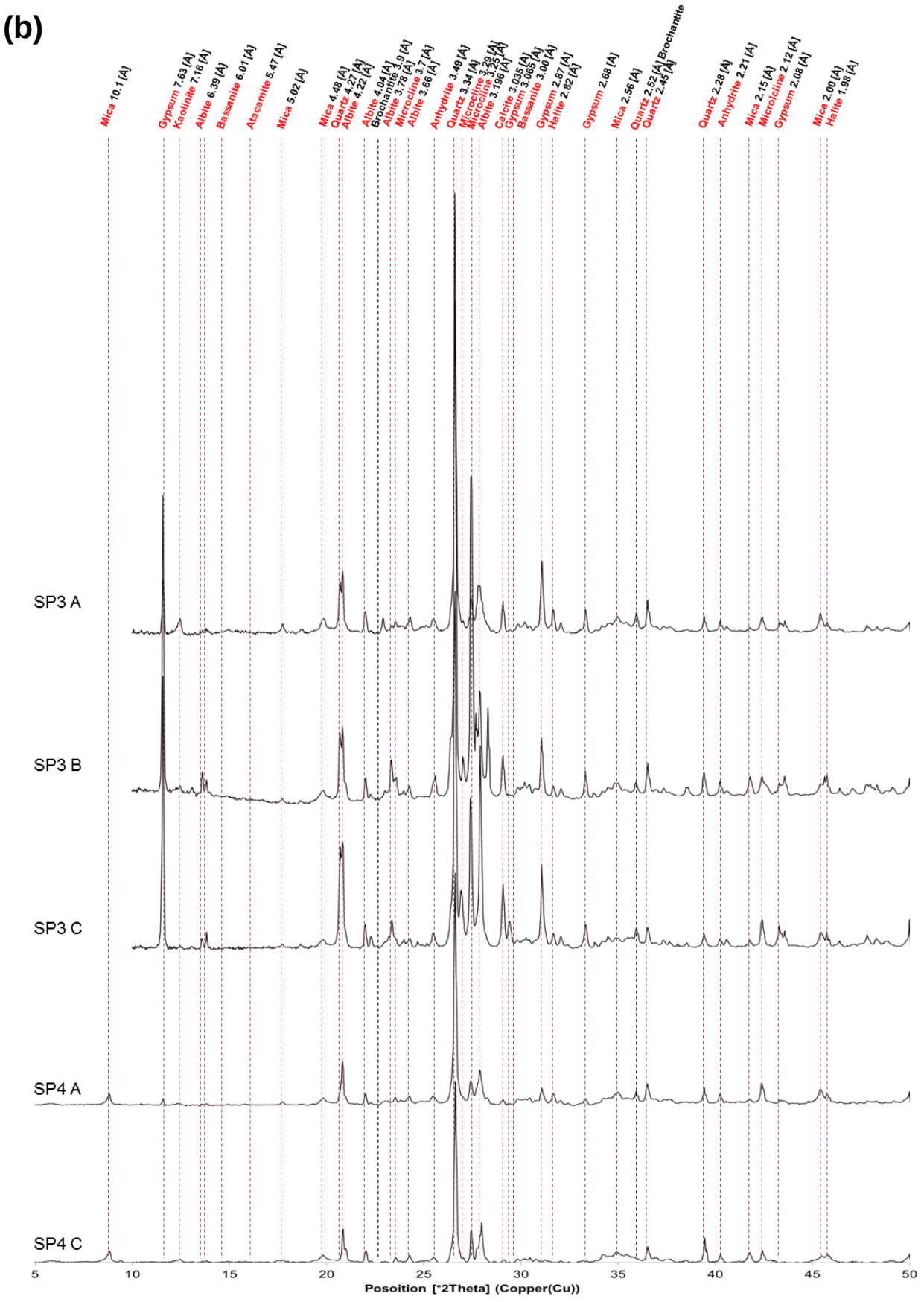

Figure 3.4 (Continued): Powder XRD patterns for SP3 and SP4. The red dashed lines indicate the dominant peaks of each mineral identified along with their d-distance value and mineral name. The absent brochantite peak positions are indicated with black dashed lines.

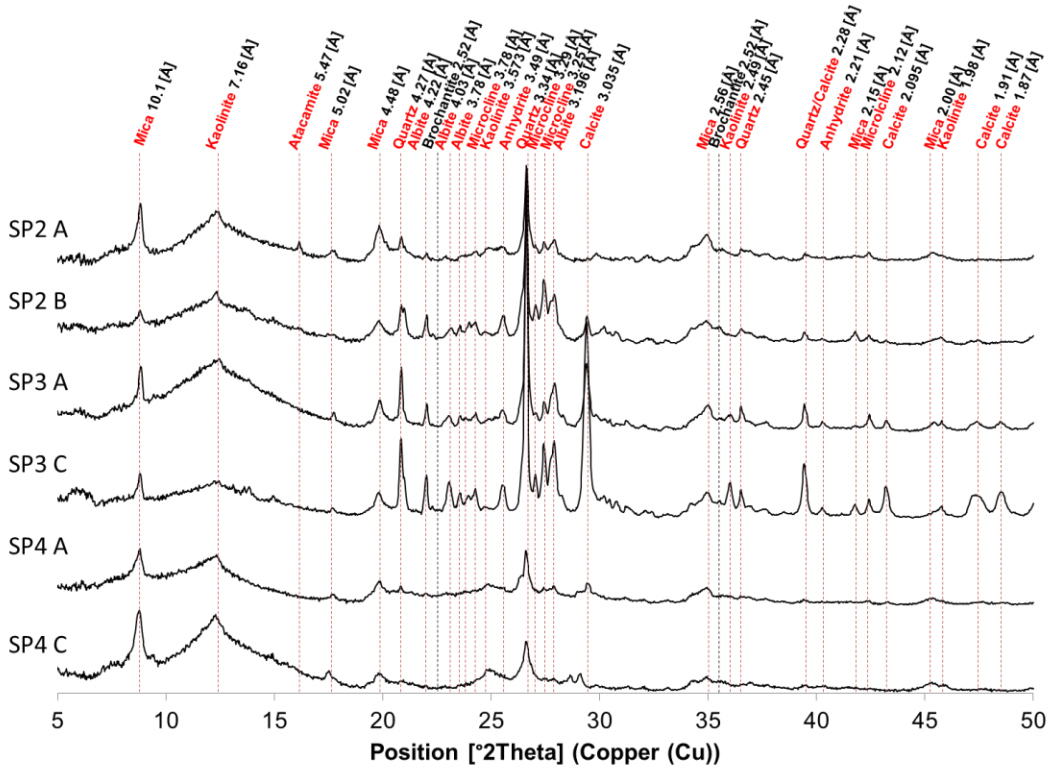

Figure 3.5: XRD patterns of clay extracts from profiles SP2, SP3 and SP4. The red dashed lines indicate the dominant peaks of each mineral identified, along with their d-distance value and mineral name. The absent brochantite peaks are indicated with black dashed lines.

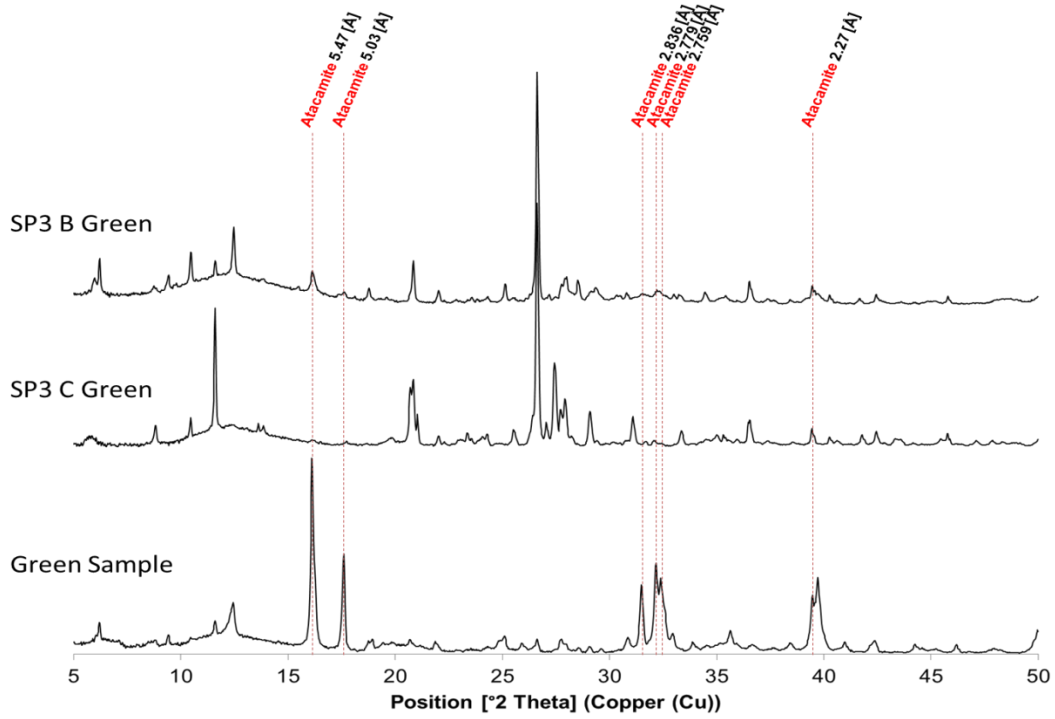

Figure 3.6: The XRD pattern of the green mottles collected in the B and C horizons of the SP3 soil profile is compared to the XRD pattern of the green soil collected in the Green Sample. The red dashed lines indicate the dominant peaks of each mineral identified along with their d-distance value and mineral name.

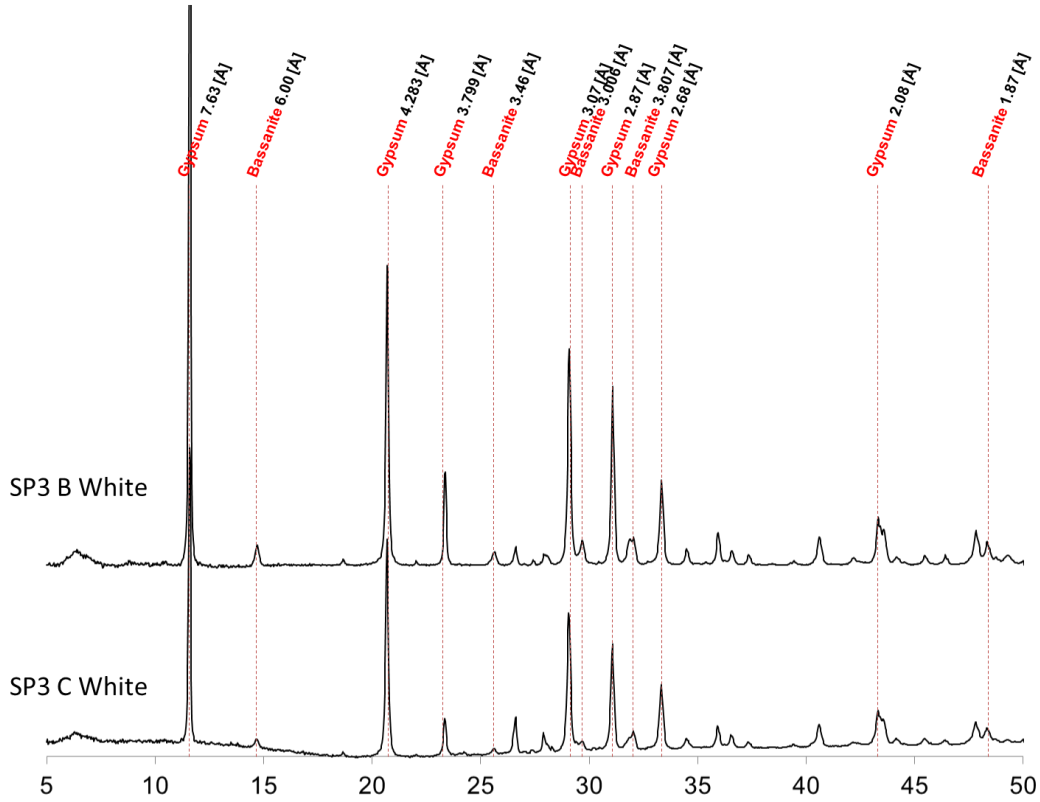

Figure 3.7: XRD patterns of the white mottles in collected in horizon B and C in the SP3 soil profile. The red dashed line indicates the dominant gypsum and bassanite peaks identified along with their d-distance value and mineral name.

3.4 Discussion

The soil samples in the area immediately surrounding the mine (profiles SP1 and SP2) are highly heterogeneous and show signs of disturbance. These soils are therefore best classified as Witbank soils (containing a manmade soil deposit).The soil samples outside the perimeter of the mine (SP3 to SP5) show clear clay and sand stratifications, inferring these soils are relatively young alluvial soils (Dundee soils).

The bulk chemical analysis of the soil indicates that the soil contains high concentrations of both major and trace elements (Table 3.2 and Table 3.3). These elements could either be present as primary and secondary minerals or bound to the soil structure through cation exchange or chemisorption. In this study the focus is to determine the secondary mineral phases retaining these elements in the soil.

The results of the soil characterization indicate that the mining activity at Spektakel has been the major factor influencing the evolution of the chemistry of the soil surrounding the site. In addition, during the time of mining, water from the Buffels River was used in the processing of ore (A. Rozendaal, .Pers. Comm). Analysis done on the Buffels River water indicates that its water comprises of 97.99-164.01 mg/l Na^{+}, 19.88-33.12 mg/l Mg^{2+}, 348.87-339.8 mg/l Cl^{-} and 0.04-0.085 mg/l Cu^{2+} (Hohne and Hansen, 2008). The highly evaporative conditions of this arid area resulted in the accumulation of these elements in the topsoil surrounding the site. This is indicated by the elevated bulk concentration of NaO (Table 3.2) and the elevated soluble Na^{+} and Cl- concentrations of the equilibrium soil solutions (Table 3.4).

The unlined and exposed copper sulphide rich tailings dumps that were produced during the ore processing have been identified as the main distributors of large quantities of Cu^{2+} into the soil surrounding site. Studies performed on sites similar to Spektakel, indicate that that Cu^{2+} concentrations in the soil surrounding the tailings dumps can range between 300 and 4000 mg/kg (Antonijević *et al.*, 2012; Kelm *et al.*, 2009). These observations correlate with the Cu^{2+} concentrations present at Spektakel. The bulk Cu^{2+} observed in the soil at Spektakel is present in concentrations which exceed the intervention value of 130 ppm Cu^{2+} prescribed by the DSSG guidelines (Table 3.3) (Dutch Soil Screening Guidelines, 2009). This elevated concentration of Cu^{2+} in the soil could become a health risk for the plant life and the inhabitants surrounding the site if it becomes mobilized. It has been reported that elevated Cu^{2+} concentrations are toxic to humans (Brewer, 2010; Davis and Mertz, 1987), animals at concentration higher than 4000 ppm (Davis and Mertz, 1987) and plants (Balsberg Pahlsson, 1989; Fernandes and Henriques, 1991).

Preliminary soil analysis performed by Hohne and Hansen (2008) provide an indication of the background chemical composition of the soil in the region. This data indicates a mean Cu^{2+} concentration of 6.2mg/kg. The 25th percentile is 24 mg/kg, while the 75th percentile is 49 mg/kg. This indicates that the Cu^{2+} concentration in the soil surrounding the tailings dumps at Spektakel exceeds the regional background concentration by a significant amount.

The solution analysis of the redissolved tailings crust (Table 3.5) emphasizes the contribution the tailings dumps make to the total Cu^{2+}, SO_4^{2-} ,Mg^{2+} and other trace metals present in the soil. During rain events exposed sulphate and copper salts, at the surface of the tailings, dissolve forming acidic Cu^{2+}, SO_4^{2-} and Mg^{2+} rich solutions (Table 3.5). The elevated concentrations of Cu^{2+} and SO_4^{2-} present on the tailings, (Table 3.3 and Table 3.5) are the remnants of unprocessed copper sulphide minerals. These exposed minerals are oxidized over time, leaving the tailings laden with mobile copper and sulphate:

$$Cu_2S + 4H_2O \rightarrow 2Cu^{2+} + SO_4^{2-} + 4H^+ \quad \text{[Eq 1]}$$

The oxidation of these sulphide minerals produces acid mine drainage (AMD) solutions in the tailings, thus acidifying both the soil as well as the tailings (Akcil and Koldas, 2006). These solutions migrate through the tailings, dissolving the soluble salts present in the soil and accumulating Cu^{2+}, SO_4^{2-} and Mg^{2+} (along with Na^{2+}, Cl^- and K^+) in the surface horizons of the soil surrounding the site (Table 3.4).

Despite the addition of acidity, when the soil is placed in equilibrium with water, the results indicate that the pH of the soil solution is circumneutral and the mobile Cu^{2+} concentration is as low as 0.02 mmol/l (Table 3.4) in some cases. The circumneutral pH is achieved by the dissolution of calcite (Figure 3.5) as the acidic tailings solution migrates through the soil and reacts with calcite. The addition of hydroxyl and carbonate groups absorbs the excess protons, buffering the solution to a neutral pH.

$$CaCO_{3\,Calcite} + H^+ \rightleftharpoons Ca^{2+} + HCO_3^{2-} \quad \text{[Eq 2]}$$

$$HCO_3^{2-} + H_2O \rightleftharpoons H_2CO_3 + OH^- \quad \text{[Eq 3]}$$

In conjunction with this the solutions that move through the soil dissolve the soluble salts, depleting the topsoil of soluble ions especially Cl^-. Both the equilibrium solution data (Table 3.4) and the XRF data (Table 3.2 and Table 3.3) indicate a decrease in elemental concentration moving down the soil profiles. The same depletion is observed in the samples further away from the site (Table 3.4).

The most noticeable result observed in the soil solutions, is that the Cu^{2+} and Cl^- concentrations (Table 3.4) differ from the tailings pond solutions (Table 3.5). Compared to the leach pond solution the soil solutions have an elevated Cl^- concentration and a reduced

Cu^{2+} concentration (Table 3.4). The mineralogy of the soil provides an indication of which mineral phases these elements are bound to.

The bulk mineralogical analysis of the soil samples (Figure 3.4a and Figure 3.4b) indicates that the mineralogy of the soil correlates with the mineralogy of the granite-gneiss domes of the Koperberg Suite (Schoch and Conradie, 1990). This indicates that the weathering of these granite-gneiss domes is the main contributor to the mineralogy of the soil. Apart from the presence of kaolinite (Figure 3.5), a secondary clay mineral produced by the weathering of the feldspar in the soil (Espejo *et al.*, 1993), the clay phase is predominantly dominated by primary minerals. This suggests that there has been minimal weathering of primary minerals to secondary minerals. This low abundance of clay minerals reduces the capacity of the soil to sequester contaminants on cation exchange sites. This indicates that the Cu must be bound to secondary Cu mineral phases.

The secondary minerals present in the soil are dominated by the evaporate minerals halite, calcite, gypsum and bassanite (Figure 3.5). The abundance of halite correlates with the elevated concentrations of soluble Na^{2+} and Cl^{-} present in the soil (Table 3.4). The presence of gypsum is expected due to the elevated SO_4^{2-} and Ca^{2+} concentrations introduced by the tailings and calcite in the soil respectively. The calcite abundance increases down the soil profiles which indicate that the acid mine solutions are dissolving the calcite and lowering the buffer capacity of the soil.

Currently no literature indicates which primary copper minerals are present at the Spektakel mine site. However research performed on the mines surrounding Spektakel indicates that the dominant primary copper minerals in the area are bornite, chalcopyrite and chalcocite. These sites also contain variable quantities of pyrrhotite, pyrite, galena and sphalerite (Gadd-Claxton, 1981). None of these primary minerals were observed in the soil surrounding the Spektakel mine (Figure 3.4a, Figure 3.4b, Figure 3.5), only secondary copper minerals were present. The main secondary Cu^{2+} mineral observed in the soil surrounding the site is atacamite. Atacamite is a common secondary Cu^{2+} phase first described in the weathered portions of sulphide deposits in the arid Atacama Desert and is also found in chloride rich environments such as the modern seafloor (Hannington, 1993). The atacamite in the soil occurs dominantly in the top horizons of the soil profiles (Figure 3.4a, Figure 3.4b and Figure 3.5). Atacamite is known to form through the replacement of calcite in a copper chloride rich solution (Garrels and Stine, 1948). This instantaneous reaction removes most of the copper from the solution preventing further migration though the soil profile. As the calcite is dissolved through atacamite formation more atacamite will form and copper will be able to migrate deeper into the soil profile.

The most striking aspect about this observation is that atacamite is the only secondary Cu^{2+} mineral observed at the site and that no secondary copper sulphate mineral was identified (Figure 3.5, Figure 3.6 and Figure 3.7). This does not correlate with the site characteristics, as the tailings solutions are dominated by Cu^{2+} and SO_4^{2-} indicating that some form of copper sulphate mineral would be expected to be present in the soil.

3.5 Conclusion

The aim of the chapter was to characterise the chemistry of the tailings ponds solution and the soil surrounding the tailings dumps at the Spektakel mine. Analysis of the tailings solution indicates that the solution is acidic and contains elevated Cu^{2+}, SO_4^{2-} and Mg^{2+} concentrations with little soluble Cl^-. The bulk chemical analysis of the soil indicates that the soil contains elevated major and trace metals, mainly SO_4^{2-}, Cl^- and Mg^{2+}, with a bulk Cu^{2+} concentration exceeding the DSSG intervention value. These elements accumulate in the top soil through evaporation as a result of the arid climate of the area. The equilibrium soil solution data indicates that when the soil becomes waterlogged after a rain event, the salts in the top soil dissolve enriching the solution with respect to SO_4^{2-}, Cl^- and Mg^{2+} at a circumneutral pH. Only a small amount of Cu^{2+} is dissolved in the equilibrium soil solution compared to the tailings pond solution. This indicates that despite the high Cu^{2+} concentration in the leachate water, the majority of the Cu^{2+} is retained in the soil. The mineralogical data of the soil indicates that the soil contains a range of primary minerals and secondary evaporate minerals. From this data it was concluded that atacamite is the only secondary copper mineral in the soil surrounding the tailing, as no brochantite was observed.

The mineralogical data indicates that the soil is enriched in calcite, the dissolution of this calcite results in the circumneutral pH of the soil. This same pH effect contributes to the formation of atacamite through the replacement of calcite. This precipitation of atacamite through the dissolution of calcite stabilizes the mobile Cu^{2+} fraction preventing it from moving through the soil profile. In order to acquire a better understanding of the longevity of this Cu^{2+} retention mechanism in the soil we need to understand the physicochemical controls on the formation and dissolution of atacamite in the soil.

4 Physicochemical controls on the formation of secondary Cu minerals

4.1 Introduction

The soil characterization analyses conducted in the previous chapter indicates that the soil contains elevated concentrations of SO_4^{2-}, Cl^- and Cu^{2+}. These elements accumulate in the soil during rain events when the Cu^{2+} and SO_4^{2-} rich tailings solution percolates through the tailings into the soil. Compared to the tailings solution the soil solution contains more soluble Cl^- and less soluble Cu^{2+}. A mineralogical analysis has indicated that atacamite is the only secondary copper mineral present in the soil, as no brochantite was detected. To date no work has been conducted at Spektakel to determine the mechanisms active in the soil during the formation of secondary copper mineral phases.

The research conducted on atacamite focused mainly on the formation and stability of atacamite in a marine environment with little reference to a terrestrial setting (Pollard *et al*, 1989; Reich *et al*, 2008). It is evident from literature that atacamite and its polymorphs paratacamite and clinoatacamite ($Cu_2(OH)_3Cl$) are the prevailing secondary Cu minerals present in supergene oxide zones of Cu deposits in the Atacama Desert (Hannington, 1993). In contrast to this atacamite is a common secondary Cu phase present in the weathered portions of sulphide deposits of the modern seafloor (Hannington, 1993). Stability diagrams based on Gibbs free energy calculations for the basic copper salts, indicate that tenorite should be the stable product of seafloor weathering of Cu sulphides. However, Woods and Garrels (1986) interpreted their free energy calculations to indicate that atacamite is the more likely stable phase at the pH and Eh of normal seawater.

The free-energy data reported by Woods and Garrels (1986) indicate that atacamite and paratacamite are equally stable in surface seawater when in equilibrium with the atmosphere at a CO_2 partial pressure of $10^{-3.5}$ bar. However, because their stabilities are so close, the preferred species depends criticality on the local $p(CO_2)$ which may be a function of temperature, depth and local biological activity (Woods and Garrels, 1986). The thermodynamic properties of the species are not the only mechanism contributing to the formation of these minerals. Formation kinetics, nucleation and growth play an important role in the crystallisation of these basic copper salts. Woods and Garrels (1986) noted that under experimental conditions the rate of crystallization (which is strongly dependent on the concentration of dissolved Cu^{2+} and the ratio of Cl^- and H^+ in solution) controls the formation of which particular species is formed. This was deduced from the fact that paratacamite

($Cu_4Cl_2(OH)_6$), the dimorph of atacamite, formed under acidic conditions and atacamite under more alkaline conditions (Woods and Garrels, 1986).

Research conducted by Rose (1976) determined that under acidic, oxidising conditions, Cu^+ and Cu^{2+} are carried in seawater (saline) solutions dominantly as cuprous chloride complexes ($CuCl^{2-}$ and $CuCl_3^{2-}$) and Cu^{2+} ions. The release of Cu^{2+} and the stability of $CuCl^{2-}$ and $CuCl_3^{2-}$ complexes under these conditions allow the solubility of Cu-bearing phases in excess of 1000 ppm. The solubility of copper is highest at a low pH, decreasing sharply at slightly alkaline pH values. This results in the precipitation of atacamite where the oxidizing solutions come into contact with ambient seawater. In contrast, atacamite will dissolve readily in fresh water and therefore is rare in subaerial environments.

The chemical conditions necessary for brochantite formation are not as well understood as those for atacamite formation. Brochantite is a secondary copper hydroxy sulphate mineral often observed in the oxidized zones of copper deposits (Zamana and Usmanov, 2007). It is the most common copper hydroxy sulphate mineral found in nature (Woods and Garrels, 1986) and is known to precipitate in solutions with a Cu^{2+} concentration of 8.56 kg/l (Zamana and Usmanov, 2007). The poorly constrained chemical conditions necessary for the formation of brochantite mean that it is unclear as to why brochantite is not observed in the Spektakel soils, despite the high sulphate signature of the soil solution.

To understand how the chemical mechanisms in the soil behave during the formation of atacamite and other secondary minerals, all the characteristics at the site need to be taken into account. According to literature the circumneutral pH and the presence of calcite (Chapter 3) will be the main characteristics contributing to the formation of atacamite in the soil. The analyses conducted in the previous chapter indicate that calcite is dominant in the subsoil horizons surrounding the tailings dumps. Along with this, the evaporative conditions, due to the arid climate, accumulates elevated concentrations of Cl^-, SO_4^{2-} and Cu^{2+} in the form of evaporate minerals.

The aim of this chapter is to determine why the copper hydroxy chloride mineral atacamite ($Cu_2(OH)_3Cl$) forms in preference to its sulphate equivalent brochantite ($Cu_4(OH)_6SO_4$). Two types of experiments were conducted to determine this. Firstly the influence of varying Cl^- and SO_4^{2-} activities on Cu mineral formation was determined and secondly the effect of evaporation on Cu mineral formation was determined.

4.2 Materials and Methods

4.2.1 Mineral formation experiment with change in absolute Cl^- and SO_4^{2-} concentration

4.2.1.1 Solution preparation and experimental procedure

To determine the effect that varying Cl^- and SO_4^{2-} concentrations and the presence of calcite will have on secondary Cu mineral formation, various synthetic solutions were prepared. The Cl^- and SO_4^{2-} concentration range of the synthetic solutions are based on the concentrations observed in the saturated paste extracts (Chapter 3). The concentrations were adjusted in five steps, in samples S1 to S5. The Cu^{2+} concentration was kept constant at 0.1M throughout all five steps (Table 4.1). To regulate the Cl^- and SO_4^{2-} concentrations NaCl and Na_2SO_4 were added. The experiment was executed in triplicate for each of the five different concentration combinations. The solutions were placed in 200ml Erlenmeyer flasks, 50ml of solution and 1g of calcite powder were added to each of the containers. The containers were covered with Parafilm, to minimize evaporation, and left to equilibrate at 25 ˚C in a MRC temperature controlled unit for one month. After equilibration the solutions were extracted and analysed for the change in Cu^{2+}, Cl^- and SO_4^{2-} concentration via ICP-MS and IC analysis to determine the change in solution composition. The precipitate was extracted, dried and analysed for mineral composition using XRD analysis. (*Refer to Chapter 2*)

Table 4.1: Theoretical compositional range of solutions S1 to S5 (in mol/l) to perform the mineral formation experiment in the presence of calcite.

Sample	Cl^-	SO_4^{2-}	Cu^{2+}
	Concentration (mol/l)		
S1	0.500	0.010	0.100
S2	0.250	0.025	0.100
S3	0.100	0.100	0.100
S4	0.025	0.250	0.100
S5	0.010	0.500	0.100

4.2.2 Evaporation experiment of a synthetic solution with a composition similar to a solution in equilibrium with the soil

4.2.2.1 Synthetic solution preparation

A synthetic soil solution, modelled on the saturated paste extract of the SP2 A soil horizon, was used in the evaporation experiment as this sample contains atacamite, gypsum and high concentrations of Cu^{2+}. To prepare the solution the salts were added individually and left to fully dissolve prior to the addition of the next salt. The sequence of salt addition of (1) $CaCl_2$, 2) $MgSO_4$, 3) $MgCl_2$, 4) NaCl, 5) KCl, 6) $CuCl_2$ and 7) $NaHCO_3$ was used to reduce mineral precipitation during preparation. Immediately after the dissolution of all the salts the solution was filtered through a 0.45µm Whatman Duradisc 25 NYL disposable syringe filter with polypropylene housing, to remove any suspended precipitate that formed. The evaporation experiment was conducted immediately after filtration in order to prevent additional precipitation prior to the initiation of the experiment.

Table 4.2: Comparison between the composition of the original saturated paste extract from the SP2 A soil horizon (SPE) (Chapter 3) and the synthetic solution prepared to use in the evaporation experiment (NC Evap). Concentration of the solutions are expressed in mg/l

	Samples SP2 A	
	SPE	NC Evap
Elements	**Concentration (mg/l)**	
Ca^{2+}	923.9	846.7
K^{+}	597.2	549.1
Mg^{2+}	5428.9	5436.0
Na^{+}	5683.3	5765.3
Cl^{-}	17567.4	13331.2
SO_4^{2-}	13692.2	10192.3
Cu^{2+}	193.3	169.9
$HCO3^{-}$	10.7	21.4
pH	4.9	4.9

4.2.2.2 Evaporation procedure and sample collection

Two treatments were used in the evaporation experiments. In one treatment 1g of $CaCO_3$ powder was added to the solution (labelled as CC Evap) and in the second treatment $CaCO_3$ was omitted from the solution (labelled as NC Evap). Both treatments were run in triplicate. The synthetic SP2 A solution was divided equally into six 800ml acid washed glass flasks and 300g of solution was added to each container. All six containers were placed in a temperature controlled unit at 25˚C and the solutions were sampled at 24 hour intervals. This sampling involved collecting an aliquot of solution, measuring the pH and weighing the glass container to determine the loss in weight.

With evaporation, the ions in solution become concentrated increasing the solution density, making a gravimetric determination of water loss difficult. In order to eliminate this change in density, the total weight of salt in the solution of each sample was calculated using the total dissolved salts (TDS) values (Figure 4.4). The total salt weight was subtracted from the weight of the solution at each specific collection, to determine the total weight of water remaining in the container. Using the weight of water still remaining in the container the concentration factor of each solution was determined as follow:

$$CF = \frac{W_{Initial}}{W_{Remain}} \qquad \text{[Eq 4]}$$

where the concentration factor (CF) is equal to the initial weight of the solution ($W_{Initial}$), after the total salt weight was subtracted, divided by the remaining solution weight (W_{Remain}), after the total salt weight was subtracted. The increase in CF represents the loss of fluid as the solution evaporates.

The pH measurement was conducted by submerging the pH probe as far as possible into the evaporating solution in an attempt to get as accurate as possible a reading (*Refer to Chapter 2*). Towards the end of the evaporation experiment the volumes of the solution in the containers were too low to collect an accurate pH reading.

The collected aliquots were filtered with a 0.2 µm GVS Cellulose Acetate Membrane Syringe Filter. Each of the filtered aliquots were diluted with MiliQ deionized water and stored in a 50ml centrifuge tube. The dilution factor of each filtered aliquot was determined by using the concentration of the previous collection. Diluted samples were placed in a refrigerator at 4˚C, to prevent precipitation of minerals, and sealed to prevent leaks. Each of the diluted samples were analysed for cations and anions. After all free water had been evaporated from the flasks the crystal precipitate at the bottom of the containers was collected and prepared for XRD powder analysis. (*Refer to Chapter 2*)

4.2.3 Analytical methods

The major cations were analysed by means of ICP-AES and the trace cations were analysed using ICP-MS. The anions were analysed with a Methrohm 761 compact ion chromatograph (IC). The mineral analysis was conducted by means of X-Ray diffraction analysis. (*Refer to Chapter 2*)

4.2.4 PHREEQC modelling

The evaporation was modelled using PHREEQC 2.18.3.5570 (Parkhurst and Appello, 1999). The basis of the model is set up to replicate the conditions of the evaporation experiment. A temperature of 25 °C and a CO_2 partial pressure of $10^{-3.5}$ were used for all simulations. The solution composition of sample NC Evap was used as the initial solution. The evaporation process is simulated by removing water, in moles, from the solution in the same volumetric increments observed in the evaporation experiment. To replicate the evaporation of NC Evap and CC Evap, the solution composition of NC Evap was used for both samples. However in order to replicate CC Evap, the simulation was placed in Equilibrium with 1 mol of calcite. The SIT (Specific Ion-Interaction Theory) database was used due to the high ionic strength of the solutions (Parkhurst and Appello, 1999).

The chemical composition of each of the collected samples was modelled in PHREEQC to determine the percentage error of the solution data as well as the activity and molality of the respective ions. This made it possible to compare the composition of the evaporation samples with the PHREEQC model, as PHREEQC does not calculate molarity only molality. The activity data was used, along with the pH, to track the stability of atacamite and brochantite during the experiments.

4.3 Results

4.3.1 The effect of absolute Cl^- and SO_4^{2-} concentrations on Cu secondary mineral formation

The initial composition of the solutions S1 to S5 (Table 4.3) closely resembles the theoretical solution composition (Table 4.1). After the solutions reacted with the calcite the Cu^{2+} concentrations decreased from approximately 100 mmol/l to less than 0.0028 mmol/l. The SO_4^{2-} concentration decreased in all the samples. An increase in Cl^- is observed in S3 to S5. The pH of the samples increases from between 4.29 and 4.68, to between 7.44 and 8.05 (Table 4.3).

Table 4.3: Chemical composition of the initial solution (a) (before calcite was added) vs. the composition of the solution after the experiment was completed (b). The concentration of the solutions is expressed in mol/l.

(a)	Initial concentration			
	Cl^-	SO_4^{2-}	Cu^{2+}	
Sample		mmol/l		pH
S1	488.49	7.84	102.81	4.29
S2	218.31	18.88	89.23	4.26
S3	79.93	71.37	103.91	4.54
S4	15.68	189.47	85.53	4.63
S5	6.83	429.89	84.63	4.68

(b)	Concentration after			
	Cl^-	SO_4^{2-}	Cu^{2+}	
Sample		mmol/l		pH
S1	475.20	7.61	0.0028	7.62
S2	183.12	9.14	0.0028	7.44
S3	85.07	17.92	0.0028	7.75
S4	16.95	146.26	0.0049	8.05
S5	7.08	386.42	0.0403	7.98

The XRD patterns of samples S1 to S5 indicate the formation of gypsum, atacamite and malachite (Figure 4.1). Using to the peak intensity as an indication of the quantity of mineral formed, it becomes apparent that the decrease in SO_4^{2-} and Cl^- concentration (Table 4.3) can be related to the formation of SO_4^{2-} and Cl^- minerals. Sample S1 and S2 (high Cl^- and low SO_4^{2-}) formed atacamite and little to no gypsum. Sample S3 (equal Cl^- and low SO_4^{2-})

formed more gypsum than atacamite. Samples S4 and S5 (high SO_4^{2-} and low Cl^-) predominantly formed gypsum with minor malachite. Brochantite was not detected in any of the treatments.

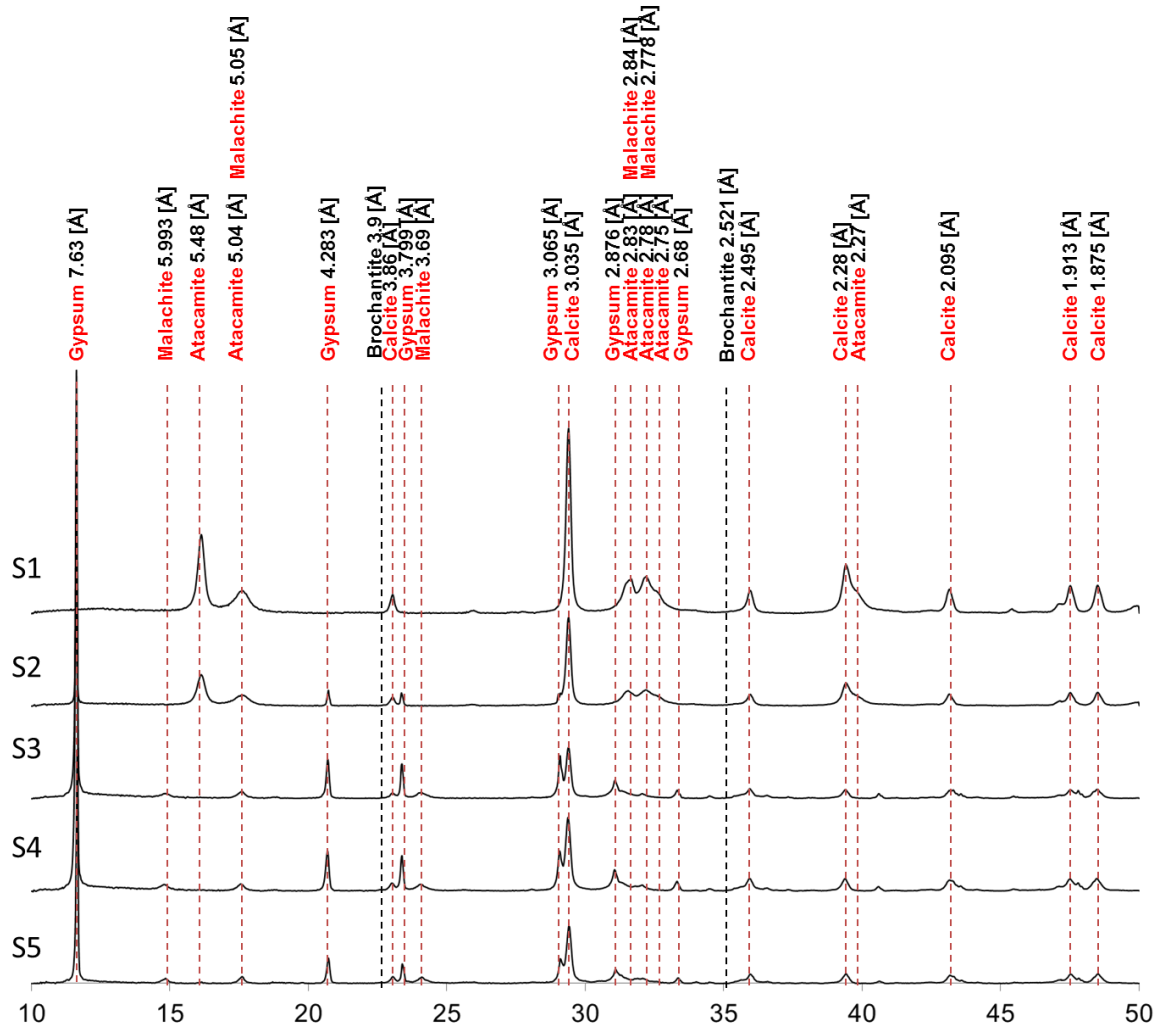

Figure 4.1: XRD patterns for samples S1 to S5. The minerals identified in each of the samples are indicated along with the d-distance which correlates with each peak. The concentration of the ions in each of the solutions, before and after the experiment, is displayed in Table 4.3. The black dashed lines indicate the position where the two most intense peaks for brochantite should occur.

4.3.2 The effect of evaporation on secondary Cu mineral formation in the presence and absence of calcite

4.3.2.1 Evaporation experiment vs. PHREEQC model

This section details a comparison between the data collected during the evaporation experiment and the modelled data produced by the PHREEQC evaporation simulation. The data collected during evaporation is expressed as NC Evap (no calcite added to solution) and CC Evap (calcite added to solution). The PHREEQC simulation data is expressed as CC Sim (in equilibrium with calcite) and NC Sim (not in equilibrium with calcite).

4.3.2.2 Evaporation rate

During the experiment a difference in evaporation rate between NC Evap and CC Evap was observed (Figure 4.2). Initially, the evaporation rate is similar, at collection number six the concentration rate of NC Evap starts to decrease relative to CC Evap. In the final stages of evaporation the colour of the NC Evap solution changed from transparent to yellow, this change was not observed in CC Evap. At the end of evaporation experiment the precipitate in CC Evap was dry and the precipitate in NC Evap remained a moist paste. The moist precipitate of NC Evap was left at 25 °C for an extended two weeks to determine if it would dry completely, but it did not. To determine how the NC Evap solution would evolve if complete evaporation occurred the concentration factor of CC Evap was used for NC Sim.

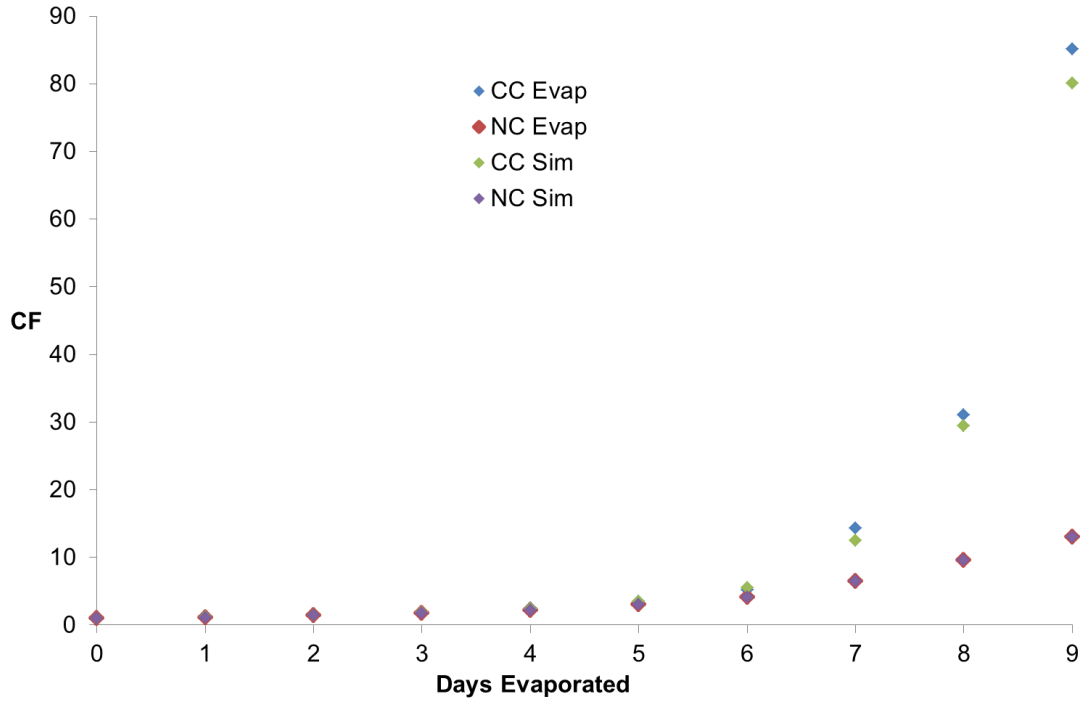

Figure 4.2: Comparison between the rates of evaporation, illustrated as the change in concentration factor (CF), of each collected sample in CC Evap, CC Sim, NC Evap and NC Sim. Each data point is indicated with a (◆) and distinguished by a different colour.

4.3.2.3 Solution pH and total dissolved salts (TDS)

The pH of the evaporation experiment and the PHREEQC simulation follow a similar trend (Figure 4.3). In the case of CC Evap and CC Sim the pH of the solution increases from 4.89 to 7.64 with calcite addition. During evaporation the pH of CC Evap and CC Sim remains in the circumneutral range. The pH of CC Sim increases more than CC Evap during initial evaporation as well as decreasing more toward the end of evaporation comparatively. The pH evolution of NC Evap and NC Sim indicates that the pH decreases during evaporation. Toward the end of evaporation NC Evap becomes more acidic than NC Sim.

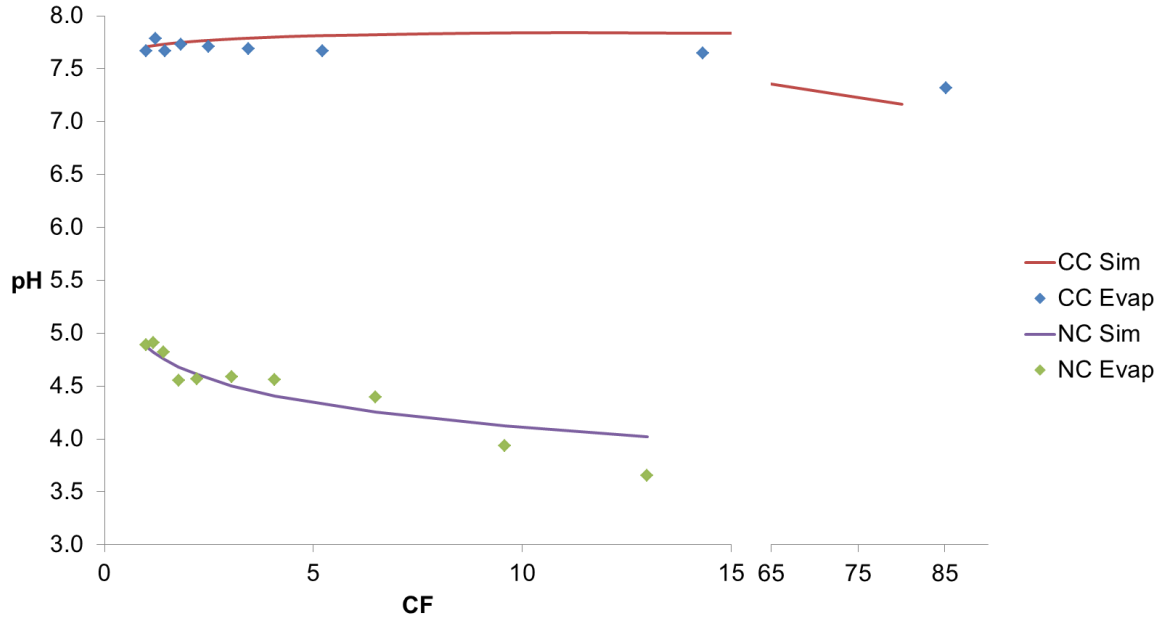

Figure 4.3: Comparison of the pH evolution between the evaporation experiment [CC Evap (◆), NC Evap (◆)] and the PHREEQC model [CC Sim (−), NC Sim (−)]. The X-axis of the graph is reduced to amplify the pH change of NC Evap.

The accumulation of the total dissolved salts (TDS) of the evaporation and simulation follow a similar trend during initial evaporation (Figure 4.4). However, in the final stages of evaporation the TDS of CC Evap starts to decrease whereas the TDS of CC Sim continues to increase. The NC Evap solution did not evaporate to the same CF as CC Evap thus this observation could not be made for NC Evap. The TDS of CC Sim and NC Sim increases linearly throughout the simulation.

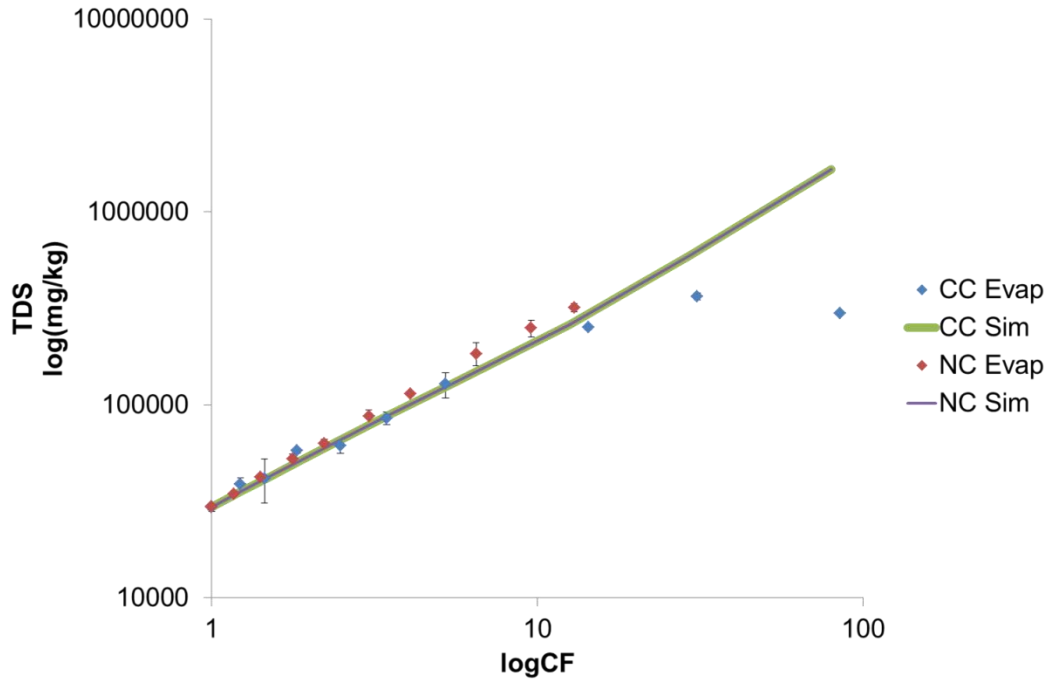

Figure 4.4: The change in the total dissolved salts (TDS) of the evaporation samples and the PHREEQC simulation. The TDS as used here is the SUM total of the major ions expressed as log(mol/kg) vs. logCF. Error bars indicate the calculated standard deviation for the evaporation data. Refer to Figure 4.3 for symbols.

4.3.2.4 Evolution of ion concentration during evaporation

The concentration of Cl^-, Na^+, SO_4^{2-} and K^+ in CC Evap increases during the initial stages of evaporation and decreases toward the end of evaporation (Figure 4.5a). The CC Sim indicates that the concentration of Cl^-, Na^{2+}, SO_4^{2-} and K^+ remains conservative throughout the simulation. The final Mg^{2+} and Ca^{2+} concentration of CC Sim deviates strongly from CC Evap. The Mg^{2+} concentration of CC Evap increases with evaporation and starts to stabilize at logCF 5. The Mg^{2+} concentration of CC Sim increases initially and starts to decrease after logCF 5. The Ca^{2+} concentration of CC Evap increases between logCF 1 and 2 and then start to decrease. The Ca^{2+} concentration of CC Sim decreases from the start, stabilizing at logCF 13 and increases in the final simulation step.

The activity of Cl^-, Na^+, Mg^{2+}, SO_4^{2-} and K^+ in CC Evap increases during the initial stages of evaporation and decreases at the end of evaporation (Figure 4.5b). The activities of Na^{2+}, Mg^{2+} and K^+ in CC Sim follow the same trend as the CC Evap activities. The Cl^- activity in CC Sim increases in the final step of the simulation. The SO_4^{2-} and Ca^{2+} activity of CC Sim deviates strongly from CC Evap. The SO_4^{2-} activity of CC Evap has a close to linear trend whereas the SO_4^{2-} activity of CC Sim starts with a stable positive trend and decreases after logCF 10. The Ca^{2+} activity of CC Evap increases between logCF 1 and 2 and decreases during evaporation the rest of the evaporation. The Ca^{2+} activity of NC Sim starts with a close to stable trend which increases after logCF 10.

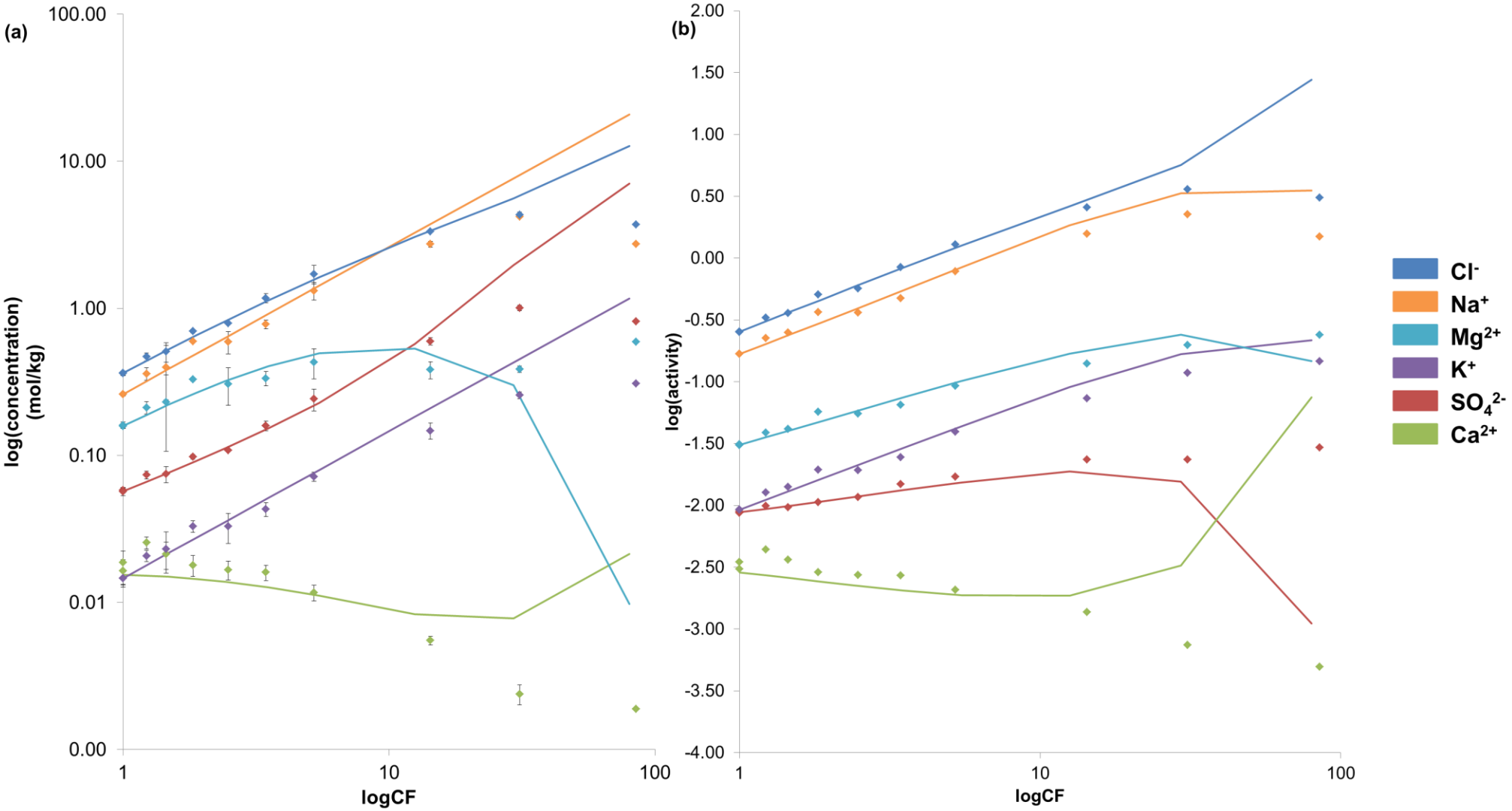

Figure 4.5: Comparison between the log(concentration) and log(activity) of CC Evap (◆) and CC Sim (−). (a) log(concentration) in mol/kg vs. logCF of CC Evap and CC Sim. (b) log(activity) vs. logCF of CC Evap and CC Sim. The calculated standard deviation is indicated with error bars for the NC Evap data.

The evolution of NC Evap is only plotted to a logCF of 13 as NC Evap did not evaporate to the same extent as CC Evap. Too aid in the understanding of how the solution would evolve if NC Evap evaporated completely the NC Sim data is plotted against the CF calculate for CC Evap (Figure 4.6).

The concentration of Cl^-, Na^+, SO_4^{2-} and K^+ in NC Evap increases during evaporation (Figure 4.6a). The NC Sim data indicates that the concentration of Cl^-, Na^{2+}, SO_4^{2-} and K^+ evolves in a fashion similar to NC Evap up to logCF 13 and remains conservative throughout the simulation. The Mg^{2+} and Ca^{2+} concentrations of NC Sim, however deviate strongly from NC Evap. The Mg^{2+} concentration of NC Evap increases with evaporation and starts to stabilize at logCF 5, whereas the Mg^{2+} concentration of NC Sim increases initially and then decreases after logCF 13. The Ca^{2+} concentration of NC Evap increases between logCF 1 and 2 after which it decrease until it reaches logCF 13. The Ca^{2+} concentration in NC Sim decreases from the start, levels out after logCF 10 and then increases in the final simulation step.

The activity of Cl^-, Na^+, Mg^{2+} and K^+ in NC Evap increases during the initial stage of evaporation (Figure 4.6b). The activity of Na^{2+}, Mg^{2+} and K^+ in CC Sim follow the same trend as the NC Evap showing a decrease in the final simulation step. The Cl^- activity of NC Sim increases in the final step of the simulation. The SO_4^{2-} and Ca^{2+} activity of NC Sim deviates strongly from NC Evap. The SO_4^{2-} activity of NC Evap has a stable linear evolution during evaporation while the SO_4^{2-} activity of NC Sim initially evolves linearly and then decreases at the end of the simulation. The Ca^{2+} concentration of NC Evap increases between logCF 1 and 2 and then starts to decrease to logCF 13. The Ca^{2+} concentration in NC Sim decreases from the start, stabilizes at logCF 13 and increases in the final simulation steps.

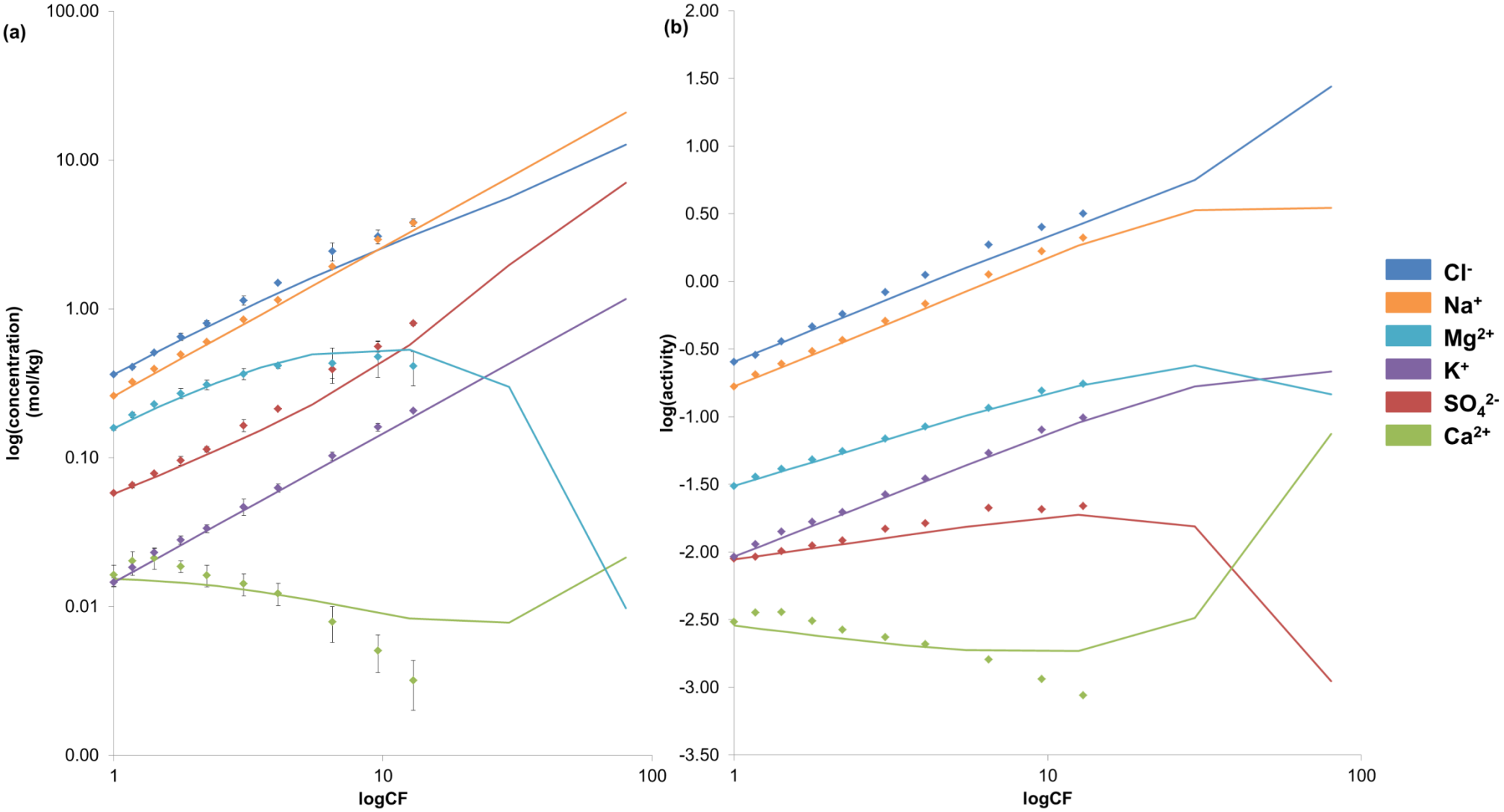

Figure 4.6: Comparison between the log(molality) and log(activity) of NC Evap (◆) and NC Sim (−). (a) log(molality) in mol/kg vs. logCF of NC Evap and NC Sim. (b) log(activity) vs. logCF of NC Evap and NC Sim. The CF used for NC Sim is based on the CF from CC Evap. The calculated standard deviation is indicated with error bars for the NC Evap data.

The change in Cu^{2+} concentration and activity during evaporation is shown in Figure 4.7. The concentration of Cu^{2+} is conservative in CC Sim, NC Evap and NC Sim (Figure 4.7a). After calcite was added to the CC Evap solution Cu^{2+} is removed from the solution reducing the concentration from 169 mg/l to 0.4 mg/l. When the calcite settled on the base of the container a green precipitate formed on the surface of the calcite powder. The activity of Cu^{2+} evolves along a trend similar to the molality (Figure 4.7b).

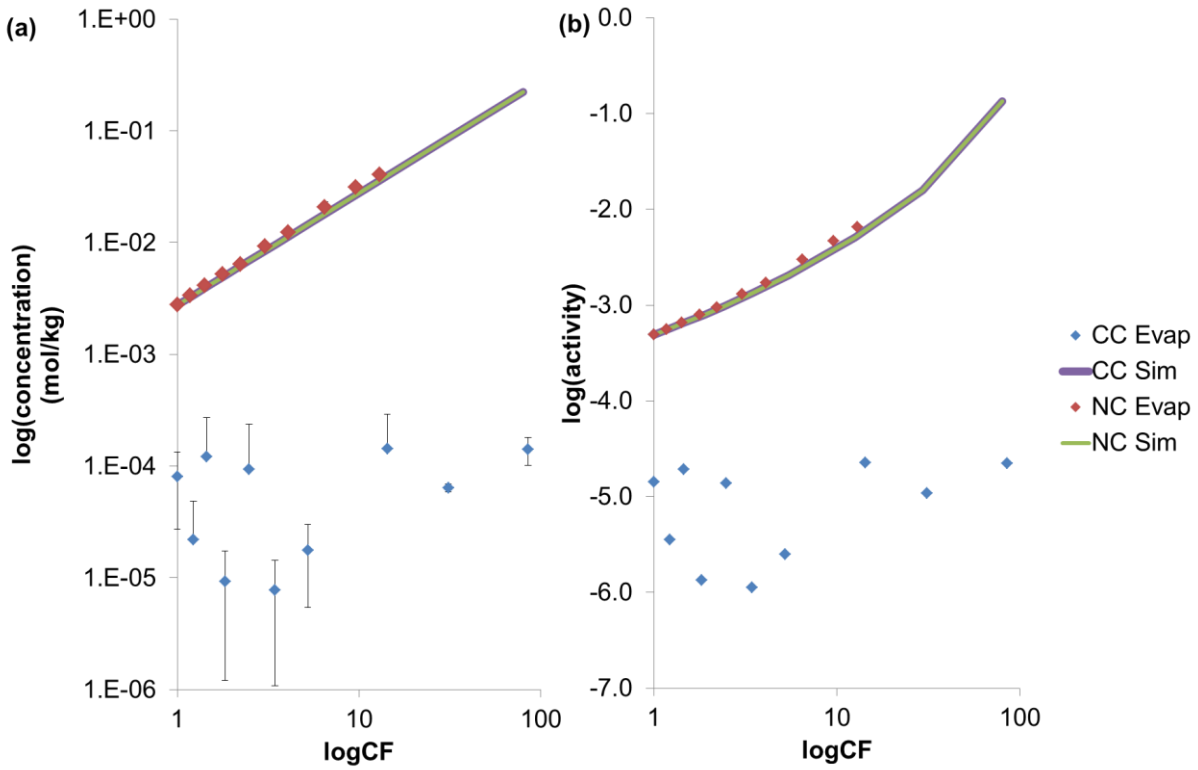

Figure 4.7: Comparison of the evolution of Cu^{2+} during evaporation (CC Evap and NC Evap) and the PHREEQC simulation (CC Sim and NC Sim) in the presence and absence of calcite: (a) change in log(concentration) of Cu^{2+} expressed in mol/kg vs logCF, (b) change in log(activity) of Cu^{2+} vs logCF. Refer to Figure 4.3 for symbols.

4.3.2.5 Mineralogy of the precipitate collected after completed evaporation

The mineral precipitate collected, after evaporation of CC Evap and NC Evap, indicates that different minerals form in the presence and absence of calcite. The minerals that formed in CC Evap are gypsum, starkeyite (leonhardtite) ($MgSO_4 \cdot 4H_2O$), halite and atacamite. The minerals present in the NC Evap precipitate are bassanite, kieserite ($MgSO_4 \cdot H_2O$) and halite (Figure 4.8). Mineral abundance is proportional to the concentration of ions, that contribute to the formation of the various minerals, in solution.

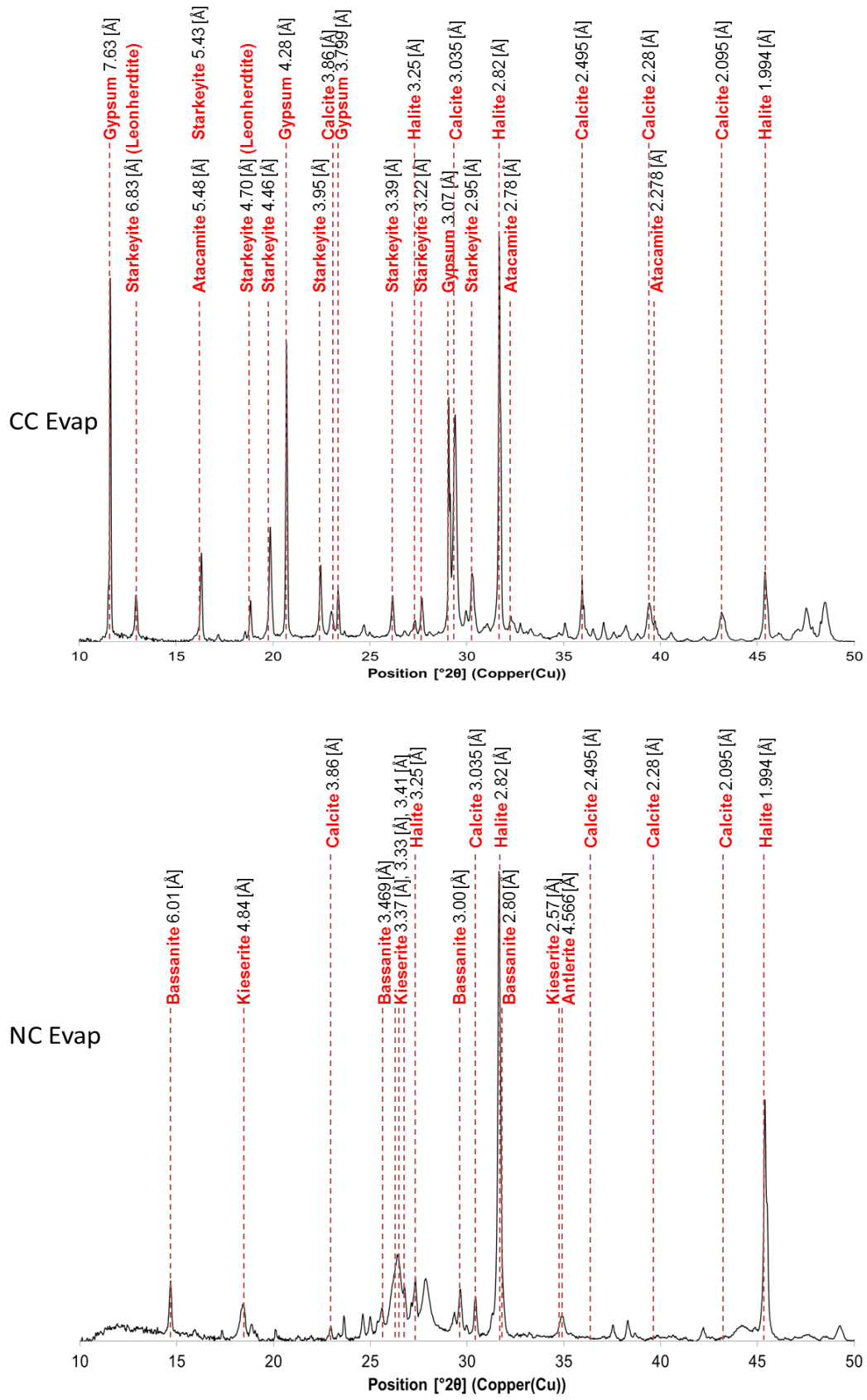

Figure 4.8: XRD patterns of air dried precipitate collected after evaporation of CC Evap and NC Evap. The red dashed lines indicate the main peaks of each identified mineral. Each identified mineral name and d-distance is indicated.

4.4 Discussion

The purpose of this research was to determine the chemical mechanisms active in the soil surrounding the Spektakel mine tailings and how they influence secondary copper mineral formation. Specifically it was to determine why the sulphate rich environment at the mine favours the formation of a copper chloride mineral (atacamite) over its sulphate counterpart (brochantite).

4.4.1 The effect of chloride and sulphate concentrations on secondary Cu mineral formation

The initial experiment investigated how the ratio of Cl^- to SO_4^{2-} influences the formation of atacamite and brochantite in the presence of calcite. It was found that the mobility of Cu^{2+} in a solution, containing Cl^- and SO_4^{2-}, is controlled by the pH and the activity of the Cl^- and SO_4^{2-} ions, these findings are consistent with that of Mann and Deutscher (1977). The low pH values (4.29 – 4.68) (Table 4.3) of the initial solutions is due to the hydrolysis of Cu^{2+}, as described by the following equation:

$$Cu^{2+} + 2H_2O \rightleftharpoons Cu(OH)_2 + 2H^+ \quad \text{[Eq 5]}$$

The addition of calcite adds carbonate ions to the system buffering the pH through the following mechanism:

$$CaCO_{3\,Calcite} + H^+ \rightleftharpoons Ca^{2+} + HCO_3^{2-} \quad \text{[Eq 6]}$$

$$HCO_3^{2-} + H_2O \rightleftharpoons H_2CO_3 + OH^- \quad \text{[Eq 7]}$$

Thus, the dissolution of calcite increases the Ca^{2+} concentration of the sample solution and increases the gypsum forming potential of the high SO_4^2 solutions S3 to S5 (Table 4.3). This observation correlates with the XRD data (Figure 4.1) that indicated gypsum formed in the solutions with elevated SO_4^{2-} concentrations. Conversely, the reduced SO_4^{2-} concentrations of samples S1 and S2 did not result in the formation of gypsum.

The XRD data of samples S1 to S5 indicate that atacamite and malachite were the only copper minerals that formed during the experiment and no brochantite was observed. Work conducted by Mann and Deutscher (1977) shows that the change in Cl^- and SO_4^{2-} activity influences the mobility of Cu^{2+} in the presence of carbonate, resulting in the formation of different copper mineral phases. To do this they calculated which mineral phases restrict the mobility of Cu^{2+} in solution with changing Cl^- and SO_4^{2-} activities. It was determined that in acidic solutions the increase in SO_4^{2-} and Cl^- activity lowers the activity of Cu^{2+} in solution. Increasing SO_4^{2-} activity produced antlerite and brochantite, whereas increasing Cl^- activity produced atacamite. In an alkaline solution, depending on the SO_4^{2-} activity, malachite limits

the mobility of Cu^{2+} (Figure 4.9). Stability diagrams based on the calculations by Mann and Deutscher (1977) indicate how the change in Cl^- and SO_4^{2-} activity influences mineral stability at a pH between 2 and 12 (Figure 4.9). The pH, along with the Cl^- and SO_4^{2-} activities of sample S1 to S5, before and after calcite addition, were plotted on these diagrams. The results from the experiment correlate with the conclusions of Mann and Deutscher (1977). In sample S3, S4 and S5, after calcite addition, the high pH and SO_4^{2-} activity along with a low Cl^- activity favours the formation of malachite (Figure 4.9) as is observed in the XRD patterns (Figure 4.1). In sample S1 and S2, after calcite addition, the high Cl^- and low SO_4^{2-} activity favour the formation of atacamite (Figure 4.9) in agreement with the XRD mineral analysis (Figure 4.1).

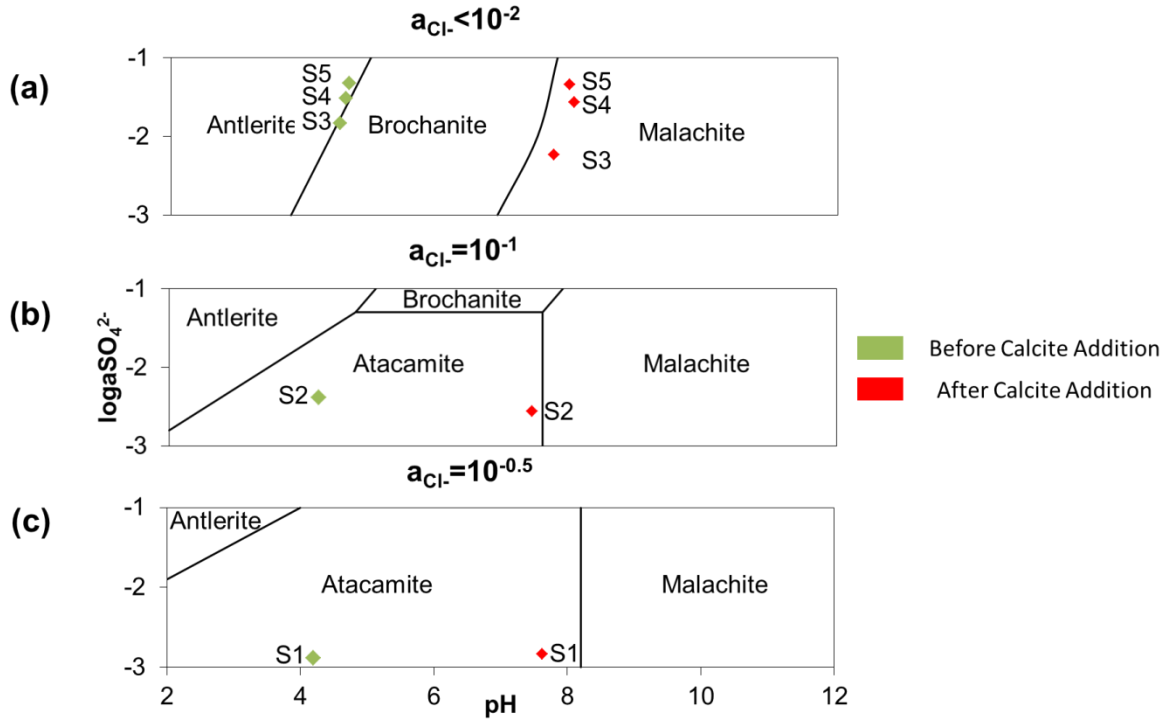

Figure 4.9: Stability diagram indicating the mineral phases that limit the mobility of Cu^{2+}, at different Cl^- and SO_4^{2-} activities, in solution before and after the addition of calcite (modified from Mann and Deutcher, 1977). The solution compositions of sample S1 to S5 (◆), before and after calcite addition, were plotted on the diagram to indicate the mineral stability of each solution before and after the experiment. The results are expressed as the log activity of SO_4^{2-} ($\log SO_4^{2-}$) vs pH

The solution composition of S4 and S5 replicates the composition of the tailings pond solution (Table 3.5), i.e. elevated SO_4^{2-} and reduced Cl^- concentrations relative to the soil present at the site. At a pH similar to the tailings pond solution (4.46 (Table 3.5)), prior to the addition of calcite, antlerite/brochantite will be the stable phase in these solutions (Figure 4.9a). The composition of solution S3 represents the solution composition of the equilibrium soil solutions, consisting of a similar Cl^- and SO_4^{2-} concentrations (Table 3.4). This solution will plot in the brochantite stability field at low pH. When calcite is added to solutions S3, S4 and S5, the pH increases to above 7 forming a solution that favours malachite stability. It is

only when the SO_4^{2-} concentration is decreased and the Cl^- concentration is increased, in solutions S1 and S2, that the solutions start to favour atacamite stability.

These results do not correspond with observations made in the Spektakel soils. The soil contains elevated Cl^- and SO_4^2, similar to S3, however atacamite is still the dominant secondary copper mineral phase. No malachite or brochantite is observed. This indicates that changes in absolute Cl^- and SO_4^{2-} concentrations are not the only mechanism that is effecting secondary copper mineral formation.

4.4.2 The effect of evaporation on the formation of secondary copper mineral formation

To determine which other chemical mechanisms influence the formation of secondary copper minerals in the soil at Spektakel, focus was placed on the environmental conditions at the site. The main environmental parameter influencing the soil at Spektakel is the arid climate. Namaqualand is known for its very hot and dry summer months when temperatures can reach up to 38°C (Francis *et al.*, 2007). This causes the soil of the Namaqualand to act like a shallow ephemeral aquifer with a saline lake characteristic, promoting the formation of secondary minerals (Francis *et al.*, 2007). After a rain event the fluid that is in equilibrium with the soil, evaporates before it has time to filter through the soil profile or flow away from the site. This causes salt to build up in the surface horizons of the soil profiles near the tailings.

This experiment investigated how the evaporation of a solution in equilibrium with the soil surrounding the site, influences secondary copper mineral formation. The data collected from the evaporation experiment is compared to a PHREEQC simulation which replicates the experiment. The data produced by the PHREEQC simulation correlated well with the data obtained from the evaporation experiment giving confidence as to the accuracy of the data. This result helps promote the validity of using a model to help predict the outcome of experimental data.

The results of the evaporation experiment showed that the rate of evaporation of CC Evap was faster than NC Evap, an observation identical to those of Lazar *et al.* (1983). The NC Evap samples formed a yellow gel-like substance after a CF of 13 which remained stable for the remainder of the experiment without further water loss. This could represent increased amounts of structural water being included in the structure of the precipitated minerals. It is also not clear as to why the presence of calcite prevented this from occurring in the CC Evap treatment. It is still unclear why the evaporation rate is higher in CC Evap or why NC Evap would not evaporate to complete dryness.

During evaporation the pH of CC Evap remained circumneutral and the pH of NC Evap followed a decreasing trend. This difference in pH behaviour of each of the two solutions is controlled by the same mechanism as in the previous experiment. The hydrolysis of Cu^{2+} reduces the pH of the initial solution before evaporation starts. The addition of calcite to CC Evap removes the Cu^{2+} ions (Figure 4.7) discontinuing the hydrolysis reaction and neutralizing the solution by adding carbonate ions through the dissolution of calcite (Figure 4.3). During the evaporation of NC Evap Cu^{2+} behaves conservatively accumulating in solution (Figure 4.5). Thus the hydrolysis reaction and associated lowering of the pH during evaporation continues (Figure 4.3).

The evolution of dissolved species during the evaporation experiment and simulation are given in Figure 4.5 and Figure 4.6 respectively. Initially the solutions are in chemical equilibrium producing a charge balance of equal molar equivalent concentrations (m) of cations and anions:

$$m\text{Cations}(+) = m\text{Anions}(-) \qquad \text{[Eq 8]}$$

In the case of this experiment this charge balance is as follows:

$$2m_{Ca^{2+}} + 2m_{Mg^{2+}} + m_{Na^{+}} + m_{K^{+}} + m_{H^{+}} = 2m_{SO_4^{2-}} + m_{Cl^{-}} + m_{HCO_3^{-}} + 2m_{CO_3^{2-}} + m_{OH^{-}} \qquad \text{[Eq 9]}$$

As the solution evaporates the ions become more concentrated in the solution. When the solution becomes saturated with respect to a specific mineral that mineral will start to precipitate reducing the concentration of those ions in solution. To maintain the chemical equilibria both cations and anions are removed maintaining a neutral charge.

During the evaporation it was observed that the TDS of CC Evap decreases toward the end of evaporation and the TDS of NC Evap remained conservative (Figure 4.4) indicating that some of the conservative ions in CC Evap precipitated during the final stages of evaporation. However, calcite has the capacity to adsorb both metallic and non-metallic elements (Comans and Middelburg, 1987; Zachara *et al.*, 1991). It is therefore possible that during the final stages of evaporation, the ions in CC Evap adsorbed onto the calcite crystal surface reducing the total concentration of soluble salts in solution.

Hardie and Eugster (1970) have done extensive research on the evolution of saline brine solutions with chemical compositions similar to the equilibrium soil solutions from Spektakel. They produced a chemical model that predicts the evolution of these saline solutions during evaporation. According to Hardie and Eugster (1970) during evaporation the first phase to precipitate will be $CaCO_3$ removing both Ca^{2+} and CO_3^{2-} from the solution. In a solution with a $2m_{Ca^{2+}} > Alkalinity$ ratio, all the carbonate species will be removed. Consequently little to no $CaCO_3$ will precipitate from the NC Evap solution, as the alkalinity is very low. Alternatively, as in the case of CC Evap, the general abundance of calcite will mask any extra calcite formation. The second step in the evaporation model of Hardie and Eugster (1970) predicts the precipitation of gypsum and, thus, the removal of both Ca^{2+} and SO_4^{2-} from the solution. In this evaporation experiment, before evaporation was initiated, both the CC Evap and NC Evap solutions were in equilibrium with gypsum. This indicates that the initial phase to precipitate will be gypsum rather than calcite. As solutions CC Evap and NC Evap evaporated the Ca^{2+} concentration increased and only started to decrease at CF 1.5 (Figure 4.10). The results in Figure 4.11 indicate that when the Ca^{2+} concentration starts to decrease the SO_4^{2-} concentration increases at a lower rate, compared to the rest of the evaporation, in CC Evap indicating that gypsum started to precipitate. A similar change in Ca^{2+} and SO_4^{2-} concentration is not observed in NC Evap, as the low Ca^{2+} concentration masks any noticeable decrease in SO_4^{2-}. The results from the PHREEQC simulation do not correlate with the evaporation results, as the simulation predicts that gypsum precipitation should occur from the start of evaporation (Figure 4.10). The reason for the Ca^{2+} concentration increase in the final stages of the PHREEQC simulation is unclear.

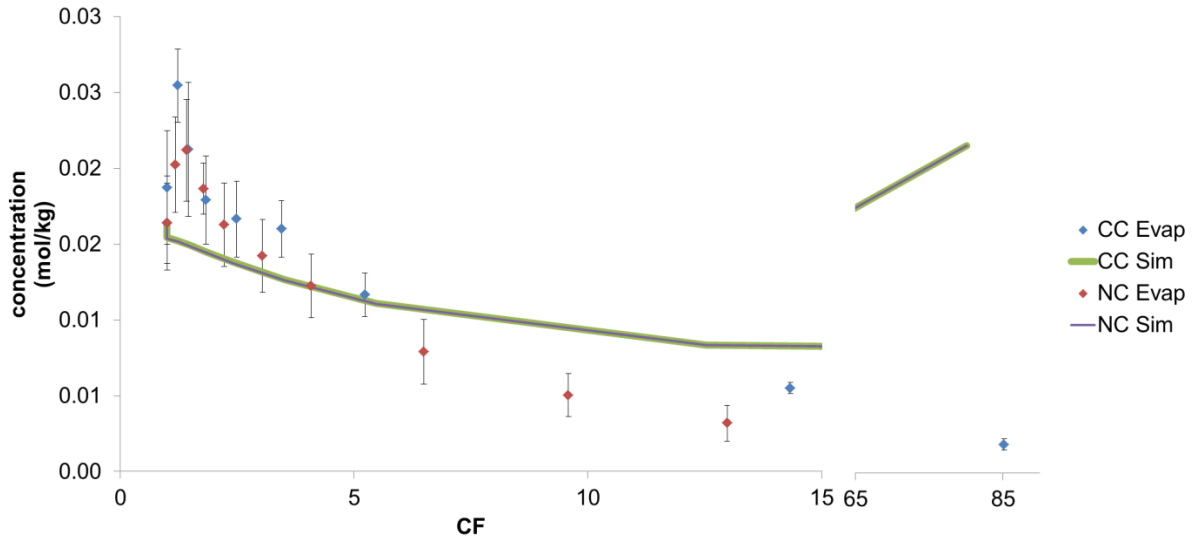

Figure 4.10: Change in Ca^{2+} concentration during the evaporation of CC Evap, NC Evap, CC Sim and NC Sim. The results are expressed as concentration (mol/kg) vs CF. Refer to Figure 4.3 for symbols.

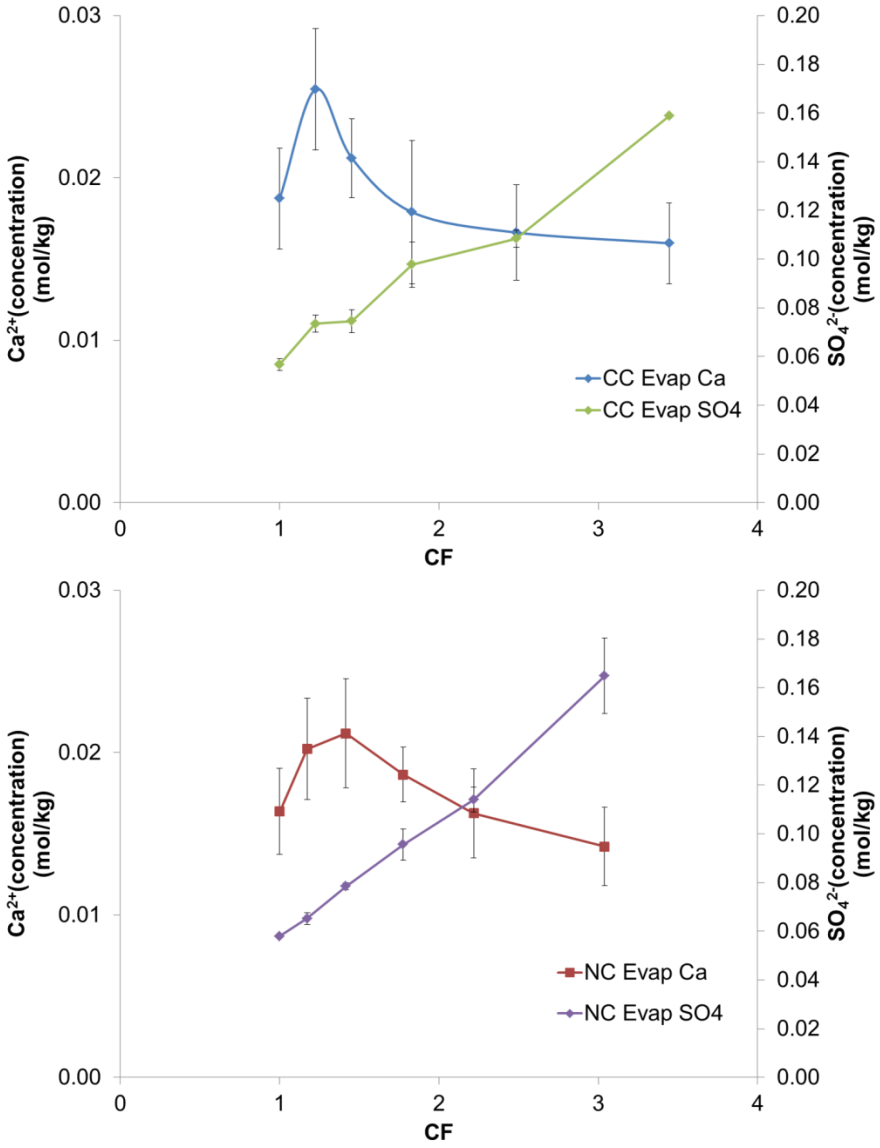

Figure 4.11: Comparison between the decreases in the concentration of SO_4^{2-} (mol/kg) vs. Ca^{2+} (mol/kg) during gypsum precipitation in the evaporation experiment (a) CC Evap Ca (◆–), CC Evap SO4 (◆–),(b) NC Evap Ca (■–) and NC Evap SO4 (■–)

It was this observation of gypsum formation that lead to the second section of the Hardie and Eugster evaporation model (1970) being referred to as a chemical divide. It predicts that the evaporation of a solution in equilibrium with gypsum with a 1:1 SO_4^{2-} and Ca^{2+} ratio removes both Ca^{2+} and SO_4^{2-} at a similar rate without changing the Ca^{2+}/SO_4^{2-} ratio in the solution. However the evaporation of a solution with $Ca^{2+} < SO_4^{2-}$ (as in this experiment) the SO_4^{2-} ions will accumulate while the Ca^{2+} ions are depleted (Figure 4.12). This uneven chemical divide is observed in both CC Evap and NC Evap during evaporation (Figure 4.12). The data from the PHREEQC simulation predicts the same Ca^{2+} and SO_4^{2-} evolution for CC Evap and NC Evap. The increase in Ca^{2+} concentration towards the end of the CC Sim and NC Sim (CF = 15) is difficult to explain as a similar increase was not observed in the evaporation experiments (Figure 4.12).

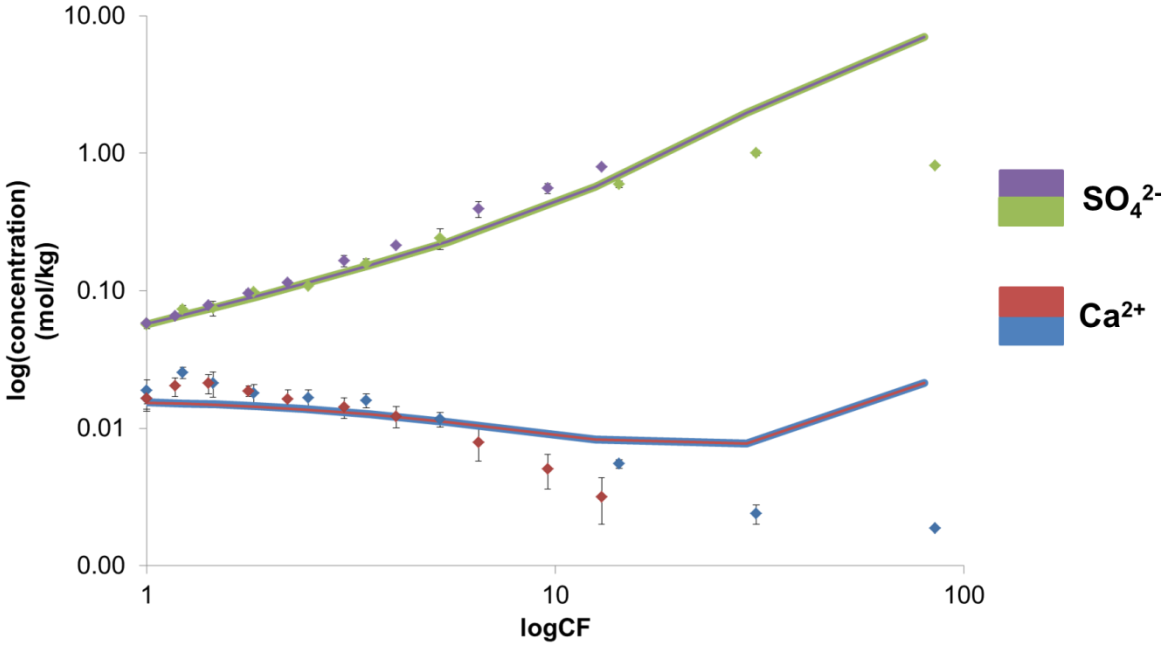

Figure 4.12: Indication of the chemical divide between Ca^{2+} and SO_4^{2-} for the evaporation experiment (CC Evap and NC Evap) indicated with a (◆) and the PHREEQC simulation (CC Sim and NC Sim) indicated with a (−) expressed in log mg/l vs. CF. The colours indicate the SO_4^{2-} and Ca^{2+} concentration in both the presence of calcite (CC) and absence of calcite (NC). The simulation results for CC and NC are identical resulting in the lines masking each other. The line thickness of each sample was adjusted in an attempted to make the results more clear. The error bars indicate the calculated standard deviation of the results.

Aside from the evolution of the ions mentioned up to this point, the rest of the ions in the solution remained conservative until final evaporation. The only difference was observed in the evolution of Cu^{2+} in CC Evap in comparison with NC Evap (Figure 4.13). The Cu^{2+} concentration of NC Evap, CC Sim and NC Sim behave conservatively during evaporation. After calcite is added to CC Evap the Cu^{2+} concentration is decreased from $2.77x10^{-3}$ mol/kg to $1.1x10^{-4}$ mol/kg (Figure 4.13). This indicates that the addition of calcite has a strong effect on the retention of Cu^{2+} in the solution.

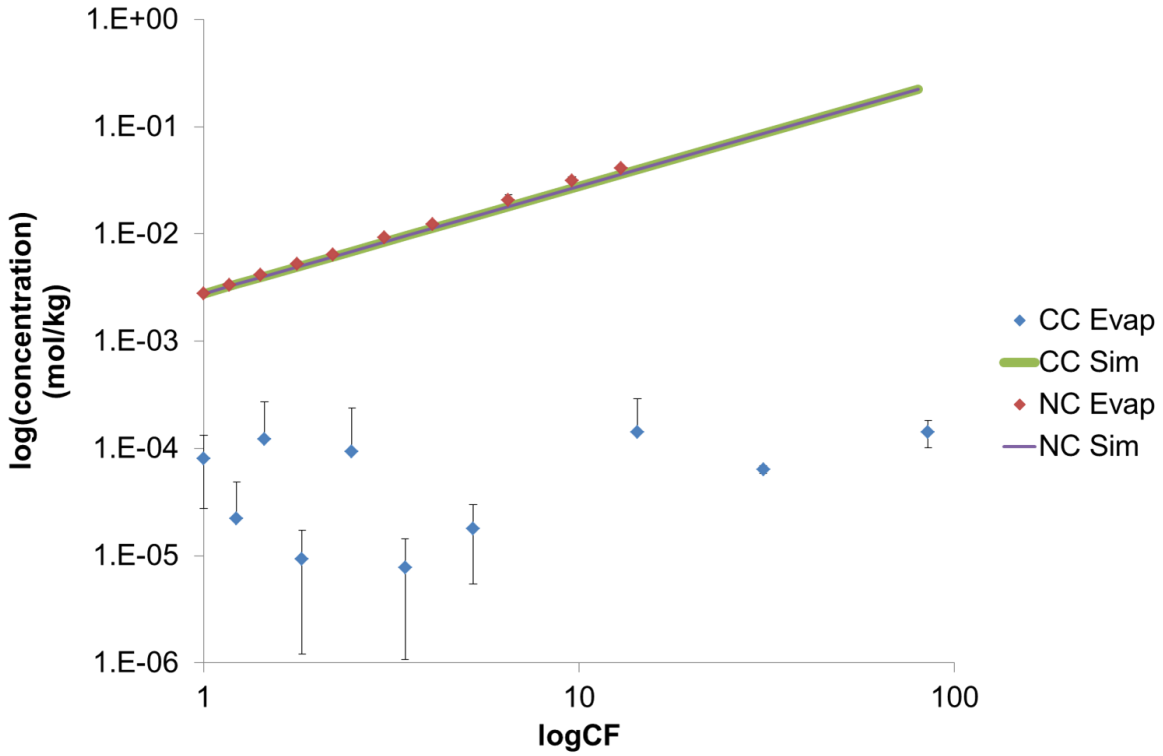

Figure 4.13: Indication of the evolution of Cu^{2+} during the evaporation experiment (CC Evap and NC Evap) and PHREEQC simulation (CC Sim and NC Sim). The results indicate the log(concentration) of Cu^{2+} in mol/kg vs logCF. The error bars indicate the calculated standard deviation of the results. Refer to Figure 4.3 for symbols.

The reaction between calcite and Cu^{2+} was first described by Garrels and Stine (1948) who noticed that calcite is replaced by atacamite in a $CuCl_2$ solution. The mechanism describing this reaction consists of two interrelated, but separate reactions (Equation 1). The mechanism dictates that atacamite formation cannot occur without the formation of a carbonate ion. As H^+ is produced by the hydrolysis reaction of $CuCl_2$ the pH of the solution decreases. This lowered pH causes the dissolution of calcite producing carbonate and OH^- ions on the surface of the calcite. As the Cu^{2+} and Cl^- in solution come in contact with the OH^- on the calcite surface, atacamite saturation is exceeded and it is precipitated onto the calcite surface. Precipitation of $Cu_2(OH)_3Cl$ starts at an approximate pH of 4 (Sharkey and Lewin, 1972). The amount of atacamite formed does not have to be equivalent to the amount of calcite dissolved (Garrels and Stine, 1948).

$$4CuCl_2 \leftrightarrow 4Cu^{2+} + 2Cl^- \leftrightarrow Cu_4(OH)_6Cl_2 \quad \text{[Eq 10]}$$

$$6H_2O \leftrightarrow 6OH^- + 6H^+ \quad \text{[Eq 11]}$$

$$3CaCO_3 \leftrightarrow 3Ca^{2+} + 3CO^{3-} \quad \text{[Eq 12]}$$

$$3H_2CO_3 \leftrightarrow 3H_2O + 3CO_2$$

Equation 1: Chemical mechanism for the replacement of calcite by atacamite (Garrels and Stine, 1948)

Precipitates were collected after evaporation was completed to provide clues regarding the evolution of the solutions. Due to the fact that the precipitate of NC Evap remained moist the sample collected from the precipitate had to be heated to 100 °C to remove the remaining water. The precipitate collected at the base of the containers in sample CC Evap and NC Evap consists of typical saline brine minerals, such as halite, starkeyite and kieserite (Figure 4.8; Lowenstein and Hardie, 1985). According to Lowenstein and Hardie (1985) the mineral composition of the precipitate that forms during the evaporation of a brine solution depends on the composition of the evaporating solution. In most instances the precipitate consists of a single dominant mineral species. It has been documented that in most arid saline environments halite is the dominant secondary mineral phase (Lowenstein and Hardie, 1985). This correlates with the precipitate collected in CC Evap and NC Evap which has a dominant halite signature (Figure 4.8). As has been mentioned the presence of gypsum is expected according to the Hardie and Eugster evaporation model (1970; Figure 4.8). The heating of the precipitate from NC Evap altered the chemistry of the mineral species observed in NC Evap and CC Evap. The heating of the precipitate dehydrated gypsum ($CaSO_4 \cdot 2H_2O$) to form bassanite ($2CaCO_3 \cdot H_2O$) in NC Evap (Mees and Stoops, 2003). Similarly starkeyite ($MgSO_4 \cdot 4H_2O$) dehydrated to form kieserite ($MgSO_4 \cdot H_2O$). The only copper mineral observed in the precipitate samples was atacamite as no other secondary copper minerals could be identified.

To understand how evaporation influenced the evolution of the solution chemistry with respect to secondary Cu minerals, the change in solution chemistry was plotted on an oxidised Cu^{2+} mineral stability diagram (Figure 4.14 and Figure 4.15). The initial solution composition of CC Evap and NC Evap plot in the atacamite-paratacamite stability field, adjacent to the brochantite and antlerite stability fields (Figure 4.14). After the addition of calcite to CC Evap the chemical composition of the solution changes placing the solution chemistry close to the atacamite-paratacamite and tenorite field boundary. The only difference between these two solutions at this stage is the pH. The addition of calcite increases the pH of CC Evap which influences the evolution of the solution. However during evaporation the chemical composition of CC Evap and NC Evap remain in the atacamite-paratacamite stability field. The activity of SO_4^{2-} never reaches the optimum brochantite activity range, thus correlating with the observation made in Figure 4.5 and Figure 4.6, indicating that the increase in SO_4^{2-} activity is less than the molality of SO_4^{2-} during evaporation.

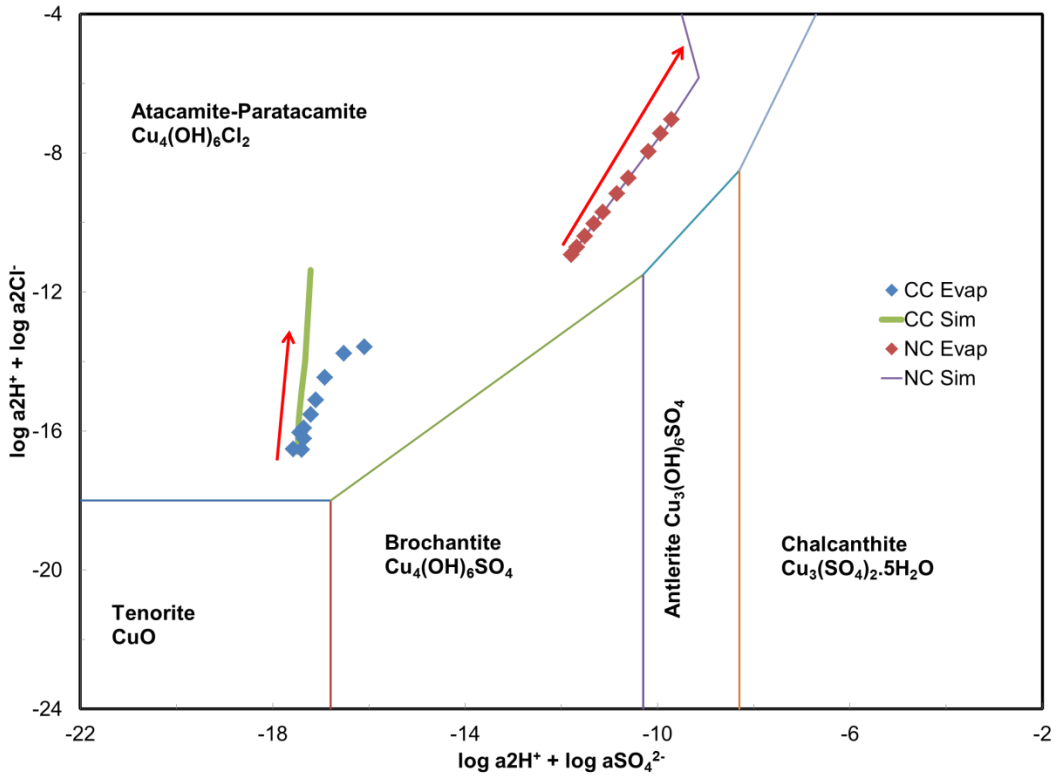

Figure 4.14: Stability diagram illustrating the relative stability fields of oxidized copper minerals at 25 °C calculated using thermodynamic data provided by Woods and Garrels (1986). The activity values of Cl^- and SO_4^{2-} were calculated with PHREEQC running the SIT database. Predicted pH values were used for the CC Sim and NC Sim the collected pH values were used for CC Evap and NC Evap. For symbols refer to Figure 4.3. The arrows indicate the direction of the evolution of the ions during evaporation.

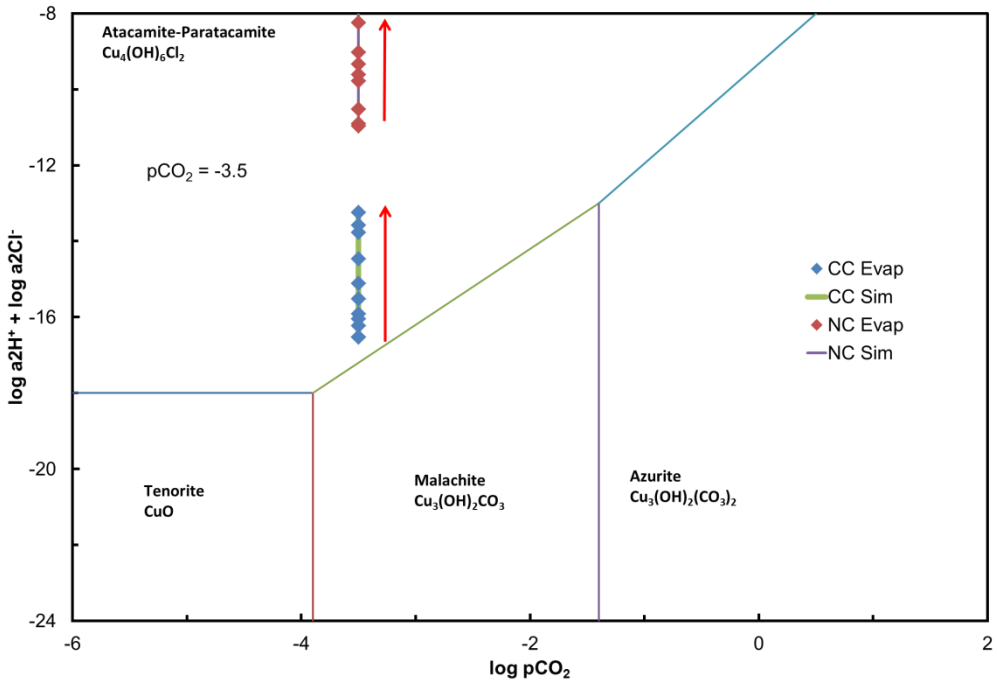

Figure 4.15: Stability diagram illustrating the relative stability fields of oxidized copper minerals at 25 °C calculated with the free energy of formation values used by Woods and Garrels (1986) at CO_2 partial pressures of $10^{-3.5}$. The activity values of Cl^- and SO_4^{2-} were calculated with PHREEQC running the SIT database. For symbols refer to Figure 4.3. The arrows indicate direction of the evolution of the ions during evaporation.

The difference between the activity and molality of SO_4^{2-} indicates that some other factor is inhibiting its evolution. It has been noted that Mg^{2+} and SO_4^{2-} can form ion pairs in solution (Martin, 2000). This correlates with the elevated Mg^{2+} concentration observed in the equilibrium soil solutions determined in Chapter 3. The mechanism predicted by Atkins and Petrucci (1966) indicates:

$$Mg^{2+}\,(aq) + SO_4^{2-}\,(aq) = [Mg(WW)SO_4] = [Mg(W)SO_4] = [MgSO_4] \qquad \text{[Eq 13]}$$

where W represents the water molecule trapped in between the ions. A comparison between the activities of SO_4^{2-}, $MgSO_4$ (aqueous complex) and Cl^- (Figure 4.16) indicates that the activity of SO_4^{2-} in all the experiments is lower than activities of Cl^- and $MgSO_4$ (aqueous complex). This indicates that the formation of these $MgSO_4$ complexes reduces the activity of free SO_4^{2-} in solution. The increased Cl^- activity and reduced SO_4^{2-} activity provide the ideal conditions for the formation of atacamite formation rather than brochantite, or indeed any other copper sulphate mineral. The unique chemical characteristic of the Spektakel soil, thus provide the ideal conditions for the formation of atacamite over brochantite.

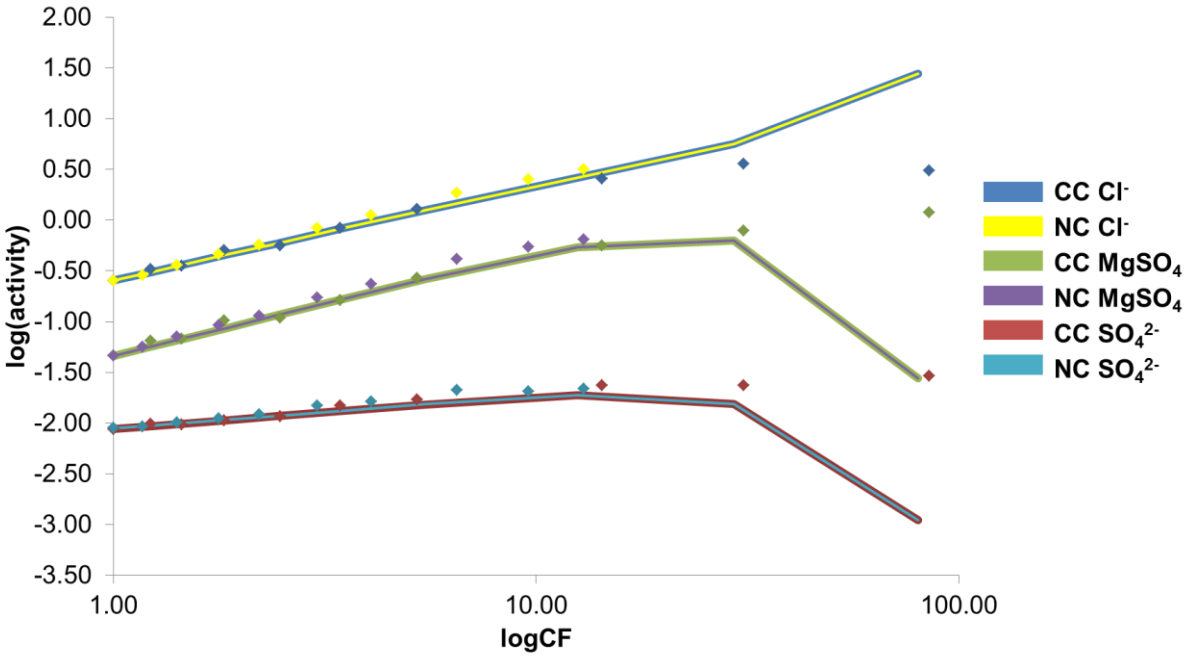

Figure 4.16: Comparison of the activities of Cl^-, SO_4^{2-} and $MgSO_4$ (aqueous complex) in the evaporation experiment (CC Evap and NC Evap) indicated with (◆) and the PHREEQC simulation (CC Sim and NC Sim) indicated with (−). Indicated as log(activity) vs logCF. Each colour represents the activity of a specific ion for both the evaporation experiment and the PHREEQC simulation. The simulation results for CC Sim and NC Sim are identical resulting in the lines masking each other. The line thickness of each sample was adjusted in an attempted to make the results more clear.

4.5 Conclusion

The focus of this chapter was to determine the physiochemical controls on the formation of secondary copper minerals in the soil at the Spektakel mine site. The initial formation experiment indicated that SO_4^{2-} and Cl^- activity combined with pH are the dominant factors controlling the formation of atacamite over brochantite in the presence of calcite. The evaporation experiment indicated that the chemical evolution of the solution in equilibrium with calcite differs from the solution excluding calcite. The addition of calcite to the evaporation solution buffered the pH in the circumneutral range, triggering the formation of atacamite through the calcite replacement mechanism. The elevated sulphate and increased calcium concentrations that occur, due to calcite dissolution, result in conditions perfect for the formation of gypsum.

The evaporation of the solution excluding calcite indicated that Cu^{2+} will remain conservative, accumulating in the solution. As the solution becomes more concentrated during evaporation, magnesium sulphate aqueous complexes form which reduce the activity of free sulphate ions in the solution. This reduced SO_4^{2-} activity and increased Cl^- favoured the formation of the chloride mineral atacamite over the sulphate end member brochantite or any other copper sulphate mineral.

5 The stability of atacamite under conditions of decreased salinity and increased acidity

5.1 Introduction

The research in the previous chapters shows that the soil surrounding the Spektakel site contains high concentrations of Cu^{2+} and that atacamite is the dominant, secondary Cu phase retaining Cu^{2+} in the soil. Dissolution of the atacamite has the potential to leach large quantities of Cu^{2+} into the Buffels River and Buffels River aquifer. This has serious implications for the surrounding community as these are the main sources for both drinking water and irrigation. To understand the long term impact that the dissolution of atacamite will have on the ground and surface waters surrounding the site it is crucial to understand the stability of atacamite and how it will behave if the geochemical conditions in the soil suddenly changed.

Little research has been conducted on the stability of atacamite and most of the literature focuses on the formation of atacamite in arid saline environments (Cameron *et al.*, 2007; Hannington, 1993; Reich *et al.*, 2008). These studies concluded that atacamite formation requires saline water, rather than fresh meteoric water, as atacamite dissolves rapidly or changes phase when exposed to fresh meteoric water (Reich *et al.*, 2008). It has also been noted that some assemblages of cupric hydroxy minerals, atacamite, brochantite, malachite, and tenorite, respond rapidly to changes of solution composition, in most cases, within weeks (Woods and Garrels, 1986). Contrary to these studies, research conducted by Miles *et al.* (1998) indicates that atacamite is insoluble in water.

The soil conditions at Spektakel, to some extent, correlate with the conditions required for atacamite formation indicated in the aforementioned studies. The solutions on the surface of the tailings dams contain elevated concentrations of mobile Cu^{2+}, Mg^{2+} and SO_4^{2-}. During rain events these elements are mobilized and filter through the tailings into the soil. These solutions dissolve the halite present in the soil and form acidic Cl^-, Mg^{2+}, SO_4^{2-} and Cu^{2+} rich solutions. When this solution reacts with the calcite in the soil the pH of the solution is neutralized and Cu^{2+} is removed and retained in the soil as atacamite. The saturated paste extracts performed in Chapter 3 indicate that after a sporadic rain event, when the soil containing atacamite becomes waterlogged the solution becomes enriched with Cl^-, SO_4^{2-} and Mg^{2+} at a circumneutral pH. These experiments showed that only a fraction of the Cu^{2+} relative to the original tailings solutions becomes mobilized, indicating that atacamite remains, to a large extent, stable under these circumneutral conditions. The focus of this

chapter is to determine how atacamite will react should continued rain events remove the elevated Cl^- concentration and calcite buffering capacity of the soil.

The effect of pH on the dissolution rate of atacamite was determined both in the presence and absence of chloride. This will replicate how atacamite will behave in both the saline equilibrium soil solutions discussed in Chapter 3 and solutions with reduced soluble ion concentrations. To limit external factors influencing the dissolution, pure atacamite was synthesized.

5.2 Materials and methods

5.2.1 Atacamite preparation

Synthetic atacamite crystals were prepared according to the method proposed by Sharkey and Lewin (1972) that produces a 3g atacamite yield by adding 1g of powdered calcite to a 0.1M $CuCl_2$ solution. To increase the atacamite yield, the initial quantities of the formation solution and calcite was multiplied by a factor of ten. One litre of 1.0M $CuCl_2$ solution was prepared and set to stir on a magnetic stirrer. In total, 10g of calcite power was added to the stirring solution. The calcite powder was added in 2g increments to prevent the solution from bubbling over due to the CO_2 gas release during the reaction. After the calcite was added the solution was left to stir for 24 hours to complete the reaction.

At completion of the reaction the atacamite minerals remained suspended in solution. A 0.5M $Mg(NO_3)_2$ solution was used to help flocculate the atacamite minerals and wash the remaining Cu^{2+} and Cl^- ions from the mineral surface. This was achieved by decanting 40ml of the atacamite-$CuCl_2$ solution and 10ml of 0.5 $Mg(NO_3)_2$ solution into a 50ml centrifuge tube. The tubes were vortexed for 5 minutes to remove as much of the remaining Cu^{2+} and Cl^- from the mineral surface as possible. The tubes were centrifuged for 15 minutes at 3500 rpm to flocculate atacamite crystals. The washing and flocculation was repeated until all the atacamite crystals were removed from the initial solution. The collected atacamite crystals were washed with a 0.2M $Mg(NO_3)_2$ solution until the bulk of the remaining Cu^{2+} and Cl^- was removed. The solution was checked for Cl^- with $AgNO_3$ after each wash. After washing, the crystals were dried overnight at 50 °C and milled into a powder using an agate mortar and pestle. The dry milled sample was sent for XRD mineral analysis to determine the purity of the sample.

5.2.2 Dissolution experiment parameters

The dissolution experiment was designed to replicate the conditions present in the soil. The solutions used for the experiment consist of MiliQ Deionized water (DI water) and a 0.5M NaCl solution (chloride solution). The acidity of the solutions was adjusted in four increments (5.5, 5.0, 4.5 and 4.0) to replicate how the acidic tailings solutions will influence atacamite dissolution during rain events.

Before the pH adjustment experiment was performed 0.4 g of atacamite was equilibrated with 40 ml of DI water and chloride solution respectively, to determine the solubility of atacamite before the pH was reduced. The solutions were stirred for two hours collecting samples at different time intervals (Figure 5.1).

During the pH adjustment experiment, identical experimental procedures were performed on both the deionized water and saline solution samples. The experiment was performed on a solution with a 1:10 atacamite solution ratio. A 50ml glass container was filled with 40 ml of solution and 0.4 g of atacamite added. Before the pH adjustment was performed, atacamite was added to the solution and a 0.7 ml aliquot of sample was collected to determine the initial Cu^{2+} concentration. After commencement of the pH adjustment, the first sample was only collected when the solution reached the pH specified for that run. A 0.7 ml aliquot of solution was collected incrementally at 1,2,3,4,5,10 and 20 minutes. The collected aliquots were filtered with a 0.2 µm GVS Cellulose Acetate Membrane Syringe Filter. The filtered aliquot was diluted ten times with MiliQ deionized water and stored in a 10ml centrifuge tube. Each of the solutions were analysed for its Cu^{2+} concentration by means of ICP-MS (*Refer to Chapter 2*)

Unfortunately the solutions could not be buffered to a set pH before atacamite addition as organic solvents tend to complex with Cu^{2+} (Cardoso Fonseca *et al.*, 1992). The pH of the solutions was adjusted by adding 1M HNO_3 by means of a Methrohm Titrano Autotitrator. The drawback of this method is that the time required to reach each pH is different. This results in different initial Cu^{2+} concentrations for each of the solutions.

5.2.3 Calculations

The significance between the difference of the initial pH and Cu^{2+} concentration of DI water and the chloride solution was determined by performing a one-tailed t-test. The calculations were performed in Microsoft Excel.

The buffering capacity (B_c) of the DI water and chloride solution was determined by dividing the difference between the initial pH and the pH after atacamite addition to the sample (ΔpH) by the concentration of H^+ added (ΔH^+) to the solution to reach that specific pH.

$$B_c = \frac{\Delta pH}{\Delta H^+} \quad \text{[Eq 14]}$$

5.3 Results

Figure 5.1 illustrates the change in Cu^{2+} concentration in DI water and the chloride solution after both solutions were equilibrated with atacamite for 120 minutes (7200 seconds). The results indicate that more Cu^{2+} was released in DI water than in the chloride solution. The Cu^{2+} remained stable in the Chloride solution, a slight increase in Cu^{2+} is observed in the DI water.

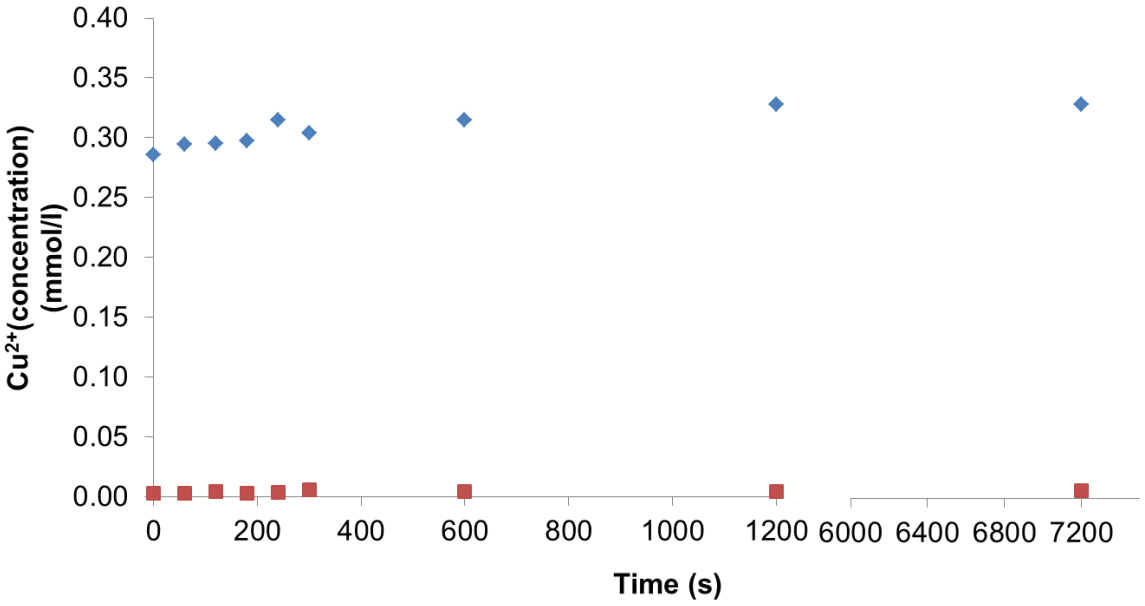

Figure 5.1: Change in Cu^{2+} concentration, with addition of atacamite, over 120 min (7200 seconds) in DI water (◆) and the chloride solution (■). The time is expresses in seconds passed (s). The concentration of Cu^{2+} is expressed in mmol/l.

The average initial Cu^{2+} concentration, after atacamite addition (Figure 5.2), indicates that significantly more (n=6, P<0.01) Cu^{2+} is released in DI water than in the chloride solution. After atacamite addition the average concentration of Cu^{2+} in DI water increases to 0.3 mmol/l and to 0.004 mmol/l in the chloride solution (Figure 5.2).

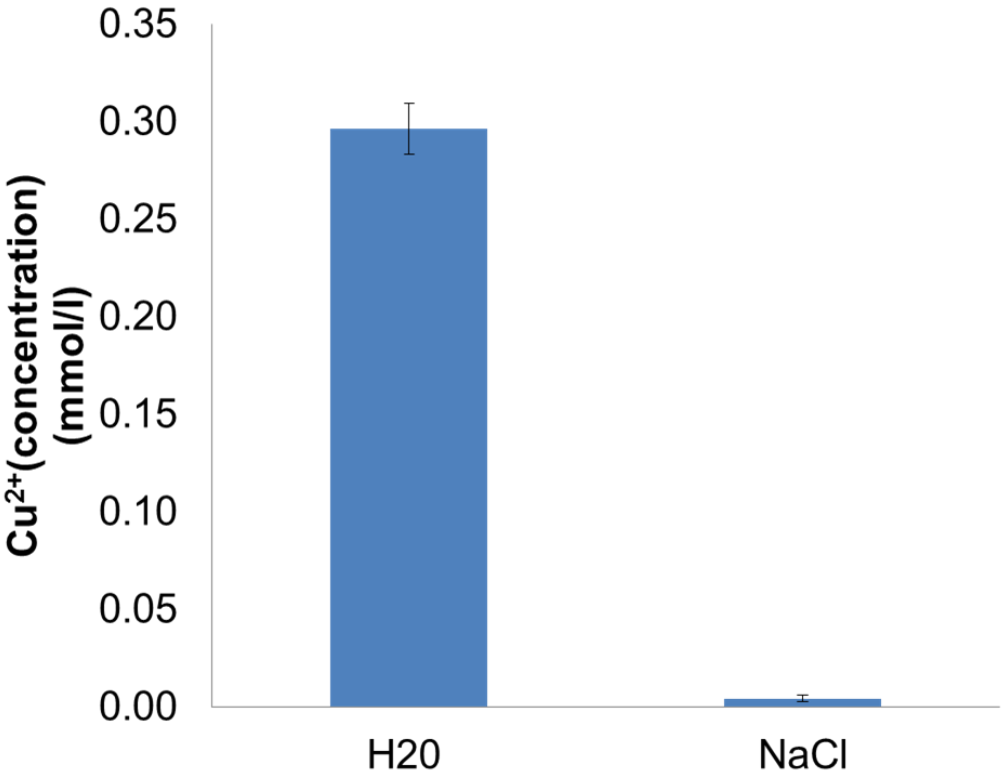

Figure 5.2: Average concentration of Cu^{2+} (expressed in mmol/l) in DI water (H_2O) and the chloride solution (NaCl) after atacamite addition. The error bars indicate the standard deviation of the Cu^{2+} concentration in each solution after atacamite addition.

The initial pH of DI water and the chloride solution is similar (Figure 5.3). After atacamite addition a significant difference in pH (n=6, P<0.01) is observed between the two solutions. The DI water pH increase to 6.17 compared to 6.7 in the chloride solution (Figure 5.3).

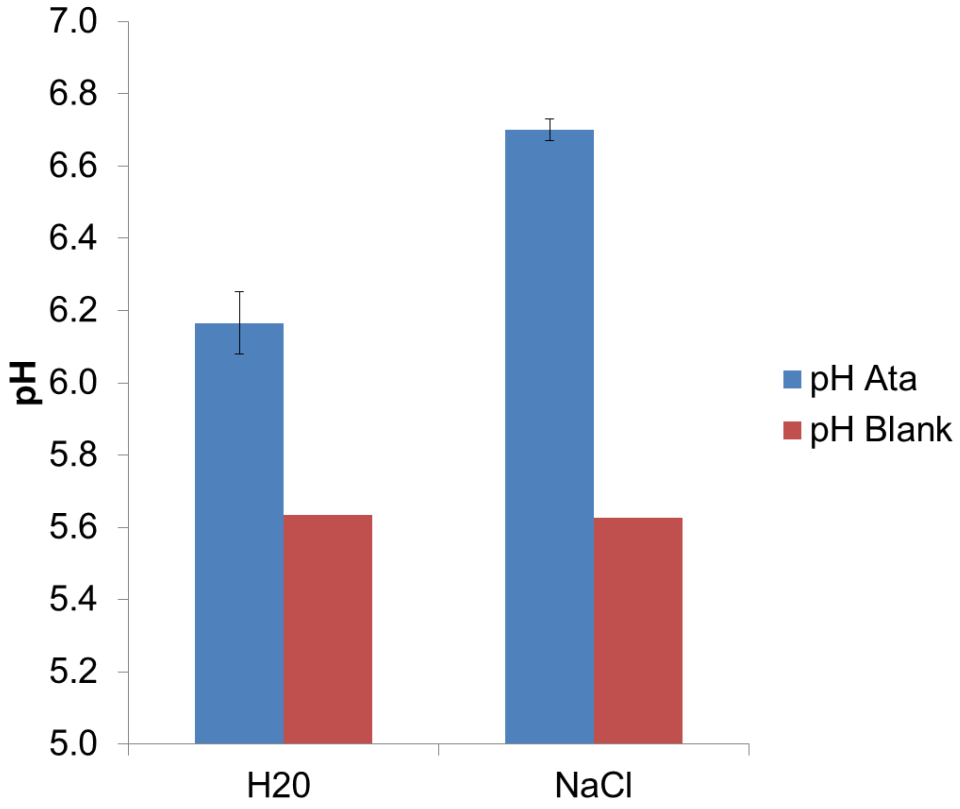

Figure 5.3: Change in solution pH before and after atacamite addition. pH Blank indicates the pH of DI water (H2O) and the chloride solution (NaCl) before atacamite addition. pH Ata indicates the pH of DI water (H2O) and the chloride solution (NaCl) after atacamite addition. The error bars on pH Ata (for both H2O and NaCl) indicate the standard deviation of the pH after atacamite addition.

The dissolution rate of atacamite with increasing acidity (Figure 5.4 and Table 5.1) indicates an elevated dissolution rate in DI water relative to the chloride solution. At pH 5.5 and 5.0 more Cu^{2+} is mobilized in DI water compared to the chloride solution (Figure 5.4a and Figure 5.4b). The initial dissolution rate is higher in DI water than in the chloride solution (Table 5.1). As the pH decreases, the volume of Cu^{2+} mobilized in the chloride solution tends to equal the concentration mobilized in DI water (Figure 5.4c and Figure 5.4d). At pH 4.5 and 4.0 (Figure 5.4c and Figure 5.4d) the dissolution rate of the chloride solution and DI water are fairly similar at 26.3 mmol/l and 31.7 mmol/l respectively (Table 5.1).

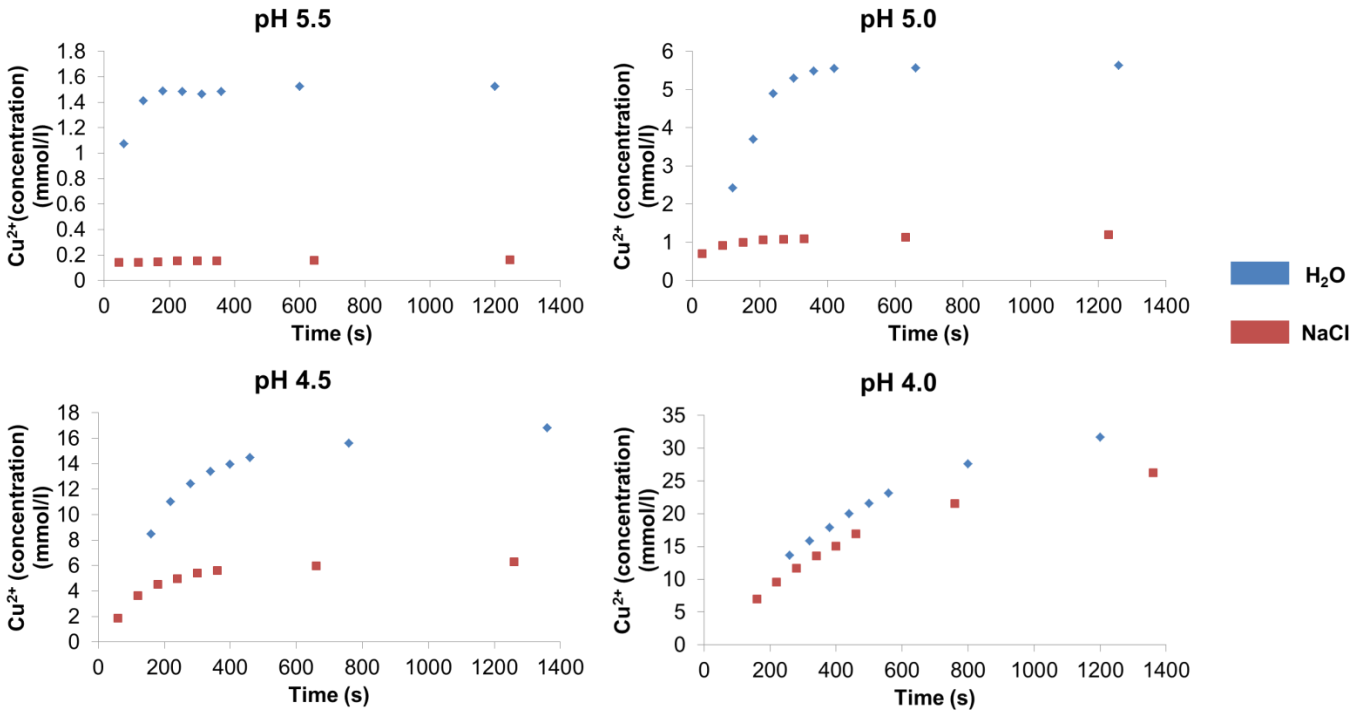

Figure 5.4: Dissolution rate of atacamite, at pH between 5.5 and 4.0, expressed as the accumulation of Cu^{2+} in mmol/l over time (in seconds (s)) in DI water (◆) (H_2O) and in the chloride solution (■) (NaCl).

Table 5.1: Initial dissolution rate of atacamite, at pH between 5.5 and 4.0, in Di water (H_2O) and the chloride solution (NaCl) expressed as the accumulation of Cu^{2+} over time ($mmol.l^{-1}.s^{-1}$)

	Initial Dissolution Rate	
	H_2O	NaCl
pH	$mmol.l^{-1}.s^{-1}$	
5.5	0.0035	0.000045
5.0	0.0206	0.00251
4.5	0.0329	0.0219
4.0	0.0354	0.0389

The results in Figure 5.5 indicate that the reaction order of atacamite dissolution in both DI water and the chloride solution is not uniform over the experimental pH range. Below pH values of 4.5, the reaction order in DI water is 1.5 with respect to pH while the reaction order of the chloride solution is 3.5 with respect to pH. At pH above 4.5 the reaction order of DI water is 0.063 with respect to pH and the reaction order of the chloride solution is 0.5 with respect to pH.

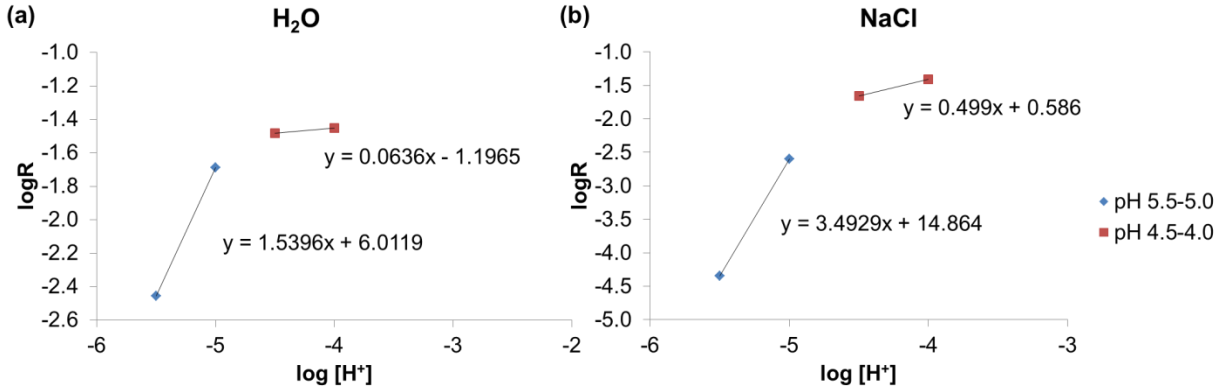

Figure 5.5: The difference in reaction order, with respect to pH, in (a) DI water (H_2O) and the (b) chloride solution (NaCl). The dissolution orders of the samples are divided into dissolution order at pH above 4.5(◆) and pH below 4.5 (■). log[H^+] indicates the concentration of protons in equilibrium with the solution (pH). logR indicates the initial dissolution rate (mmol.l^{-1}.s^{-1}) at pH between 4.0 and 5.5

The dissolution data indicates that at an identical initial pH, more Cu^{2+} is mobilized in DI water relative to the chloride solution (Figure 5.6). As the specific pH required for each solution decreases (Figure 5.6a to Figure 5.6d) the volume of acid required to reach that specific pH increases. Figure 5.6a indicates that only 1.2 mmol of [H^+] for the chloride solution and 1.75 mmol of [H^+] for DI water was required to maintain a stable pH of 5.5. At pH 5.5 the concentration of Cu^{2+} remained stable. The data indicates that the volume of acid required for reaching a pH of 5.0 and below is directly proportional to the concentration of Cu^{2+} in the solution for both DI water and the chloride solution (Figure 5.6a, Figure 5.6b and Figure 5.6c). As more acid is added to each of the solutions, more Cu^{2+} is released.

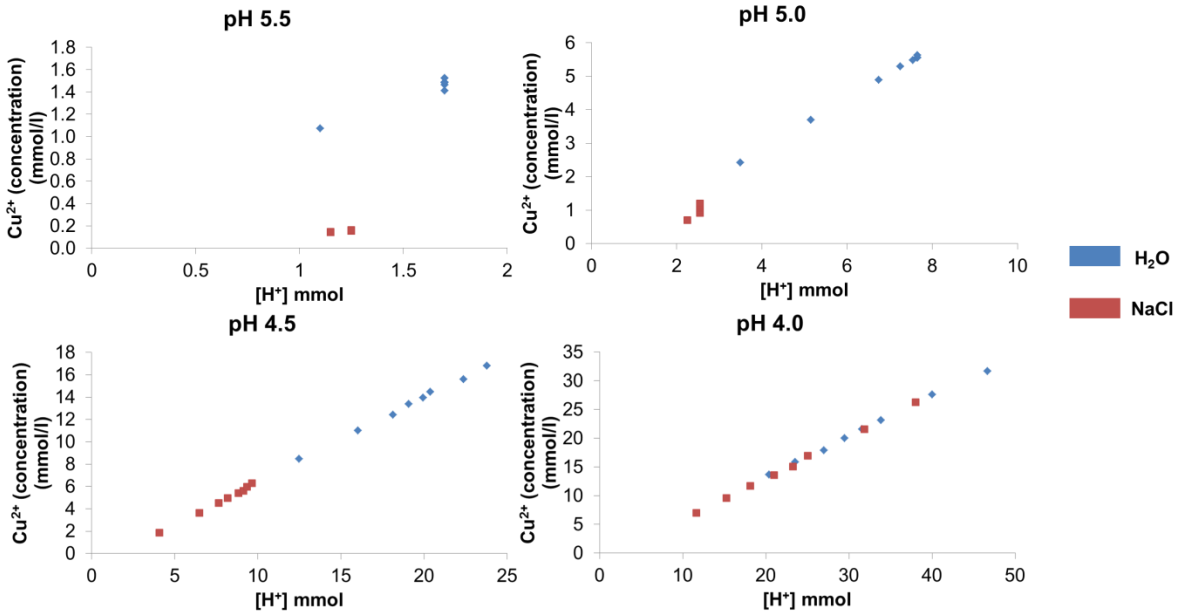

Figure 5.6: Comparison between the concentration of Cu^{2+} (in mmol/l) and the volume of acid added (in mmol $[H^+]$), in Di water (◆) (H_2O) and the chloride solution (■) (NaCl), between pH 5.0 and 4.5

Table 5.2 indicates that the buffer capacity of the chloride solution is lower than DI water indicating that DI water requires more acid to reduce its pH to the same level as the chloride solution.

Table 5.2: The buffer capacity of DI water (H_2O) and the chloride solution (NaCl) expressed as ΔpH/ Δ[H+]. ΔpH = difference between initial pH and the pH after atacamite addition. Δ[H+] = volume of acid added to reach stable pH.

Buffer Capacity		
	H_2O	NaCl
pH	ΔpH/ Δ[H^+]	
5.5	0.571	1.017
5.0	0.376	0.769
4.5	0.128	0.529
4.0	0.104	0.234

5.4 Discussion

In this chapter, the effect of pH on the dissolution rate of atacamite was examined in both the presence and absence of chloride. It has been indicated that atacamite dissolves when exposed to meteoric water and requires a saline solution to form i.e. atacamite dissolution will be reduced in a saline solution (Reich *et al.*, 2008). The concentration of Cu^{2+} observed in DI water and the chloride solution (Figure 5.2) indicates that at pH > 6 the atacamite dissolution is low. The elevated Cu^{2+} concentration in DI water compared to the chloride solution indicates that elevated Cl^- restricts atacamite dissolution. To determine if the observation made in Figure 5.1 is due to the presence of Cl^- in the solution, significance tests were performed (Figure 5.2). The results indicate that Cu^{2+} in DI water is significantly higher than in the chloride solution ($n=6$, $P<0.01$) confirming that the presence of Cl^- in the solution limits atacamite dissolution.

A similar calculation was performed to determine the significance of the change in initial pH with addition of atacamite to DI water and the chloride solution (Figure 5.3). The results indicate that the pH is significantly lower in DI water in comparison with the chloride solution after atacamite addition ($n=6$, $P<0.01$). The more acidic pH of DI water is due to the elevated Cu^{2+} concentration compared to the chloride solution. The hydrolysis effect of Cu^{2+} is more pronounced in DI water with a higher Cu^{2+} concentration reducing the pH these findings are consistent with that the results from Paulson and Kester (1980).

To understand how atacamite will react under conditions similar to those occurring in the soil the dissolution rate of atacamite was determined by decreasing the pH, in both the presence and absence of chloride (Table 5.1). This replicates an increase in soil acidity as the acidic tailings solutions move into the soil dissolving the calcite and thus removing the buffer capacity of the soil. The change in Cl^- concentration mimics the decrease in soil salinity when a large rainfall event dissolves the evaporate minerals and flushes the soil profile removing the soluble Cl^-. The initial dissolution rate of atacamite, at pH 5.5 and pH 5.0, is lower in the chloride solution than in DI water. At pH 4.5 and 4.0 the dissolution rate in DI water stabilizes and the dissolution rate in the chloride solution starts to match the rate of DI water. The dissolution rate data was used to calculate the difference in reaction order with respect to pH, between DI water and the chloride solution, in order to determine how dependant atacamite dissolution is on the change in pH (Figure 5.5). The results indicated that the dissolution rate in the chloride solution is more dependent on the change in pH than dissolution rate in DI water.

This correlates with the different buffer capacities of DI water and the chloride solution (Table 5.2). More acid was required to reduce the pH of DI water than was required to reduce the pH of the chloride solution. Thus, the increase in atacamite dissolution increases the buffer capacity of the solutions. The atacamite dissolution releases more OH^- molecules that consume the excess protons and forming water, thus buffering the pH. This observation is best explained by the dissolution reaction of atacamite expressed through the following dissolution equation (Woods and Garrels, 1986):

$$Cu_2(OH)_3Cl + 3H^+ \rightleftharpoons 2Cu^{2+} + Cl^- + 3H_2O \qquad \text{[Eq 15]}$$

This equilibrium equation is used to explain the influence of chloride activity on the atacamite dissolution. The stoichiometry of the solution indicates that the equilibrium constant of atacamite in solution is expressed as:

$$K_{eq}(atacamite) = \frac{[Cu^{2+}]^2\,[Cl^-]}{[H^+]^3} \qquad \text{[Eq 16]}$$

This equation indicates that to maintain equilibrium when acidity is increased the activity of Cl^- and Cu^{2+} also needs to increase. In DI water, this mechanism indicates that the increase in acidity will dissolve atacamite increasing the Cu^{2+} and Cl^- activity, favouring the forward reaction. In the chloride solution the increased Cl^- activity interferes with this mechanism. As the acidity increases less atacamite will dissolve as the elevated Cl^- activity forces the back reaction reducing the Cu^{2+} activity. This indicates that the elevated Cl^- activity of the chloride solution restricts atacamite dissolution. This explains why less acid is required to reduce the pH of the chloride solution as less atacamite is dissolved producing less OH^- molecules to consume the protons.

The soil at Spektakel is concentrated with Cl^- and has a circumneutral pH (Chapter 3), which according to the results in this chapter favour the stability of atacamite. Should a large rain event occur, the elevated water volume will dissolve the soluble chloride salts reducing the soil Cl^- concentration of the soil. A similar decrease will be observed in the pH of the soil as the acidic tailings solutions will move into the soil depleting the soil's calcite buffer capacity. It is evident from the results that this reduction in Cl^- concentration and increased acidity will increase the dissolution rate of atacamite mobilizing Cu^{2+} into the soil and surrounding water supplies.

5.5 Conclusion

The aim of this chapter was to determine how a rapid change in the chemical conditions in the soil at Spektakel will affect the dissolution rate of atacamite. Specifically, the experiments were focused on the impact that a decrease in Cl^- concentration and an increase in acidity will have on atacamite dissolution. The results indicate that, even though the dissolution rates are generally low, when atacamite is equilibrated with both deionized water and a chloride solution, significantly more Cu^{2+} is released in deionized water. The decrease in pH of the deionized water and the chloride solution indicated that the deionized water had a higher buffering capacity than the chloride solution. The reaction order data indicates that the dissolution rate of atacamite is more dependent on pH in the chloride solution than in DI water. The results suggest that the current condition in the soil at Spektakel favour the stability of atacamite. When a large rain event dilutes the Cl^- concentration of the soil and reduces the buffer capacity, atacamite dissolution will increase, mobilizing large quantities of Cu^{2+}. This will place the surrounding communities at risk as the water sources adjacent to Spektakel contribute to their main water supply.

6 General discussion

The overall aim of this study was to acquire an understanding of the physiochemical controls on the formation and stability of secondary copper minerals in the soil surrounding the Spektakel mine. Chapter 3 describes the chemical characteristics of the soils, while Chapters 4 and 5 describe a number of laboratory experiments that were designed to delineate the conditions of formation and dissolution of secondary Cu minerals. In this discussion the findings of Chapters 3, 4 and 5 are related to conditions occurring in the soil environment.

The initial characterization of the soil (Chapter 3) indicates that the soil contains elevated concentrations of major (SiO_2>Al_2O_3>K_2O>Fe_2O_3>CaO>=MgO>=Na_2O) and trace (Cu>S> Ba>Sr>Rb>Cr) elements with only Cu^{2+} exceeding the Dutch Soil Standard Guidelines (Dutch Soil Screening Guidelines, 2009). This indicates that the current copper concentration in the soil is hazardous to human health and that remediation is required to reduce the Cu^{2+} concentration. This is problematic due to the proximity of the site with respect to the water sources in the area. The Spektakel mine is situated upslope of the Buffels River which is the main water source feeding into the Buffels River aquifer. These water sources constitute the main water supply to the communities situated downstream of the site (Benito *et al.*, 2010). If the copper in the soil is mobilized and leaches into these water sources it will place the health of these communities at risk.

To determine if the water sources are at risk of mass Cu^{2+} mobilization, analyses were performed to determine how the copper and other major and trace elements accumulate and disperse in the soil profiles during and after rain events (Chapter 3). The results indicate that during rain events an acidic solution (pH 4.8) enriched in Cu^{2+}, SO_4^{2-}, Mg^{2+} accumulates on the surface of the tailings dumps. As this solution percolates through the tailings into the soil it dissolves other evaporate minerals, mainly halite, producing an acidic Cu^{2+}, SO_4^{2-}, Mg^{2+} and Cl^- rich solution. However, when the soil is placed in equilibrium with water, analysis indicates that the soil has a circumneutral pH and a much lower Cu^{2+} concentration when compared to the tailings solution. This indicates that some chemical mechanisms are buffering the pH and retaining the Cu^{2+} in the soil. The mineralogical study indicates that the Cu^{2+} is retained in the soil through the formation of the copper hydroxy chloride mineral atacamite. Neither the sulphate equivalent, brochantite, nor any other copper sulphate mineral was observed in the soil, which contrasts with the sulphate rich conditions of the soil. The results from the mineral formation experiment indicate that the circumneutral pH of the soil is achieved by the dissolution of calcite present in the soil (Chapter 4). It is this same calcite dissolution reaction which forms the basis of the Cu^{2+} retention in the soil. During

dissolution the calcite is replaced by atacamite (Garrels and Stine, 1948) (Chapter 4). This formation mechanism is controlled by activity of Cl^- and SO_4^{2-} in the soil solution. When the solution, in equilibrium with the soil, evaporates the elevated Mg^{2+} in the soil solution complexes (Martin, 2000) with SO_4^{2-} reducing the activity of SO_4^{2-} reducing its ability to complex with Cu^{2+}. This inhibits the formation of brochantite or any other secondary copper sulphate mineral.

The conditions currently present in the soil at Spektakel (circumneutral pH, high Cl^- and Mg^{2+} concentration and calcite in the soil (Chapter 3, Chapter 4 and Chapter 5)) favour the stability of atacamite reducing the risk of mass Cu^{2+} mobilization. However as continued rain events flush meteoric water through the tailings and soil surrounding Spektakel, the availability of the components involved in the mechanisms that stabilize atacamite are reduced (Chapter 3 and Chapter 4). The acidic tailings solutions dissolve the calcite in the soil reducing the soils ability to buffer its pH. As more of the tailings solution moves into the soil, it concentrates the soil with respect to SO_4^{2-} diluting the Cl^- concentration. The increased acidic soil pH, combined with the reduction in chloride concentration will reduce the ability of atacamite to form and retain Cu^{2+} in the soil (Chapter 3, Chapter 4 and Chapter 5). The increased acidity and diluted Cl^- concentration favours the dissolution of atacamite and will mobilize Cu^{2+} into the soil solutions (Chapter 5). After rain events, when the copper rich soil solution evaporates, Cu^{2+} will remain conservative in the solution (Chapter 4). The abundance of Mg^{2+} in the soil solution reduces the activity of SO_4^{2-} by forming $MgSO_4$ aqueous complexes (Martin, 2000). This reduced activity inhibits SO_4^{2-} reacting with Cu^{2+} to form a copper sulphate mineral, therefore less Cu^{2+} will be retained in the soil (Chapter 4). If the sporadic rain events continue to strip the soil of the Cu^{2+} retaining mechanisms, the acidic metal rich tailings solution will eventually percolate into the surrounding water supplies, risking the health of the people in the area.

The result of this study indicates that the tailings and the soil at the site have the potential to mobilize large volumes of Cu^{2+} into the surrounding water sources. To prevent this it is recommend that as much calcite as possible needs to be added into the soil and tailings. This is the most cost effective approach to retain the copper and, keep the soil pH neutral. A more permanent, and more expensive, solution would be to remove the copper rich tailings dumps and dispose of it at a secure hazardous waste disposal site.

7 Conclusions and further work

The overall aim of the study was to determine the physiochemical conditions governing the formation and dissolution of secondary copper minerals, specifically atacamite, in the soil at the Spektakel mine.

- The site characterization established that the soil surrounding the tailings contains elevated concentrations of major and trace elements, with a Cu^{2+} concentration exceeding the Dutch Soil Standard Guidelines (Dutch Soil Screening Guidelines, 1991). The saturated paste extracts indicate that the soils are extremely saline with a circumneutral pH. The mineralogical analysis indicates that the soil contains a range of secondary mineral phases and that atacamite is the only secondary copper phase in the soil. No brochantite or any other secondary copper sulphate minerals was observed.
- The analysis of the tailings pond solution indicates that the solution is acidic and contains elevated concentrations of Cu^{2+}, Mg^{2+} and SO_4^{2-}. The Cl^- concentration of the solution is low compared to the other elements. When this solution percolates through the tailings it accumulates Cl^- through halite dissolution forming an acidic Cu^{2+}, Mg^{2+} and SO_4^{2-} and Cl^- solution. This solution enriches the surrounding soil with respect to its chemical composition and neutralizes the soil pH through calcite dissolution. The dissolution of the calcite retains the Cu^{2+} from the solution in the soil replacing the calcite with atacamite.
- It was identified that the absolute Cl^- and SO_4^{2-} concentration is not the only mechanism governing the formation of atacamite and restricting the formation of brochantite or any other copper sulphate mineral. The main mechanism of formation relies on the pH and the activity of the Cl^- and SO_4^{2-} ions in the solution.
- The evaporation of a solution in equilibrium with the soil indicated that the elemental evolution adhered to the evaporation model described by Hardie and Eugster (1970). All the elements remained conservative during evaporation except for Ca^{2+} which was removed through gypsum precipitation. The solution containing calcite indicated that Cu^{2+} was removed after calcite addition inhibiting the formation of any other secondary copper mineral phases. The results of the solution excluding calcite, indicated that no brochantite or any other copper sulphate mineral was formed. It was concluded that due to the abundance of Mg^{2+} in the solution $MgSO_4$ aqueous complexes formed reducing the activity of SO_4^{2-}, reducing the ability of SO_4^{2-} to complex with Cu^{2+}.

- It was established that in a solution with a pH > 6 and a high chloride concentration atacamite will remain stable. As the solution becomes more acidic and less concentrated with respect to Cl^-, dissolution rate of atacamite will increase mobilizing more Cu^{2+}.
- The overall conclusion that follows from this study is that the current chemical conditions of the soil favour the formation and stability of atacamite, thus retaining Cu^{2+} in the soil. As the acidic tailings solutions flush through the soil during sporadic, rain events, it concentrates the soil with respect to SO_4^{2-}, decreasing the Cl^- concentration and dissolving the calcite in the soil. This reduced soil pH and lowered Cl^- concentration favours atacamite dissolution and will result in the leaching of large quantities of Cu^{2+} into the surrounding water bodies contaminating the water supply.

The results of the study indicate that more work can be conducted at Spektakel. In the future more focus should be placed on determining the distribution of copper with respect to the site. How does the concentration of Cl^- combined with the reduction in pH influence atacamite dissolution? Do the “heuweltjies” influence the migration pathway of Cu^{2+} in the soil? Additional analyses should be conducted to determine whether or not Cu^{2+} is present in the Buffels River and Buffers River aquifer.

8 References

Akcil, A. & Koldas, S. 2006. Acid mine drainage (AMD): Causes, treatment and case studies. *Journal of Cleaner Production,* 14, 1139-1145.

Antonijević, M.M., Dimitrijević, M.D., Milić, S.M. & Nujkić, M.M. 2012. Metal concentrations in the soils and native plants surrounding the old flotation tailings pond of the copper mining and smelting complex bor (serbia). *Journal of Environmental Monitoring,* 14, 866-877.

Atkinson, G. & Petrucci, S. 1966. Ion association of magnesium sulfate in water at 25°. *Journal of Physical Chemistry,* 70, 3122-3128.

Balsberg Pahlsson, A.M. 1989. Toxicity of heavy metals (Zn, Cn, Cd, Pb) to vascular plants. *Water Air Soil Pollution,* 66, 163-171.

Benedict, P.C., D. Wiid & A.K. Cornelissen(eds.) 1964. *Progress report on the geology of the O'okiep Copper District.* The geology of some ore deposits in Southern Africa. Vol. 2 South Africa: Geological Society of South Africa.

Benito, G. 2010. Management of alluvial aquifers in two Southern African ephemeral rivers: Implications for IWRM. *Water Resources Management,* 24, 641-667.

Brewer, G.J. 2010. Risks of copper and iron toxicity during aging in humans. *Chemical Research in Toxicology,* 23, 319-326.

Cairncross, B. 2004. History of the Okiep Copper District, Namaqualand, Northern Cape Province, South Africa. *Mineralogical Record,* 35, 289-317.

Cameron, E.M., Leybourne, M.I. & Palacios, C. 2007. Atacamite in the oxide zone of copper deposits in Northern Chile: Involvement of deep formation waters? *Mineralium Deposita,* 42, 205-218.

Cardoso Fonseca, E., Claudino Cardoso, J., Estela Martins, M. & Margarida Vairinho, M. 1992. Selective chemical extraction of Cu from selected mineral and soil samples: Enhancement of Cu geochemical anomalies in Southern Portugal. *Journal of Geochemical Exploration,* 43, 249-263.

Clifford, T.N., Gronow, J., Rex, D.C. & Burger, A.J. 1975. Geochronological and petrogenetic studies of high-grade metamorphic rocks and intrusives in Namaqualand, South Africa. *Journal of Petrology,* 16, 154-188.

Comans, R.N.J. & Middelburg, J.J. 1987. Sorption of trace metals on calcite: Applicability of the surface precipitation model. *Geochimica Et Cosmochimica Acta,* 51, 2587-2591.

Davis, G.K. & Mertz, W. 1987. Copper, *Trace elements in human and animal nutrition.* Vol. 1. New York: Acadamic Press.Pages 301-364 in

Desmet, P.G. 2007. Namaqualand—A brief overview of the physical and floristic environment. *Journal of Arid Environments,* 70, 570-587.

Dutch Soil Screening Guidelines. 2012. *Dutch Soil Screening Guidelines.* [Online]. Available: http://www.esdat.net/Environmental%20Standards/Dutch/ENGELSE%20versie%20circulaire%20Bodemsanering%202009.pdf [13 November 2012].

Ellis, F. 2002. Contribution of termites to the formation of hardpans in soils of arid and semi-arid regions of South Africa. *In: 17th World Congress of Soil Science, Bangkok, Thailand, August 2002.*

Ellis, F. & Lambrechts, J.J.N. 1994. Dorbank, a reddish brown hardpan of South Africa - A proto-silcrete? *In: 15th World Congress of Soil Science, Acapulco, Mexico.*

Espejo, R., Vicente, M.A., Molina, E. & Barragan, E. 1993. Kaolinite formation from feldspars: Study of a weathering profile in gneiss from the Iberian Hercynian Massif. *Mineralogica Et Petrographica Acta,* 35 A, 209-216.

Fernandes, J. and Henriques, F. , 1991. Biochemical, physiological, and structural effects of excess copper in plants. *The Botanical Review*, 57, 246-273.

Francis, M.L., Fey, M.V., Prinsloo, H.P., Ellis, F., Mills, A.J. & Medinski, T.V. 2007. Soils of namaqualand: Compensations for aridity. *Journal of Arid Environments,* 70, 588-603.

Gadd-Claxton, D.L. 1981. *The economic geology of the Okiep copper deposits, Namaqualand, South Africa. Unpublished thesis.* Grahamstown, South Africa: Rhodes University.Masters.

Garrels, R.M. & Stine, L.O. 1948. Replacement of calcite by atacamite in copper chloride solutions. *Economic Geology,* 43.

Geller, W., Klapper, H. & Salomons, W. 1998. *Acidic mining lakes: Acid mine drainage, limnology and reclamation.* New York: Springer-Verlag.

Gibson, R.L. & Kisters, A.F.M. 1996. The geology and mineralization of the Okiep Copper District: An overview. *South African Journal of Geology,* 99, 105-106.

Hahn, B.D., Richardson, F.D., Hoffman, M.T., Roberts, R., Todd, S.W. & Carrick, P.J. 2005. A simulation model of long-term climate, livestock and vegetation interactions on communal rangelands in the semi-arid succulent karoo, Namaqualand, South Africa. *Ecological Modelling,* 183, 211-230.

Hannington, M.D. 1993. The formation of atacamite during weathering of sulfides on the modern seafloor. *Canadian Mineralogist,* 31, 945-956.

Hardie, L.A. & Eugster, H.P. 1970. The evolution of closed-basin brines. *Mineral Society of America Special Papers*, 3, 273-290.

Hohne, S. & Hansen, R.N. 2008. Preliminary conceptual geo-environmental modal of the abandoned copper mines of the Okiep Copper District, Namaqualand, Northern Cape, *Sustainable development through mining.* Vol. 1. Council for Geoscience.Pages 1-70.

Holland, J.G. & Marais, J.A.H. 1983. The significance of the geochemical signature of the proterozoic gneisses of the Namaqualand metamorphic complex with special reference to the Okiep Copper District, in Botha, B.J.V.(ed.). *Namaqualand metamorphic complex.* Vol. 10. Geological Society of South Africa. Pages 83-91.

Kelm, U., Helle, S., Matthies, R. & Morales, A. 2009. Distribution of trace elements in soils surrounding the El Teniente Porphyry Copper Deposit, Chile: The influence of smelter emissions and a tailings deposit. *Environmental Geology,* 57, 365-376.

Kelso, C. & Vogel, C. 2007. The climate of Namaqualand in the nineteenth century. *Climatic Change,* 83, 357-380.

Kisters, A.F.M., Charlesworth, E.G., Gibson, R.L. & Anhaeusser, C.R. 1996. Steep structure formation in the Okiep Copper District, South Africa: Bulk inhomogeneous shortening of a high-grade metamorphic granite-gneiss sequence. *Journal of Structural Geology,* 18, 735-751.

Land Type Survey Staff. 1987, Land type survey staff. Land types of the maps 2816 Alexander Bay, 2818 Warmbad, 2916 Springbok, 2918 Pofadder, 3017 Garies, 3018 Loeriesfontein. Memoirs on the. Agricultural and Natural Resources.of South Africa. No 9.

Lazar, B., Starinsky, A., Katz, A., Sass, E. & Ben-Yaakov, S. 1983. The carbonate system in hypersaline solutions: Alkalinity and CaCO3 solubility of evaporated seawater. *Limnology & Oceanography,* 28, 978-986.

Lombaard, A.F. & The Exploration Department Staff of the O'okiep Copper Company Ltd. 1986. The copper deposits of the Okiep Copper District, Namaqualand, *Mineral deposits of Southern Africa.* Geological Society of South Africa: Johannesburg, 1421-1445.

Lowenstein, T.K. & Hardie, L.A. 1985. Criteria for the recognition of salt-pan evaporites. *Sedimentology,* 32, 627-644.

MacKellar, N.C., Hewitson, B.C. & Tadross, M.A. 2007. Namaqualand's climate: Recent historical changes and future scenarios. *Journal of Arid Environments,* 70, 604-614.

Mann, A.W. & Deutscher, R.L. 1977. Solution geochemistry of copper in water containing carbonate, sulphate and chloride ions. *Chemical Geology,* 19, 253-265.

Martin, S.T. 2000. Phase transitions of aqueous atmospheric particles. *Chemical Reviews,* 100, 3403-3453.

Mees, F. & Stoops, G. 2003. Circumgranular bassanite in a gypsum crust from eastern algeria - A potential palaeosurface indicator. *Sedimentology,* 50, 1139-1145.

Miles, R.D., O'Keefe, S.F., Henry, P.R., Ammerman, C.B. & Luo, X.G. 1998. The effect of dietary supplementation with copper sulfate or tribasic copper chloride on broiler performance, relative copper bioavailability, and dietary prooxidant activity. *Poultry Science,* 77, 416-425.

Miller, D. 1995. 2000 years of indigenous mining and metallurgy in Southern Africa - A review. *South African Journal of Geology,* 98, 232-238.

Mortlock, R.A. & Froelich, P.N. 1989. A simple method for the rapid determination of biogenic opal in pelagic marine sediments. *Deep Sea Research Part A, Oceanographic Research Papers,* 36, 1415-1426.

Newmark, N. 2010. Formation and stability of secondary copper minerals in the soils of Spektakel copper mine. *Honours Thesis, Stellenbosch University.*

Parkhurst, D.L. and Appello, C.A.J. , 1999. PHREEQC - A computer program for the speciation, batch reaction, onedimentional transport, and inverse geochemical calculations.

Paulson, A.J. & Kester, D.R. 1980. Copper(II) ion hydrolysis in aqueous solution. *Journal of Solution Chemistry,* 9, 269-277.

Reich, M. 2008. Atacamite formation by deep saline waters in copper deposits from the Atacama Desert, Chile: Evidence from fluid inclusions, groundwater geochemistry, TEM, and 36Cl data. *Mineralium Deposita,* 43, 663-675.

Rose, A.W. 1976. Effect of cuprous chloride complexes in the origin of red-bed copper and related deposits. *Economic Geology,* 71, 1036-1048.

Rozendaal, A. Water of the buffels river used in ore processing at Spektakel. personal communication.

Schoch, A.E. & Conradie, J.A. 1990. Petrochemical and mineralogical relationships in the Koperberg Suite, Namaqualand, South Africa. *American Mineralogist,* 75, 27-36.

Sharkey, J.B. & Lewin, S.Z. 1972. Thermochemical properties of the copper(II) hydroxychlorides. *Thermochimica Acta,* 3, 189-201.

Smalberger, J.M.(ed.). 1975. *Aspects of the history of copper mining in Namaqualand, 1846 - 1931.* Vol. 1 Cape Town: C. Struik

Soil Classification Group(ed.). 1991. *Soil classification, A taxonomic system for South Africa.* Vol. 2 Republic of South Africa: The Department of Agricultural Development Republic of South Africa

Sparks, D.L. (eds.) 1996. *Methods of soil analysis - Part 3 Chemical Methods.* Soil Science Society of America Book Series Number 5. Vol. 4 Madison, WI: Soil Science Society of America, Inc

Vigneault, B., Campbell, P.G.C., Tessier, A. & De Vitre, R. 2001. Geochemical changes in sulfidic mine tailings stored under a shallow water cover. *Water Research,* 35, 1066-1076.

Woods, T.L. & Garrels, R.M. 1986. Phase relations of some cupric hydroxy minerals. *Economic Geology,* 81, 1989-2007.

Zachara, J.M., Cowan, C.E. & Resch, C.T. 1991. Sorption of divalent metals on calcite. *Geochimica Et Cosmochimica Acta,* 55, 1549-1562.

Zamana, L.V. & Usmanov, M.T. 2007. Thermodynamic and hydrogeochemical formation conditions of brochantite as a crystalline hydrate: A case of the Udokan Copper Deposit. *Doklady Earth Sciences,* 413, 269-271.